

In cooperation with the U.S. Army Corps of Engineers, Chicago District, and the Metropolitan Water Reclamation District of Greater Chicago

# Methodology, Data Collection, and Data Analysis for Determination of Water-Mixing Patterns Induced by Aerators and Mixers

Water-Resources Investigations Report 00-4101



U.S. DEPARTMENT OF THE INTERIOR  
U.S. GEOLOGICAL SURVEY

In cooperation with the U.S. Army Corps of Engineers, Chicago District, and the Metropolitan Water Reclamation District of Greater Chicago

# **Methodology, Data Collection, and Data Analysis for Determination of Water-Mixing Patterns Induced by Aerators and Mixers**

By Gary P. Johnson, Nancy J. Hornewer, Dale M. Robertson, Darren T. Olson, and Josh Gioja

Water-Resources Investigations Report 00-4101

Urbana, Illinois  
2000

**U.S. DEPARTMENT OF THE INTERIOR**  
**BRUCE BABBITT, Secretary**

**U.S. GEOLOGICAL SURVEY**  
**Charles G. Groat, Director**

The use of firm, trade, and brand names in this report is for identification purposes only and does not constitute endorsement by the U.S. Geological Survey.

For additional information write to:

District Chief  
U.S. Geological Survey  
221 North Broadway Avenue  
Urbana, Illinois 61801

Copies of this report can be purchased from:

U.S. Geological Survey  
Branch of Information Services  
Box 25286  
Denver, CO 80225-0286

# CONTENTS

Abstract.....	1
Introduction .....	1
Purpose and Scope.....	2
Description of Study Sites .....	2
Acknowledgments .....	3
Methodology and Equipment .....	3
Methodology.....	3
Aerators and Mixers .....	7
Aerators .....	7
Submersible Mixer.....	8
Surface Mixer .....	8
Velocity Measurements.....	8
Acoustic Doppler Velocimeter.....	8
Acoustic Doppler Current Profiler.....	12
Water-Quality Measurements .....	12
Instruments .....	12
Docks, Thermistor Strings, and Anemometer.....	13
Microprofiler.....	13
Fluorometer and Dye .....	14
Data Collection .....	14
Tank Tests .....	14
Egan Quarry Tests (1996 and 1997) .....	15
Raw Data .....	17
Analysis of Data .....	18
Tank Tests .....	18
Egan Quarry Tests (1996).....	19
Single-Aerator Tests .....	19
Strongly Stratified Conditions .....	19
Weakly Stratified Conditions.....	22
Multiple-Aerator Tests.....	22
Measurements and Model Simulations of Plume Characteristics .....	29
Breakdown of Stratification in Egan Quarry .....	38
Egan Quarry Tests (1997).....	40
Aerators and Submersible Mixer .....	40
Surface Mixer .....	43
Summary.....	46
References Cited.....	48
Appendix 1. Maps of Data Collection Locations .....	51
Appendix 2. CD-ROM Data Base (in back of report)	

## FIGURES

1. Photograph showing test tank at the U.S. Army Corps of Engineers Waterways Experiment Station, Vicksburg, Mississippi .....	2
2–3. Maps showing:	
2. Location of Egan Quarry, Schaumburg, Illinois .....	4
3. Bathymetry of Egan Quarry, August 1995 .....	5
4. Schematic of bubble plume with multiple entrainments and detrainments .....	6

5–14.	Photographs showing:	
5.	Fine-bubble and coarse-bubble aerators used during the tank tests at the U.S. Army Corps of Engineers, Waterways Experiment Station .....	7
6.	Coarse-bubble aerator and frame used during tests in Egan Quarry .....	8
7.	Air compressor/manifold system used to deliver compressed air to aerators .....	9
8.	Submersible mixer (A) and mount (B) used during tests in Egan Quarry .....	10
9.	Surface mixer operating in Egan Quarry.....	11
10.	Acoustic Doppler Velocimeter and mount used during tests in Egan Quarry .....	11
11.	Acoustic Doppler Current Profiler and mount used during tests in Egan Quarry.....	12
12.	Water-quality-monitoring equipment and floating dock used during tests in Egan Quarry.....	13
13.	Microprofiler used in water-quality measurements during tests in Egan Quarry.....	14
14.	Turner flow-through fluorometer used to track the dye movement in the axisymmetric intrusion during tests in Egan Quarry .....	15
15.	Three-dimensional view of the test tank at the U.S. Army Corps of Engineers, Waterways Experiment Station, showing velocity-vector axes.....	22
16–21.	Two-dimensional plots of velocity vectors induced by aerators in a test tank at the U.S. Army Corps of Engineers, Waterways Experiment Stations for:	
16.	Test ASA .....	23
17.	Test ASB.....	24
18.	Test ALC .....	25
19.	Test ALD .....	26
20.	Test BSE.....	27
21.	Test BSF .....	28
22–34.	Diagrams showing:	
22.	Velocity field induced from a single aerator during strongly stratified conditions [test eg962s (a.m.)], Egan Quarry, 1996.....	29
23.	Dissolved oxygen concentrations prior to and during single-aerator test in strongly stratified conditions [test eg962s (a.m.)], Egan Quarry, 1996 .....	30
24.	Fluorometric data recorded during single-aerator test eg962s (a.m.) after injection of dye at the aerator head, Egan Quarry, August 27, 1996.....	31
25.	Microstructure data collected as the microprofiler ascended vertically to the water surface of Egan Quarry, (A) prior to turning on the air compressor (initial conditions) on August 27, 1996, at 11:33 a.m., (B) at 12.3 meters from the center of the rising-bubble plume at 12:19 p.m., (C) at 10.7 meters from the center of the rising-bubble plume at 12:35 p.m. and (D) at 29.0 meters from the center of the rising-bubble plume at 1:03 p.m.....	32
26.	Velocity field induced from a single aerator during weakly stratified conditions (test eg964d), Egan Quarry, 1996.....	33
27.	Dissolved oxygen concentrations prior to and during a two-aerator test in strongly stratified conditions (test eg964s), Egan Quarry, 1996 .....	34
28.	Physical characteristics of a rising bubble-plume from Schladow's (1992) model for a bubble plume rising through a 12.2-meters strongly stratified water column with an aerator at 11.6 meters and an air-flow rate of 0.022 cubic meter per second, Egan Quarry .....	36
29.	Physical characteristics of a rising bubble-plume from Schladow's (1992) model for a bubble plume rising through a 12.2-meters weakly stratified water column with an aerator at 11.6 meters and an air-flow rate of 0.022 cubic meter per second, Egan Quarry .....	37
30.	Observed water temperature from August 28 to September 3, 1996, in Egan Quarry.....	39
31.	Simulation by the Dynamic Lake Model-Hourly (DLM-hr) of water temperature in Egan Quarry with aeration, 1996.....	41
32.	Simulation by the Dynamic Lake Model-Hourly (DLM-hr) of water temperature in Egan Quarry without aeration, 1996.....	42
33.	Water-velocity profiles during test eg973s, 6.1 meters west and 32 meters west of the submersible mixer, Egan Quarry, 1997.....	44
34.	Water-velocity profiles during test SM2, 16.7 meters east and 49 meters east of the surface mixer, Egan Quarry, 1997.....	45
35.	Photograph showing data collection set-up during the SM3 test, Egan Quarry, July 24, 1997.....	46

36.	Diagram showing dissolved oxygen data of a west to east cross-section in Egan Quarry during test SM3, July 24, 1997.....	47
-----	--	----

TABLES

1.	Air-flow rate and corresponding letter designation in data file names for tank tests, Waterways Experiment Station.....	15
2.	Summary of test configurations during summer 1996 listed in order of performance, Egan Quarry, Illinois .....	16
3.	Summary of test configurations during summer 1997 listed in order of performance, Egan Quarry, Illinois .....	17
4-9.	Summary tables of six tank tests, Waterways Experiment Station	
4.	Test ASA.....	18
5.	Test ASB.....	19
6.	Test ALC.....	19
7.	Test ALD .....	20
8.	Test BSE.....	20
9.	Test BSF .....	21
10.	Comparison of measured and estimated plume characteristics for eg962s (a.m.) and eg964d at Egan Quarry.....	35

CONVERSION FACTORS, VERTICAL DATUM, AND ABBREVIATIONS

Multiply	By	To obtain
<b>Length</b>		
centimeter (cm)	0.3937	inch
meter (m)	3.281	foot
kilometer (km)	0.6214	mile
<b>Area</b>		
hectare (ha)	2.471	acre
<b>Volume</b>		
cubic centimeter (cm <sup>3</sup> )	0.06102	cubic inch
cubic meter (m <sup>3</sup> )	0.0008107	acre-foot
<b>Flow rate</b>		
meter per second (m/s)	3.281	foot per second
cubic meter per second (m <sup>3</sup> /s)	2119	cubic foot per minute
centimeter per second (cm/s)	0.03281	foot per second
millimeter per second (mm/s)	0.003281	foot per second
cubic meter per minute (m <sup>3</sup> /min)	35.31467	cubic foot per minute
<b>Mass</b>		
kilogram (kg)	2.205	pound avoirdupois
<b>Mass Density</b>		
kilogram per cubic meter (kg/m <sup>3</sup> )	0.0624297	pound per cubic foot

Temperature in degrees Celsius (°C) may be converted to degrees Fahrenheit (°F) as follows:

$$^{\circ}\text{F} = (1.8 \times ^{\circ}\text{C}) + 32$$

**Concentrations of chemical constituents** in water are given either in milligrams per liter (mg/L) and micrograms per liter (µg/L).

**Other abbreviations used in this report:**

MHz	Megahertz
Hz	Hertz
mS/cm	millisiemen per centimeter
hp	horsepower
V	volt
kHz	kilohertz

# Methodology, Data Collection, and Data Analysis for Determination of Water-Mixing Patterns Induced by Aerators and Mixers

By Gary P. Johnson, Nancy J. Hornewer, Dale M. Robertson, Darren T. Olson, *and* Josh Gioja

## Abstract

The U.S. Geological Survey collected and analyzed data to describe mixing patterns induced by aerators and mixers to aid in the calibration and verification of a three-dimensional hydrodynamic model. During September 1995, three-dimensional water-velocity profiles were collected during the operation of fine-bubble and coarse-bubble aerators in a test tank at the U.S. Army Corps of Engineers Waterways Experiment Station. Three-dimensional water-velocity, water-temperature, pH, dissolved oxygen concentration, and specific conductivity profiles were collected during operation of a coarse-bubble aerator in a reservoir in Schaumburg, Illinois, during summer 1996 and summer 1997, during strongly stratified and weakly stratified conditions. The effects of a submersible mixer alone and in combination with coarse-bubble aerators and a surface mixer alone also were investigated during summer 1997. The mixing patterns induced by the operation of aerators, submersible mixers, and surface mixers were described and compared with mixing patterns predicted by model simulations.

Bubble-plume characteristics during tests in strongly stratified and weakly stratified conditions in the reservoir were documented and compared with characteristics simulated by different models. Lemckert and Imberger's model simulates an entrainment rate similar to the rate measured during a test in the reservoir under strongly stratified conditions, whereas Schladow's one-dimensional model appears to underestimate the total entrainment rate by about 50 percent.

Schladow's model was accurate during weak stratification but underestimated the radius of the plume during strong stratification.

For 5 days during daylight hours, water-temperature profiles were collected continuously during the operation of four aerators. Water temperatures in the reservoir were significantly affected by the operation of the aeration system. These changes were compared to simulations from a one-dimensional Dynamic Lake Model (DLM) simulation. DLM accurately simulated changes as a result of aeration, including daily changes.

On the basis of temporal and spatial dissolved oxygen measurements, the volumetric quantity of oxygen in the reservoir was quantified before and after operation of a submersible mixer. A net loss of oxygen was calculated. This net loss may have resulted from a net warming of water throughout the reservoir or submerged supersaturated water releasing oxygen when the water came in contact with the atmosphere.

## INTRODUCTION

The U.S. Army Corps of Engineers, Chicago District (Corps) is designing a flood-control reservoir to store excess stormwater and sewage from combined sewer overflows (CSO's) as part of the Chicagoland Underflow Plan/Tunnel and Reservoir Plan (CUP/TARP). During storms, CSO will be diverted through dropshafts into a series of deep tunnels under Chicago, Illinois, and surrounding areas. The tunnels will route the CSO to a flood-control reservoir.

The reservoir will store the CSO until the water can be treated at the Stickney Water Reclamation Plant. The Corps is designing a coarse-bubble aeration system to prevent stratification and anoxic conditions from developing in the reservoir. Submersible mixers, surface mixers, and/or other devices may be required to enhance water movement in the reservoir.

The design of the aeration system will be based on the results of simulations made with the numerical model MAC-3D (Bernard, 1996), developed by the U.S. Army Corps of Engineers, Waterways Experiment Station (WES). MAC-3D is a finite-volume numerical model for three-dimensional incompressible flow, which has been extended to compute the flow produced by bubble aerators (Bernard, 1997).

The U.S. Geological Survey (USGS), in cooperation with the Corps and the Metropolitan Water Reclamation District of Greater Chicago (MWRDGC), conducted pilot-scale tests in a test tank at WES to provide an empirical base for adjustment and validation of the extensions to MAC-3D. The USGS also conducted field-scale tests in a reservoir (Egan Quarry in Schaumburg, Ill.) to determine the mixing patterns associated with different coarse-bubble aerator

configurations that will be compared with mixing patterns simulated with MAC-3D.

## Purpose and Scope

This report describes the test designs, configurations, instrumentation, and methods used in pilot-scale data collection and analysis in September 1995 in a test tank at WES in Vicksburg, Mississippi, and in field-scale data collection and analysis at Egan Quarry, Schaumburg, Illinois, during the summers of 1996 and 1997. Water-mixing patterns were determined by collecting three-dimensional velocity, water temperature, pH, dissolved oxygen concentration, and specific conductivity profiles during operation of combinations of aerators, a submersible mixer, and a surface mixer. Water-velocity and water-quality results for all tests conducted are included in appendix 2 (CD-ROM data base).

## Description of Study Sites

The pilot-scale tests were performed at WES in Vicksburg, Mississippi, in a cylindrical test tank (7.6-m diameter) at two water depths (fig. 1).



**Figure 1.** Test tank at the U.S. Army Corps of Engineers Waterways Experiment Station, Vicksburg, Mississippi.

Field-scale tests were conducted at a former quarry, which has been allowed to fill with water. The present-day reservoir is called Egan Quarry and is adjacent to the John E. Egan Water Reclamation Plant in Schaumburg, Ill. The plant, operated by the MWRDGC, is approximately 50 km northwest of Chicago (fig. 2).

In August 1995, bathymetric data for Egan Quarry were collected by the USGS and used to produce a contour map of the reservoir bottom (fig. 3). Horizontal-position data were collected utilizing a differentially corrected, global positioning system (GPS). Water-depth data were collected with a PTS1000 digital fathometer, or echo sounder, produced by Ocean Data Equipment Corporation. During data collection, the GPS and echo-sounder data were merged in the field with a hydrographic surveying software package (Hypack). The software produced an x, y, z file (x and y are horizontal position, and z is water depth) that was read into a mapping software (Surfer) to produce the contour map.

Egan Quarry has a surface area of approximately 6 ha and a volume of 590,000 m<sup>3</sup>. The bottom of the quarry is relatively level and typically is 13 m deep; however, some areas are as deep as 16.5 m. Ground water is the primary source of flow into the quarry, but a small portion of the total inflow is from storm-water runoff.

## Acknowledgments

The authors thank the Corps (especially Thomas Fogarty, Linda Sorn, Heather Henneman, Jennifer Miller, Lynette Moughton, and Kirston Buczak) for their help and guidance during this project. Calvin Buie, from WES, was an immeasurable asset to the data collection team. His tireless work ethic and enthusiasm, along with his pleasant demeanor, made very long days in the field not only productive but also rather enjoyable.

Richard Lanyon and Larry Walters of MWRDGC provided support at Egan Quarry by coordinating several logistic items. We also thank the city of Schaumburg for allowing use of city right-of-way on the road along the quarry during the data-collection effort.

Professor Miki Hondzo, Purdue University, assisted with some field-scale tests and provided guidance in the determination of the data-collection

sites. He also assisted with the fluorometric and microstructure data collection.

## METHODOLOGY AND EQUIPMENT

### Methodology

A general overview of bubble plumes and their characteristics is presented below in order to help understand the specific methodology used in selecting (1) locations and spacing of aerators, (2) air-flow rates through the aerators, and (3) locations for data collection.

Artificial destratification methods have been used in various forms for about 40 years. Some of these methods have included bubble aerators, mechanical stirrers, and water pumps (Cooke and others, 1986). In bubble aerators, air compressors force air through aerators at the bottom of a lake, then air bubbles are allowed to rise to the surface. As the bubbles rise, ambient water is carried with the bubbles to form a combined bubble and water plume (referred to in this report as the bubble plume). The rising-bubble plume carries deeper (colder and heavier) water until the momentum of the rising plume is no longer sufficient to keep the negatively buoyant water entrained. At this point, the water within the bubble plume is ejected (detrains), whereas the bubbles continue to rise and entrain more water. The detrained water sinks to a level of neutral density and spreads radially away from the bubble plume as an axisymmetric intrusion. In the presence of a density stratification, the buoyant plume may rise only to a terminal height; therefore, this process may be repeated several times as the bubbles rise through the water column (fig. 4, from Schladow and Fischer, 1995). This uplift and subsequent insertion of entrained water into the water column eventually can lead to a significant decrease in the stratification of the water body. The overall goal is sufficiently reduced stratification so that the water body may completely mix under natural phenomena, such as a strong wind, and remain well oxygenated throughout.

The colder and denser water that rises to the surface within the bubble plume propagates outward until the water cannot maintain itself on the surface and sinks to a level of neutral buoyancy at the plunge point. The plunge point is where the radial spreading stalls and separates the “near field” from the “far field” (Hornewer and others, 1997). Zic and others (1992)

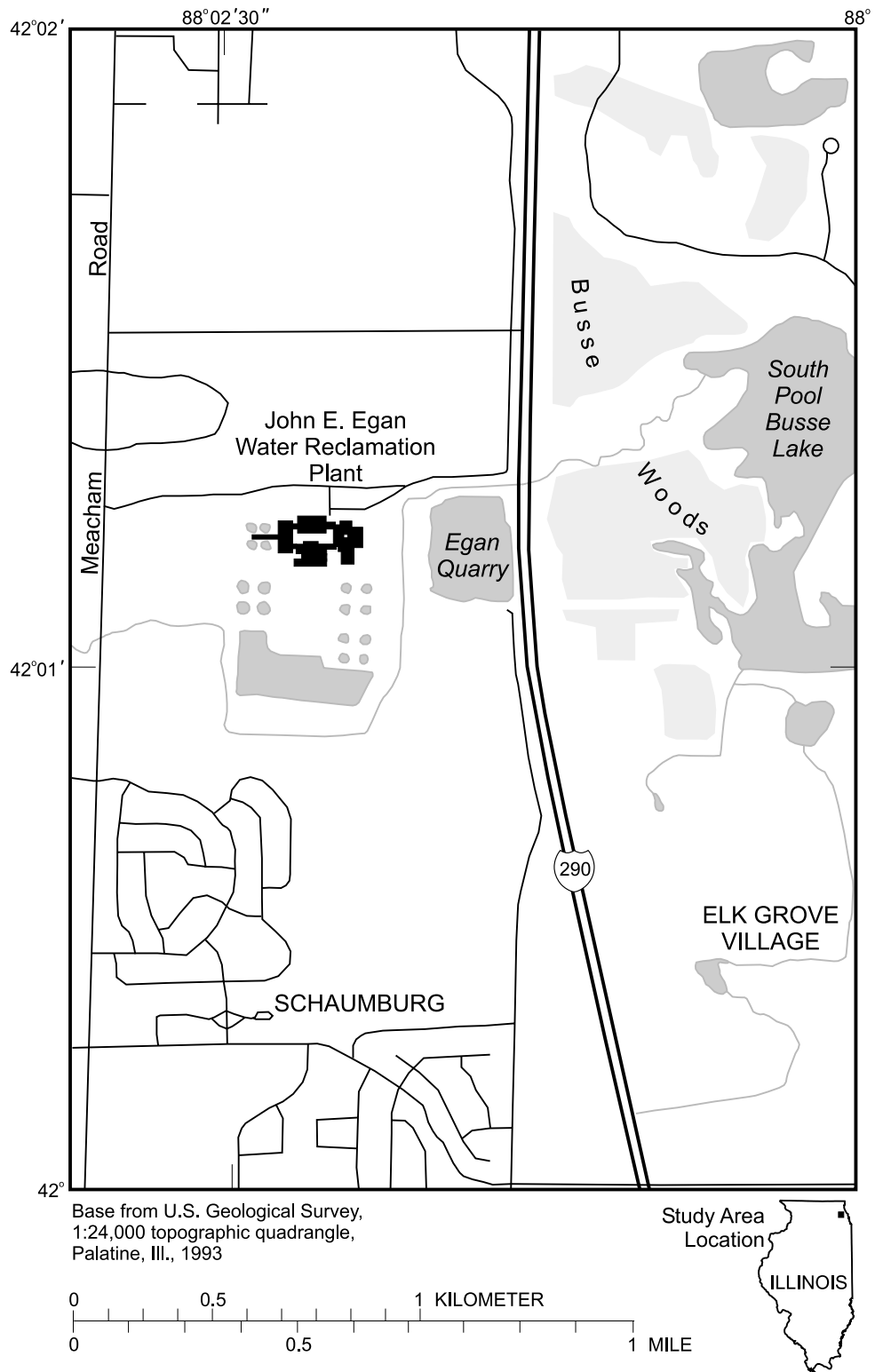


**Figure 2.** Location of Egan Quarry, Schaumburg, Illinois.

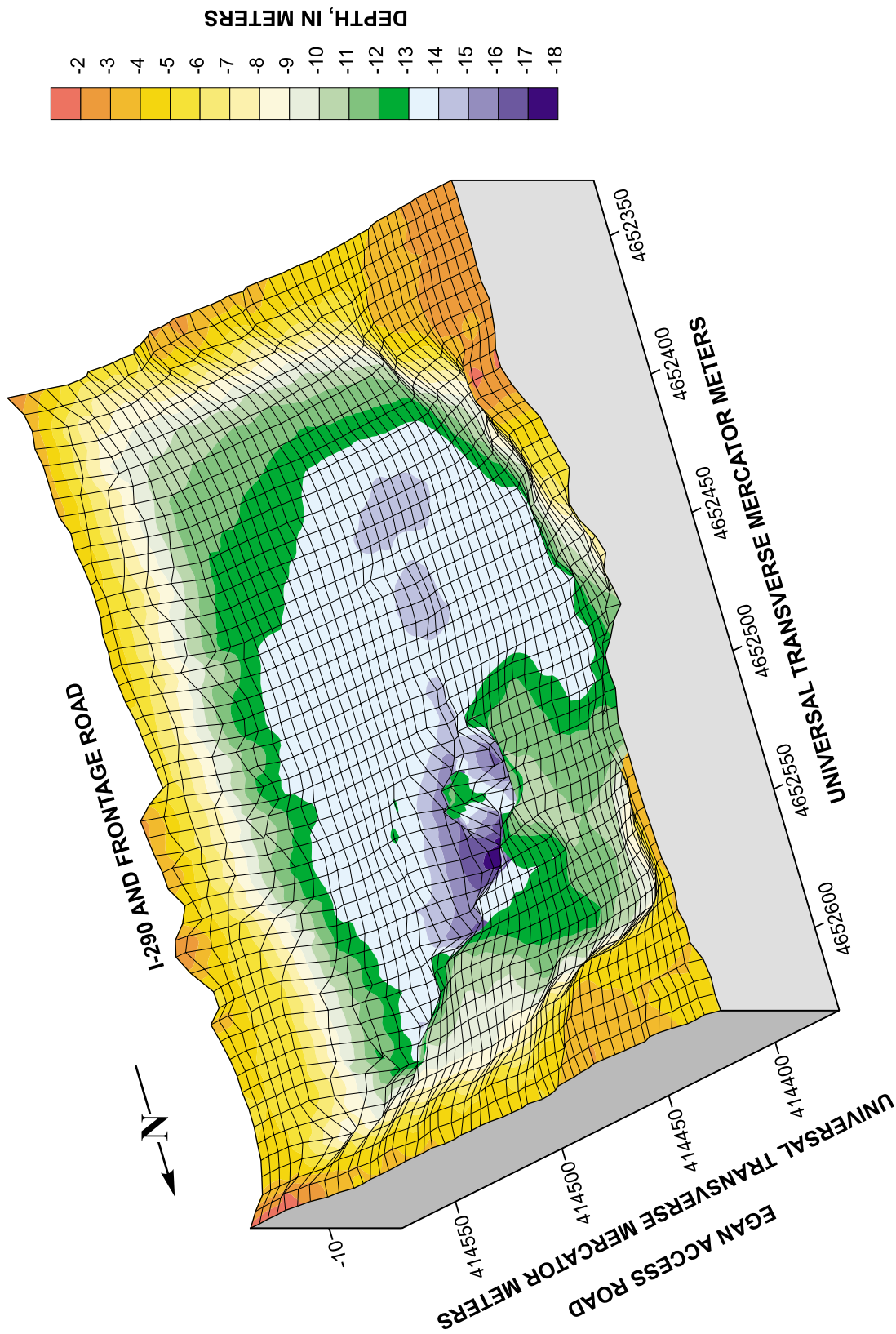
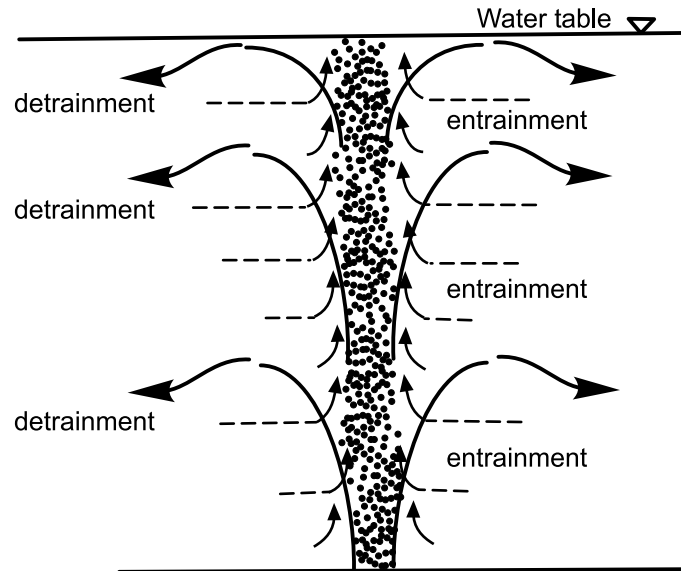


Figure 3. Bathymetry of Egan Quarry, near Schaumburg, Illinois, August 1995.



**Figure 4.** Bubble plume with multiple entrainments and detrainments (from Schladow and Fischer, 1995).

have shown in laboratory experiments that the plunge point remains a relatively fixed distance from the plume, a distance approximately equal to the depth of the water column. However, Lemckert and Imberger (1993) have shown in field experiments that the radial distance of the plunge point increases with increasing air-flow rate and decreasing strength of stratification. Upon reaching this level of neutral buoyancy, the water will continue to spread radially outward in the form of a two-dimensional axisymmetric density intrusion into the far field. Boundary conditions (sides of a reservoir or the walls of a tank) can affect these mixing patterns.

Several field tests were conducted to determine the mixing characteristics and mixing patterns induced by the operation of a single aerator. In these tests, specific bubble-plume characteristics (plume radius, plunge-point radius, and intrusion depth) were measured at different air-flow rates and with various degrees of ambient stratification. These measurements were made because many numerical models simulate these characteristics. Results from multiple-aerator field tests were used to evaluate and characterize more complex bubble-plume interactions and determine if areas were present between the aerators where very little or no mixing occurred. Other field tests were conducted to examine the interactions of closely spaced aerators and/or mixers. Finally, several tests were conducted to measure the effects of the operation of aerators placed far enough apart resulting in no interaction

between the rising-bubble plumes. The locations and distance between the aerators are described and presented in the “Data Collection” section of this report.

In determining the locations of the aerators, as well as deciding where to collect data, all factors discussed above were taken into consideration. A numerical bubble-plume model developed by Schladow (1992) and empirical relations developed by Lemckert and Imberger (1993) were used with ambient conditions in the quarry to obtain a first estimate of the size of the bubble plume, plume radius, plunge-point radius, intrusion depth, and the extent of possible interactions among adjacent plumes. Schladow’s model is described in more detail later in this report.

Generally, water-velocity, water-temperature, and water-quality data were collected in three areas: the near field [the area directly affected by the rising-bubble plume(s)], the plunge point [area where denser water sinks to a level of neutral buoyancy], and the far field [the area not immediately or directly affected by the vertical component of the bubble plume(s), approximately 30 m away from the nearest aerator]. Sampling locations were chosen at various distances from the aerator(s) and between the aerators to better describe the characteristics and mixing patterns induced by the bubble plumes and interactions among bubble plumes.

A map of the quarry for each test is provided in appendix 1 and on the CD-ROM. The locations of the aerators and/or mixers and all sampling locations are indicated on the maps. The map also illustrates the locations of the metal-cable tag lines that were used to stabilize the docks and boats used during data collection.

## Aerators and Mixers

### Aerators

A fine-bubble aerator was used during the tank tests at WES. This aerator, produced by Wilfley Weber, Inc., Denver Colorado, is a circular diffuser (22.9 cm in diameter) with a rubber surface that has tiny holes (fig. 5). The tiny holes allow air to be released in fine bubbles. The fine-bubble aerator was mounted approximately 0.6 m above the bottom of the tank.

A coarse-bubble aerator also was used during the tank tests at WES and the only type of aerator used at the Egan Quarry tests. The stainless-steel aerator, produced by Aercor, Worcester, Massachusetts, was approximately 0.6 m long and was the same type proposed for use in the final CUP/TARP design. The aerators were mounted on metal frames with 0.6-m legs, which rested on the tank and quarry bottoms (fig. 6). Therefore, the aerators were approximately 0.6 m above the bottom of the tank and quarry. In the quarry tests, all aerators were positioned at least 75 m from the edge of the quarry.

An air compressor/manifold system was designed and used to force air to the aerators. Two diesel powered 175 cubic feet per minute (4.955 m<sup>3</sup>/min) air compressors were used as the air source. The manifold system (fig. 7) dewatered and de-oiled the compressed air. Rotometers and pressure gages were used to allow accurate computation of the air flow delivered to each aerator.



**Figure 5.** Fine-bubble and coarse-bubble aerators used during the tank tests at the U.S. Army Corps of Engineers, Waterways Experiment Station, Vicksburg, Mississippi.



**Figure 6.** Coarse-bubble aerator and frame used during tests in Egan Quarry, Schaumburg, Illinois.

### **Submersible Mixer**

Submersible mixers and/or surface mixers may be used in the final CUP/TARP design. The submersible mixer used in Egan Quarry was a 4-hp direct drive, multipole motor (Flygt 4640.410). The mixer was approximately 0.61 m long and 0.51 m high with a 0.36-m diameter propeller and weighed approximately 63 kg without the mount. The motor operated on 3-phase, 460 V at approximately 860 revolutions per minute.

A mount for the submersible mixer was designed and built using standard 2-in. metal pipe to hold the mixer approximately 1.8 m above the quarry bottom. The mount also allowed the mixer to be positioned parallel to, perpendicular to, and at 45° to the quarry bottom and in different directions (fig. 8). Scuba divers positioned the mixer on the bottom of the quarry and pointed the mixer in the desired direction or angle.

### **Surface Mixer**

The effects from the operation of a surface mixer also were measured at the quarry. The surface mixer, manufactured by Aeromix Systems, Inc., Minneapolis, Minnesota, was equipped with a 100-hp electric motor, a shaft enclosed in an outer sheath, and a stainless-steel boat propeller (fig. 9). The surface-mixer assembly floated on pontoons, which were held in place by mooring lines to shore. On shore, a 460-V generator powered the motor. The propeller was angled at 45 degrees from horizontal and was approximately 0.5 m below the surface while the mixer was operating.

### **Velocity Measurements**

#### **Acoustic Doppler Velocimeter**

An Acoustic Doppler Velocimeter (ADV) was used at WES and Egan Quarry to measure



**Figure 7.** Air compressor/manifold system used to deliver compressed air to aerators.

water velocities. The ADV, manufactured by Sontek Company, San Diego, California, is an instrument that measures three-dimensional water velocities with a 10-MHz acoustic signal to measure flow in a  $0.25 \text{ cm}^3$  sampling point. Measurements are made at 25 Hz, at velocities of plus or minus 2.5 m/s, and at a velocity resolution of 0.1 mm/s (Sontek, 1994). Because the ADV measures velocity at a point, the ADV must be placed at several different depths to collect a complete profile of water velocities (from top to bottom in the water column).

The ADV used in this study was equipped with an internal compass and tilt/roll sensor (fig. 10). These devices were not used in the tank tests because the steel tank caused magnetic interference. Without these devices, water velocities were measured relative to the ADV probe and reported in terms of x, y, and z directions. Therefore, the probe must not move during

measurement. The compass and tilt/roll sensor were used in the Egan Quarry tests; thus, velocities were reported in terms of east, north, and up.

For the tank tests, a mount was designed and built that allowed the ADV to be moved radially and vertically in the tank. The mount also allowed the ADV to be oriented so that the probe tip (where the water velocity was measured) was measuring undisturbed flow. This mount also held the ADV stable during measurements. Thus, reliable three-dimensional water velocities could be measured at different radial distances and water depths in the tank.

For the Egan Quarry tests, the ADV was lowered from the boat to the desired measurement depth on a moored cable. The boat could move to different positions in the quarry. Thus, three-dimensional water-velocity measurements could be taken anywhere in the quarry.

A



B



**Figure 8.** Submersible mixer (A) and mount (B) used during tests in Egan Quarry, Schaumburg, Illinois.



**Figure 9.** Surface mixer operating in Egan Quarry, Schaumburg, Illinois.

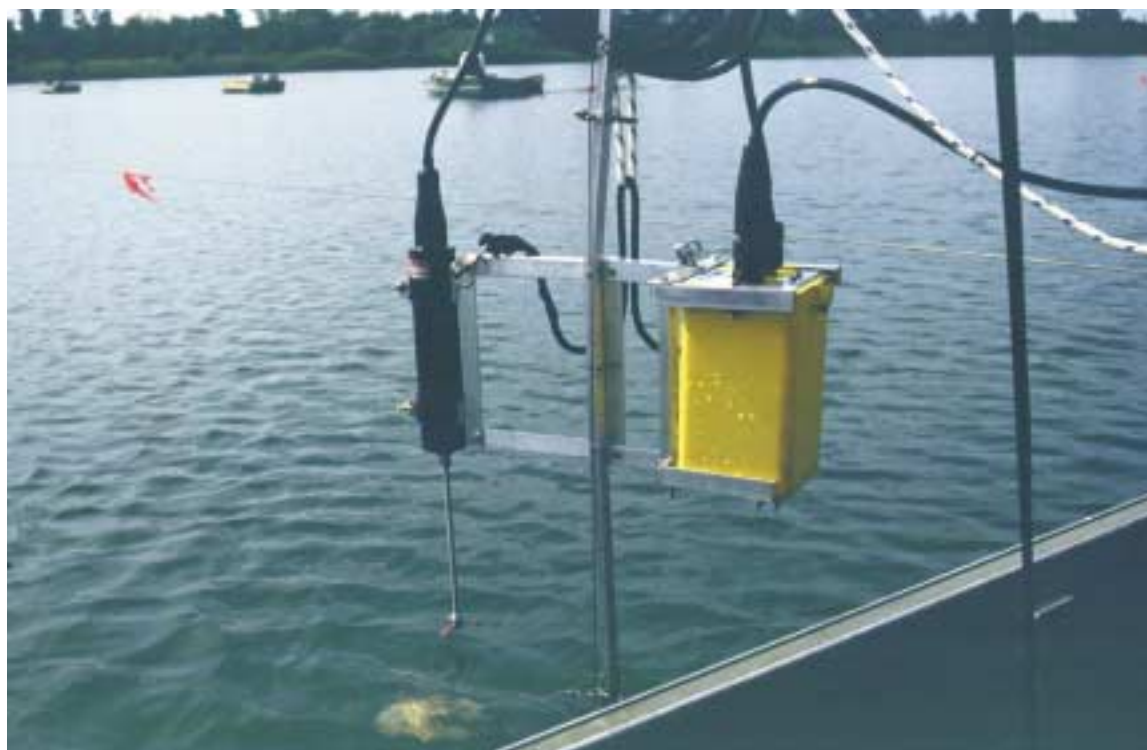


**Figure 10.** Acoustic Doppler Velocimeter and mount used during tests in Egan Quarry, Schaumburg, Illinois.

## Acoustic Doppler Current Profiler

An Acoustic Doppler Current Profiler (ADCP), manufactured by RD Instruments, San Diego, California, also was used in the tests at Egan Quarry to measure three-dimensional water velocities. Similar to the ADV, a 1200-kHz acoustic signal (other frequencies are available) was used by the ADCP to measure velocities. The ADV measures a point velocity; however, the ADCP measures water velocities throughout the water column. The ADCP measures velocities from the transducer head to a specified depth and divides this depth into uniform segments called depth cells. The collection of depth cells yields a profile of the velocities in the water column (RD Instruments, 1995). The ADCP was mounted on a boat (fig. 11), and the boat was moved to different locations in the quarry. The ADCP was used in the far field, supplementing the ADV data to obtain more frequent velocity profiles.

## Water-Quality Measurements

### Instruments

Multiparameter water-quality-monitoring instruments, manufactured by Hydrolab Corporation, Austin, Texas, were used during the Egan Quarry tests (fig. 12). Hydrolab H20's were used to measure the field parameters pH, specific conductance, water temperature, and dissolved oxygen (DO) in the quarry before, during, and after the tests. The instruments were calibrated before each test and checked after each test to ensure no calibration drift. A thermistor in the instrument was used to measure temperature, with a range of  $-5$  to  $50^{\circ}\text{C}$  and an accuracy of plus or minus  $0.15^{\circ}\text{C}$ . Specific conductance was measured by a 6-electrode cell, with a range of 0 to 100 mS/cm and an accuracy of plus or minus 1 percent of the range. A glass pH probe was used to measure pH, with a range from 0 to 14 units and an accuracy of plus or minus 0.2 units. Finally, the



**Figure 11.** Acoustic Doppler Current Profiler and mount used during tests in Egan Quarry, Schaumburg, Illinois.

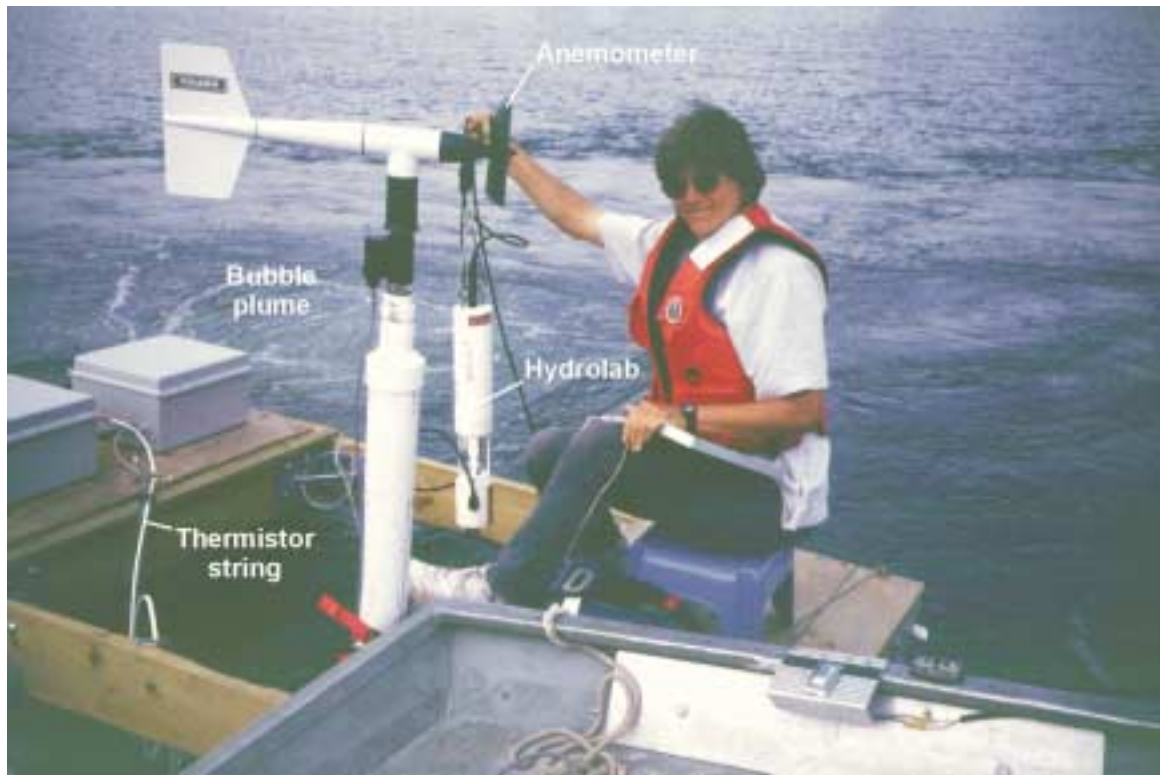


**Figure 12.** Water-quality-monitoring equipment and floating dock used during tests in Egan Quarry, Schaumburg, Illinois.

Hydrolab DO sensor had a range of 0 to 20 mg/L, with an accuracy of plus or minus 0.2 mg/L (Hydrolab, 1991).

To provide supportive evidence for the mixing patterns measured by the ADV, the field parameters were simultaneously measured at several locations during all field tests. Typically, field parameters were manually recorded at 0.5-m depth intervals in the water column.

### **Docks, Thermistor Strings, and Anemometer**

Three floating docks were constructed and positioned in different locations in Egan Quarry during the tests. The docks were used as floating data-collection platforms and for field personnel to collect water-quality data using Hydrolabs. The three docks were designated red, yellow, and green for clarity, throughout the quarry tests. Each dock held a thermistor string (white cord in bottom left of fig. 12) and electronic instruments to collect and store continuous water-temperature data. Each thermistor string had a total of 25 thermistors, spaced every 0.58 m and used to measure the water-temperature profile at each dock.

The thermistor strings were suspended vertically from each dock and anchored on the bottom of the quarry. Each thermistor string was connected to a Campbell Scientific CR-10 Datalogger sheltered in an all-weather Hoffman Box. The dataloggers collected and averaged water-temperature data. In addition, one thermistor was placed just above the water surface at each dock to measure air temperature. One dock (the red dock) was equipped with an anemometer placed 1 m above the water surface to measure wind speed and direction at the quarry (fig. 12). During each test, temperatures were measured every 2 seconds and averaged over each minute. Hourly average data also were recorded between some tests.

### **Microprofiler**

A portable, self-propelled microprofiler that records water temperature, conductivity, and pressure (for depth) also was used during some tests in the quarry (fig. 13). The Precision Measurement Engineering microprofiler was used to characterize the nature of turbulence within the plunging region and the axisymmetric intrusion. Upon deployment, the microprofiler



**Figure 13.** Microprofiler used in water-quality measurements during tests in Egan Quarry, Schaumburg, Illinois.

descended through the water at a 45° angle to a depth of approximately 12.5 m. After 5 minutes, the microprofiler ascended vertically to the water surface at a rate of approximately 0.1 m/s, recording water-quality parameters at a frequency of 100 Hz.

### Fluorometer and Dye

During one test in the quarry (single aerator during strong stratification), Rhodamine WT20 dye was injected into the rising-bubble plume at the aerator to characterize the axisymmetric intrusion. A Turner flow-through fluorometer (fig. 14) was used from a boat

to locate and track the dye movement. Dye concentration data were used to estimate the depth, thickness, and velocity of the axisymmetric current that propagated horizontally from the bubble plume. These data are characteristics that can be simulated in some numerical models.

## DATA COLLECTION

### Tank Tests

In September 1995, six sets of tests were conducted in the WES test tank. Each test used unique air-flow rates at one of two different water depths and with either the fine- or coarse-bubble aerators. Both aerators were mounted at the center of the tank, 0.6 m above the tank bottom. For each test, water-velocity profiles were measured at 3 to 5 radial distances in the tank. Data were collected at 1 Hz, with about 3 minutes of data at each point in the profiles. For the deep water tank tests, velocity data were collected near the surface and at depths of every 0.6 to 0.9 m to the bottom. For the shallow water tests, data were collected at every 0.3 m of depth.

Data files were named to describe the data collection conditions by the file name (depth of water in the tank, which aerator was operated, the air-flow rate through the aerator, the distance of the ADV from the center of the tank, and the depth of the ADV in the tank).

The first character in the file names represented the depth of water in the tank: A for a water depth of 9.54 m and B is for a water depth of 3.05 m. The second character represented whether the coarse-bubble (represented by the letter L) or fine-bubble aerator (represented by the letter S) was used. The third character (shown in table 1) represented the air-flow rate in standard cubic meters per second (SCMS) through the aerators.

The fourth character in the file names represented the radial distance [in feet (ft)] of the ADV outward from the center of the tank (A=1 ft, B=2 ft, ..., K=11 ft, L=12 ft). For example, if the letter B is the fourth character of the file name, the ADV was 2 ft from the center of the tank. The fifth and sixth characters in the file names were a two-digit number representing the depth of the ADV from the surface. For example, if "17" is in

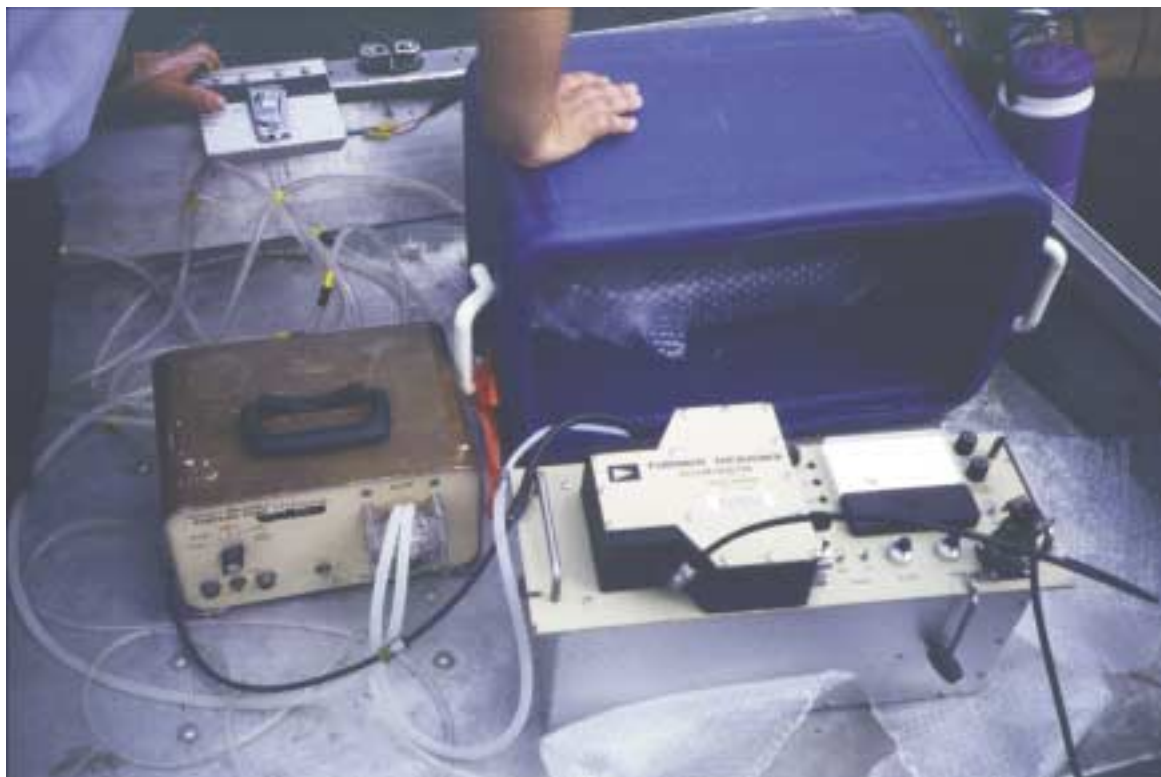


**Figure 14.** Turner flow-through fluorometer used to track the dye movement in the axisymmetric intrusion during tests in Egan Quarry, Schaumburg, Illinois.

**Table 1.** Air-flow rate and corresponding letter designation in data file names for tank tests, Waterways Experiment Station

File name letter designation	Air-flow rate, (standard cubic meters per second)
A	$5.7 \times 10^{-4}$
B	$3.1 \times 10^{-3}$
C	$6.5 \times 10^{-3}$
D	$1.4 \times 10^{-2}$
E	$1.7 \times 10^{-2}$
F	$4.2 \times 10^{-4}$

the fifth and sixth characters of the file name, then the ADV was 17 ft below the surface. Finally, the seventh character represented the orientation of the probe during the data collection. This orientation has already been used in resolving all files to a common reference.

### Egan Quarry Tests (1996 and 1997)

Two sets of five aerator tests were conducted at Egan Quarry during summer 1996 (table 2) and summer 1997 (table 3). Each year, the first set of tests were done when water in the quarry was strongly stratified, and the second set was done when water in the quarry was weakly stratified. Bubble plumes (stream of air bubbles and entrained water) react differently depending upon the relative degree of stratification; thus, weakly and strongly stratified conditions were examined. Additionally, a submersible mixer was operated during 8 of the 10 aerator tests in 1997. Finally, three tests during operation of a surface mixer were conducted during summer 1997. Maps of the quarry showing the data-collection positions and locations of aerators and mixers are included in appendix 1.

Prior to delivering air to the aerators and/or power to the mixers at the beginning of a test, a set of velocity and water-quality data was collected to establish initial conditions in the quarry. After documenting initial conditions, the compressors were turned on, allowing air to flow to the aerators. During each test, the air flow was adjusted and allowed to

**Table 2.** Summary of test configurations during summer 1996 listed in order of performance, Egan Quarry, Illinois  
 [NE, northeast; NW, northwest; SE, southeast; SW, southwest; -, not applicable; volumetric flow rate is cubic meters per second, adjusted for pressure at the aerator]

Date	Test identifier	Quarry condition	Number of aerators	Which aerators and flow rate				Aerator spacing (in meters)	Approximate number of hours aerators operated
				NE	NW	SE	SW		
<b>Initial strongly stratified conditions in the quarry</b>									
August 22, 1996	eg961s	Stratified	1	-	0.003	-	-	-	2
August 23, 1996	eg963s	Stratified	2	0.022	.022	-	-	4.6	2.5
August 24, 1996	-	Stratified	0	-	-	-	-	-	-
August 25, 1996	-	Stratified	0	-	-	-	-	-	-
August 26, 1996	eg964s	Stratified	2	.022	.022	-	-	12.2	3.8
August 27, 1996	eg962s (a.m.)	Stratified	1	-	.022	-	-	-	4
August 27, 1996	eg962s (p.m.)	Stratified	1	-	.011	-	-	-	2.8
August 28, 1996	eg965s	Stratified	4	.022	.022	0.022	0.022	12.2 by 19.8	4.5
<b>Break up began, aerators were operated for 5 days, approximately 8 hours per day, to destratify the quarry</b>									
August 29, 1996	-	Break up	4	0.022	0.022	0.022	0.022	12.2 by 19.8	8
August 30, 1996	-	Break up	4	.022	.022	.022	.022	12.2 by 19.8	11
August 31, 1996	-	Break up	4	.022	.022	.022	.022	12.2 by 19.8	10
September 1, 1996	-	Break up	4	.022	.022	.022	.022	12.2 by 19.8	8.5
September 2, 1996	-	Break up	4	.022	.022	.022	.022	12.2 by 19.8	9
September 3, 1996	-	Break up	4	.022	.022	.022	.022	12.2 by 19.8	1.5
<b>Weakly stratified conditions in the quarry</b>									
September 3, 1996	eg961d	Destratified	4	0.022	0.022	0.022	0.022	12.2 by 19.8	4
September 4, 1996	eg962d	Destratified	2	.022	.022	-	-	12.2	4
September 5, 1996	eg963d	Destratified	1	-	.012	-	-	-	3.5
September 5, 1996	eg964d	Destratified	1	-	.022	-	-	-	3
September 6, 1996	eg965d	Destratified	2	.022	.022	-	-	4.6	3.5

stabilize approximately 20 minutes before measurements were taken. The number of measurement locations increased as the number of aerators increased. When multiple aerators were tested, only one test per day was done, allowing the aerator-induced mixing patterns to diminish in the quarry between tests. The compressors were shut off between tests.

During the operation of the aerator(s), the thermistor strings collected water-temperature profiles every 2 seconds, but minute-averaged data were recorded. The locations for the thermistor strings were chosen on the basis of preliminary model simulations and generally were in the zone of substantial upward velocity (near field), just beyond the plunge point of the entrained plume, and in the far field. The far field represents the area at a distance from the aerator where the water extruded from the plume should reach an equilibrium depth. During the tests, some thermistors may have given erroneous data because of fouling or malfunction. When compared with the good thermistor data, these erroneous data are obvious; therefore, all data are provided in appendix 2.

Throughout each test, a boat with the ADV traveled to different locations in the quarry to collect velocity data that was used to define the mixing patterns induced by the aerators and mixers. Using the ADV, a complete velocity profile was collected at each location before moving to a new location. At each data-collection location, ADV velocity measurements were collected at 1 Hz, typically in 1-m increments throughout the water column. Water velocities were measured in 0.5-m increments in the area of the surface in the near field and in the area of the detrained plume. Approximately 1 minute of data were collected at each point. To view the ADCP data collected during the tests, proprietary software is needed from the manufacturer. Therefore, the ADCP data are not included in appendix 2 but are available upon request.

To help define the mixing patterns, water temperature, pH, specific conductivity, and DO profiles also were collected using Hydrolabs at each dock location and a few additional locations. Measurements were made at the surface and then every 0.5 m to the bottom. The water-quality instruments were held at each depth

**Table 3.** Summary of test configurations during summer 1997 listed in order of performance, Egan Quarry, Illinois [NE, northeast; NW, northwest; SE, southeast; SW, southwest; -, not applicable]

Date	Test identifier	Quarry stratified	Number of aerators	Which aerators and flow rate				Aerator spacing (in meters)	Mixer	Mixer, position relative to aerators	Mixer, position relative to quarry bottom	Mixer, direction pointed
				NE	NW	SE	SW					
<b>Initial strongly stratified conditions in the quarry</b>												
June 3, 1997	eg971s	Yes	1	0.022	-	-	-	No	-	-	-	
June 4, 1997	eg972s	Yes	4	.022	0.022	0.022	19.8 by 27.2	No	-	-	-	
June 10, 1997	eg973s	Yes	0	-	-	-	-	Submersible	Center of all 4	Parallel	Due west	
June 11, 1997 (a.m.)	eg974s	Yes	0	-	-	-	-	Submersible	Center of all 4	Directly up	Toward water surface	
June 11, 1997 (p.m.)	eg975s	Yes	4	.022	.022	.022	19.8 by 27.2	Submersible	Center of all 4	Directly up	Toward water surface	
<b>Break up began, aerators were operated for 4 days, approximately 8 hours per day, to destratify the quarry</b>												
June 12, 1997	-	Break up	4	0.022	0.022	0.022	19.8 by 27.2	-	-	-	-	
June 13, 1997	-	Break up	4	.022	.022	.022	19.8 by 27.2	-	-	-	-	
June 14, 1997	-	Break up	4	.022	.022	.022	19.8 by 27.2	-	-	-	-	
June 15, 1997	-	Break up	4	.022	.022	.022	19.8 by 27.2	-	-	-	-	
<b>Weakly stratified conditions in the quarry</b>												
June 16, 1997	eg971d	No	4	0.022	0.022	0.022	19.8 by 27.2	Submersible	Center of all 4 aerators	Directly up	Toward water surface	
June 17, 1997	eg972d	No	4	.022	.022	.022	19.8 by 27.2	Submersible	Between NE and NW aerators	45° toward surface	Due south	
June 18, 1997	eg973d	No	4	.022	.022	.022	19.8 by 27.2	Submersible	Between NE and NW aerators	45° toward surface	Toward SW aerator	
June 19, 1997 (a.m.)	eg974d	No	4	.022	.022	.022	19.8 by 27.2	Submersible	Between NE and NW aerators	Parallel	Due south	
June 19, 1997 (p.m.)	eg975d	No	4	.022	.022	.022	19.8 by 27.2	Submersible	Between NE and NW aerators	Parallel	Toward SW aerator	
<b>Aerators removed, and surface mixer installed</b>												
July 10, 1997	SM1	Moderate	0	-	-	-	-	Surface	-	45° toward bottom	Due east	
July 11, 1997	SM2	Moderate	0	-	-	-	-	Surface	-	45° toward bottom	Due east	
July 24, 1997	SM3	Moderate	0	-	-	-	-	Surface	-	45° toward bottom	Due east	

until the readings stabilized, generally after 1 minute.

Aerator spacing and air-flow rates for the various tests were based on operational restrictions for cleaning and maintenance of the flood-storage reservoir that might ultimately be used in the final CUP/TARP project and preliminary modeling results. These results indicated different degrees of bubble-plume interaction. An air-flow rate of 0.022 m<sup>3</sup>/s was sufficient for the bubble plumes to reach the water surface at Egan Quarry before detrainment and is comparable with the air-flow rate planned for the final CUP/TARP reservoir design. The test configurations using lower air-flow rates [test eg962s(a.m.) and eg963d during 1996] were done to approximate hydrodynamic conditions for a reservoir significantly deeper than Egan Quarry.

During the 1996 tests, single-aerator tests [eg962s(a.m.), eg962s(p.m.), eg963d, and eg964d] were done to examine specific plume characteristics (plume radius, surface-plunge point, volumetric flow rate of the intrusions, the net entrainment, and intrusion depth) at two flow rates. These characteristics were examined because many available numerical models can be applied to simulate these characteristics. Multiple-aerator tests were used to evaluate and characterize more complex bubble-plume interactions.

## Raw Data

The data from all tests described in this report are presented in appendix 2, a relational data base (Microsoft Access, version 2000) format on a CD-ROM included with this report. Working knowledge of how to use Microsoft Access would help the user to retrieve data from the CD-ROM but is not absolutely necessary. A separate README file that describes how the files can be queried is included on the CD-ROM. The README file also presents limitations of the data and explains issues that possibly may cause confusion to users. The data also are available by contacting the U.S. Geological Survey at the address at the front of this report.

## ANALYSIS OF DATA

### Tank Tests

The file names for the velocity data collected in each of the six tank tests and the processed data are given in tables 4–9. (The raw data are available on the CD-ROM included with this report or by contacting the USGS, Water Resources Division Office, in Urbana, Illinois.) The processed velocity data are resultant velocity vectors (direction and magnitude) for each location in the tank where velocity measurements were collected. The resultant velocity-vector magnitude was computed as a combination of only the x and y vectors shown in figure 15 because although the z vector may be present, it adds little information to the understanding of the general mixing patterns because the aerator was placed in the center of the circular tank. Therefore, the resultant vector and plane it represents are only two-dimensional. The direction of the vectors are referenced such that 0° represents water moving radially outward from the center of the tank, 90° represents water moving directly upward, and so on.

The resultant two-dimensional velocity vectors for each test are plotted in figures 16–21 to demonstrate the mixing patterns induced by the rising-bubble plumes. In each figure, the mixing patterns demonstrated on the shaded plane is expected to be similar throughout the tank because the tank was circular and the aerator was placed directly in the middle of the tank. Each test demonstrated the same general mixing pattern, although the pattern is best seen in figures 20 and 21. The general mixing pattern was an upward movement in the center of the tank associated with the rising bubbles, outward movement at the surface, downward movement very near the wall of the tank, and inward movement in the lower one-half of the tank. This mixing pattern was strongly affected by the walls of the tank acting as a boundary condition. The rising water, indicated by upward velocities, expanded radially with the distance from the bottom. This result indicates the rising-bubble plume entrained adjacent water that in turn entrained water over a larger area; therefore, the rising plume expanded as it passed through the water column.

The primary difference in mixing patterns among the tests was caused by the air-flow rate and the depth of the water in the tank. The higher the air-flow rate, the faster the velocities measured in the tank. This result is best seen in comparing figure 20 (air-flow rate of

**Table 4.** Summary table of tank test ASA, Waterways Experiment Station, Vicksburg, Miss.

File name	Magnitude	Direction	Z vector
ASAH01D	3.0867	10.6580	-2.0433
ASAH04D	2.4985	54.5430	.8451
ASAH07D	4.5942	78.6923	1.2204
ASAH10D	2.0575	135.2604	-.0191
ASAH13D	1.8127	49.6312	2.9539
ASAH16D	1.5363	38.7134	-.6336
ASAH19D	1.9463	-178.9932	-.7339
ASAH22D	.5703	-100.2836	1.7042
ASAH25D	1.1386	16.7103	-1.0911
ASAH28D	1.4819	-23.9278	1.0450
ASAK01L	3.7716	6.0188	.9473
ASAK04L	2.7353	38.1243	-.2126
ASAK07L	1.1434	-71.3191	2.3694
ASAK10L	1.0070	-98.7376	-1.3826
ASAK13L	2.3359	118.1119	.6115
ASAK16L	1.4282	133.6619	-.6077
ASAK19L	2.5866	-130.5735	.6939
ASAK22L	.7138	-107.5112	.5148
ASAK25L	.7567	-119.3666	1.3924
ASAK27L	1.5471	-101.6903	-.4096
ASAF01D	4.3652	19.5947	.3529
ASAF04D	3.6775	64.2177	-.6128
ASAF07D	4.6961	66.3253	.3261
ASAF10D	4.4300	102.4978	.6217
ASAF13D	2.2043	96.8026	.8486
ASAF16D	2.8828	142.8088	1.9010
ASAF19D	1.6695	148.4024	-.4404
ASAF22D	.8212	62.7282	-2.3286
ASAF25D	.8728	57.0281	.6512
ASAF28D	.8812	-19.3979	-.0567
ASAD01D	8.4362	60.2228	-1.1117
ASAD04D	7.1064	82.6704	.2714
ASAD07D	8.8330	91.6173	.3184
ASAD10D	6.3924	80.1335	2.1167
ASAD13D	4.5013	89.0119	2.1795
ASAD16D	4.9427	86.1544	3.1474
ASAD19D	2.3587	143.7635	-.1948
ASAD22D	1.2660	159.8614	-.4678
ASAD25D	1.3346	124.0870	-.8131
ASAB01R	15.2185	79.4479	-4.5725
ASAB04R	18.5054	90.2060	-.0296
ASAB07R	15.7309	97.1556	-2.7080
ASAB10R	25.2178	91.1226	-1.5720
ASAB13R	28.6883	90.8069	-.5197
ASAB16R	38.6421	89.7168	-1.2538
ASAB22R	38.5428	92.7217	-1.5286
ASAB25R	1.5479	62.3052	3.0074
ASAC00U	11.9150	2.3509	-7.5667
ASAE00U	8.3782	-4.7865	-2.5131
ASAG00U	8.4999	-6.4069	-.6897
ASAI00U	18.2448	-3.9254	.3910

**Table 5.** Summary table of tank test ASB, Waterways Experiment Station, Vicksburg, Miss.

File name	Magnitude	Direction	Y vector
ASBJ01L	5.4674	8.3274	-2.2127
ASBJ04L	2.2196	-14.3854	4.0599
ASBJ07L	.9180	-28.0427	-4.0378
ASBJ10L	1.5510	-72.5035	.5615
ASBJ13L	4.0001	-139.6619	1.2692
ASBJ16L	2.6508	-144.8324	1.5018
ASBJ19L	1.9211	-127.5653	-2.2963
ASBJ22L	1.9131	-96.2322	1.4822
ASBI01D	7.3342	6.8328	-1.1964
ASBI04D	4.7724	44.8040	-.5576
ASBI07D	5.8228	63.7656	3.4301
ASBI10D	5.6698	64.2817	-.6490
ASBI13D	3.7988	88.1002	-.0223
ASBI16D	5.4102	-173.7433	1.2320
ASBI19D	4.3850	-150.0319	-4.2969
ASBI22D	3.2055	-140.1351	1.8735
ASBI25D	1.2192	-22.3638	-1.2612
ASBE01D	11.0994	9.7834	-.8099
ASBE04D	7.4998	74.0656	.5190
ASBE07D	6.0048	93.2351	1.8605
ASBE10D	8.8761	78.7491	.8589
ASBE16D	3.8653	120.6200	-1.2564
ASBE22D	1.4678	156.6125	-1.7123
ASBE27D	1.7680	-48.6778	-.2638
ASBC01R	13.9132	36.0662	-4.6339
ASBC07R	17.6482	79.6123	2.3742
ASBC15R	7.0033	105.7183	-.3157
ASBC25R	.7709	-20.4468	1.1585
ASBL01L	4.8054	-64.1817	-1.5680
ASBL04L	9.1947	-86.4486	-.5205
ASBL07L	9.9060	-93.5797	-2.4651
ASBL12L	12.0855	-92.9979	-.4749
ASBL17L	1.6770	-101.6935	-3.4288
ASBL24L	.4193	55.1893	-.9307

**Table 6.** Summary table of tank test ALC, Waterways Experiment Station, Vicksburg, Miss.

File name	Magnitude	Direction	Y vector
ALCK01L	7.6951	6.7944	2.2832
ALCK04L	2.6084	-5.5467	.5977
ALCK07L	3.3634	-58.1721	-1.0602
ALCK10L	5.3392	-96.2933	4.9562
ALCK13L	9.5854	-100.6682	3.2642
ALCK16L	10.7765	-118.6733	-3.3841
ALCK19L	6.5552	-107.1712	-3.0737
ALCK22L	.6888	-72.1650	.9021
ALCK25L	4.7930	99.7691	1.3552
ALCH01D	21.8875	19.1280	4.9570
ALCH04D	5.7503	52.8021	1.6222
ALCH07D	10.4426	44.2788	1.0163
ALCH10D	3.4505	101.3197	3.6047
ALCH13D	7.1198	177.3895	3.6261
ALCH16D	5.7995	136.9008	1.8042
ALCH19D	2.4808	160.3513	.1577
ALCH22D	1.2468	166.7316	.8362
ALCH25D	.2867	130.3231	4.3988
ALCF01D	22.4954	22.9705	-.6462
ALCF04D	15.1467	68.4321	1.5591
ALCF07D	16.1885	69.1203	.4091
ALCF10D	9.7376	61.5134	-1.7448
ALCF13D	12.5375	62.4172	-.2656
ALCF16D	7.7049	86.9817	1.5543
ALCF19D	3.7336	149.6809	-.9341
ALCF22D	2.4357	111.7580	-.3652
ALCI01D	19.0922	8.1248	-.9717
ALCI04D	6.8919	54.0502	-2.3419
ALCI07D	7.5966	54.6142	1.1149
ALCI10D	6.0518	48.2155	2.8444
ALCI13D	6.6842	65.0198	2.8727
ALCI16D	8.8996	66.5549	4.0277
ALCI19D	7.9528	-171.9712	.7177
ALCI22D	2.4428	65.0103	-.8144
ALCI25D	5.5100	-130.8690	-.9136

$1.7 \times 10^{-2}$  SCMS) and figure 21 (air-flow rate of  $4.2 \times 10^{-4}$  SCMS).

## Egan Quarry Tests (1996)

### Single-Aerator Tests

In Egan Quarry, five tests were completed to determine mixing patterns induced by a single aerator. In 1996, three of these tests were conducted when strong stratification was present [air-flow rates of 0.003 SCMS (eg961s), 0.022 SCMS [eg962s (a.m.)] and 0.011 SCMS [eg962s (p.m.)]. Similar tests were

conducted in 1996 when the quarry was more weakly stratified [air-flow rates of 0.022 SCMS (eg964d) and 0.012 SCMS (eg963d)]. In all tests, the air flow was sufficient for the rising-bubble plume to reach the surface prior to detraining.

### Strongly Stratified Conditions

The typical mixing pattern induced by a bubble plume reaching the surface prior to detraining (described by Lemckert and Imberger, 1993) was observed during all single-aerator tests under strongly stratified conditions. To demonstrate the mixing characteristics (velocity field, plunge point, and intrusion

**Table 7.** Summary table of tank test ALD, Waterways Experiment Station, Vicksburg, Miss.

File name	Magnitude	Direction	Y vector
ALDI01D	26.7637	8.0147	-7.2123
ALDI02D	9.4394	2.1253	-.2037
ALDI04D	7.3963	57.4918	.7097
ALDI06D	7.2243	49.7343	1.0487
ALDI08D	1.3885	17.9848	-2.0635
ALDI10D	6.8701	68.3226	4.1870
ALDI12D	12.0698	64.3056	3.1154
ALDI14D	10.0863	74.5472	1.6802
ALDI16D	6.8500	123.3621	-.6806
ALDI18D	10.4657	179.8902	-5.1253
ALDI20D	4.2724	130.6200	-.3951
ALDI22D	5.3110	-169.4195	6.8940
ALDI24D	1.9558	-48.8496	3.0198
ALDI26D	3.2513	136.3514	2.0281
ALDK01L	20.5955	8.2122	-.3007
ALDK04L	4.5747	18.9973	1.1888
ALDK07L	3.6774	-43.4562	1.2445
ALDK10L	5.5536	-76.2661	-1.4610
ALDK13L	9.5543	-102.2634	-4.2658
ALDK16L	4.7420	-138.7890	-1.8246
ALDK19L	2.8832	-178.4628	-2.1646
ALDK22L	4.3700	-128.0689	-5.8604
ALDK25L	4.1105	159.8431	-2.6549
ALDF01D	28.7963	29.5686	5.6421
ALDF04D	22.2077	74.2566	1.5324
ALDF07D	33.3054	77.4830	-1.9675
ALDF13D	14.6030	101.1644	-.6759
ALDF16D	8.7740	139.6689	3.7797
ALDF19D	5.6891	83.9084	2.4873
ALDF22D	8.5977	66.9286	5.3010
ALDF25D	2.8663	-1.0028	4.2244
ALDF28D	2.6863	82.0324	1.0448

**Table 8.** Summary table of tank test BSE, Waterways Experiment Station, Vicksburg, Miss.

File name	Magnitude	Direction	Y vector
BLEF09D	10.9261	138.1720	2.3859
BLEF08D	12.1055	129.9626	4.1461
BLEF07D	12.3585	118.3906	3.6131
BLEF06D	12.1207	108.2857	3.0547
BLEF05D	11.1241	82.9269	1.8711
BLEF04D	12.2685	85.7607	-.9961
BLEF03D	9.9481	61.9820	.3801
BLEF02D	5.9787	59.2993	-.6750
BLEF01D	11.3070	18.9109	-.7304
BLEC01D	5.4535	62.2264	-.0823
BLEC02D	8.3219	73.7480	1.4638
BLEC03D	10.2285	87.0010	2.3161
BLEC04D	11.7851	93.7243	2.9456
BLEC05D	12.9166	104.8911	3.0050
BLEC06D	13.4793	112.9458	3.1631
BLEC07D	10.5490	111.4727	3.2890
BLEC08D	11.9497	137.9806	4.2599
BLEC09D	9.4333	143.6199	2.9783
BLEI01D	16.0242	.1043	-1.0453
BLEI02D	12.2669	1.6018	.4181
BLEI03D	7.3098	18.7372	1.7481
BLEI04D	3.9565	35.2651	1.2086
BLEI05D	3.3489	147.0088	.7347
BLEI06D	7.4549	157.4059	-.6245
BLEI07D	11.2031	173.1877	-6.2752
BLEI08D	12.7531	-159.6129	-4.1284
BLEI09D	11.9318	-163.4557	-.8174
BLEK01L	7.6628	-9.6853	-1.0154
BLEK02L	7.8374	-40.5169	-.2770
BLEK03L	9.2627	-57.0463	-.0366
BLEK04D	8.0600	-167.8162	.2229
BLEK05L	8.3662	-100.4167	-.3878
BLEK06L	10.1466	-116.7284	-1.4918
BLEK07L	11.4977	-129.6299	-4.1435
BLEK05LD	8.0985	-94.4557	.0649
BLEK01LD	7.1135	-6.7063	-2.2287

layer) and mixing patterns observed during strong stratification, the results from eg962s (a.m.) in 1996 are presented. Prior to test eg962s (a.m.), the quarry was strongly stratified with a surface temperature of about 26°C, thermocline at about 5 m, and bottom temperature near 8°C, and the stratification in the quarry was relatively uniform horizontally.

The velocity field and dissolved oxygen concentration measured near the end of test eg962s (a.m.) in 1996 (0.022 SCMS) indicate similar mixing patterns and are illustrated in figures 22 and 23. Similar data are available for the other tests. The mixing patterns

demonstrate that water was entrained into the plume as it rose through the water column (cool water with very low dissolved oxygen concentrations from near the bottom of the quarry together with warm water near the surface). Therefore, the bubble plume near the surface had a temperature and dissolved oxygen concentration between that at the bottom of the quarry and that at the surface. The entrained water, after reaching the surface, traveled outward from the plume and began to sink near the plunge point because the horizontal momentum was no longer adequate to overcome the negative buoyancy of the cool water. The plunge

**Table 9.** Summary table of tank test BSF, Waterways Experiment Station, Vicksburg, Miss.

File name	Magnitude	Direction	Y vector
BSFK01L	1.6819	-15.4346	0.1066
BSFK02L	2.0717	-45.3944	.5683
BSFK03L	1.6855	-74.4681	.5557
BSFK04L	2.2343	-80.8735	.6214
BSFK05L	1.9877	-98.1922	.1118
BSFK06L	1.1818	-113.4497	-.0884
BSFK07L	2.6307	-119.3524	-.1803
BSFI01D	2.5760	.3546	.6539
BSFI02D	2.2237	1.6779	.5338
BSFI03D	.9590	-7.5386	.8201
BSFI04D	.6236	-25.9076	.5528
BSFI05D	.8933	149.7910	-.0100
BSFI06D	1.5658	163.2688	-.7247
BSFI07D	2.6866	-171.0959	-1.5214
BSFI08D	3.1383	-153.7393	-.8203
BSFI09D	3.1166	-167.4110	-.2344
BSFF01D	2.3013	18.1900	.4286
BSFF02D	2.0654	38.4257	.3454
BSFF02DD	1.9416	40.1416	.2860
BSFF03D	1.9636	58.0048	-.2215
BSFF04D	2.5728	82.5495	-.7105
BSFF04DD	2.1458	78.5993	-.5774
BSFF05D	2.1645	96.2640	-.2024
BSFF06D	1.3711	120.1837	-.1326
BSFF06DD	1.8208	105.1726	-.6521
BSFF07D	2.0077	151.7500	.5082
BSFF08D	1.9204	163.8169	.7681
BSFF08DD	2.9323	162.2031	1.0846
BSFC08D	2.6971	142.5265	1.1814
BSFC07D	2.6245	119.4420	.5787
BSFC06D	3.0421	119.3823	1.0386
BSFC05D	2.7733	99.9146	.3386
BSFC04D	2.8371	99.6551	.2652
BSFC03D	2.9219	86.6656	.8288
BSFC02D	1.9550	78.0181	.3218
BSFC01D	1.8912	72.1250	.8094

point for this test was visually estimated to be about 11.4 m from the center of the rising bubbles. The detrained water sank and intruded into a layer of neutral buoyancy at a depth about 2.5–5 m from the surface. The intrusion layer was best observed at 15–20 m from the aerator (fig. 22). At this location, the spreading intrusion layer was still compressing. The depth and thickness of the intrusion layer also was confirmed and documented (fig. 24) using fluorometric dye measurements.

Microstructure data also were collected with the microprofiler (fig. 13) prior to and during test eg962s(a.m.). Microstructure data prior to the test

are shown in figure 25A. Microstructure data during the test are shown for distances of 12.3 m, 10.7 m, and 29.0 m from the center of the plume in figures 25B, C, and D, respectively. These results demonstrate very weak turbulence prior to starting the aerator. After the aerator was turned on, a great deal of turbulence was generated from the surface down to about 5 m at 10.7 and 12.3 m out from the center of the plume in the area of the plunge point. At a distance of 29.0 m from the center of the plume (far field), significant turbulence was observed only between 2 and 4 m from the surface. Turbulence between 2 and 4 m represents the effect of the spreading axisymmetric plume.

The rate of entrainment into (or detrainment from) the plume ( $Q_e$ ) in test eg962s (a.m.) was calculated by summing over the intrusion layer the products of the time-averaged horizontal velocity ( $V$ ) of a vertical section of the intrusion layer (in this case measured 17 m from the center of the plume), the thickness ( $T$ ) of the vertical section this measured velocity represents (in this case, 0.5 m because ADV velocity measurements were collected at 0.5-m increments), and the circumference of the plume ( $C$ ) (in this case, the circumference at 17 m)(eq. 1). For test eg962s (a.m.), the intrusion layer was estimated to extend 2.25–5.25 m from the surface; therefore, equation 1 was summed over a total ( $N=6$ ) vertical sections. Only the eastern component of the velocity (the component moving directly away from the aerator) was used to define the depth range of the intrusion layer. However, to obtain the horizontal velocity of each vertical section, the eastern component of the velocity and the combined eastern and northern component (eq. 2) were used. In this manner, a range in the actual horizontal velocities were estimated.

$$Q_e = \sum_{n=1}^N V_n \times T_n \times C_n \quad (1)$$

$$V = \sqrt{\left( Velocity_{east}^2 + Velocity_{north}^2 \right)} \quad (2)$$

The average horizontal velocity of the entire intruding layer was approximately 1.8–2.2 cm/s. The entrainment rate of the entire plume or the volume of the water being detrained from the plume was approximately 5.4–6.6 m<sup>3</sup>/s. The absolute accuracy of the velocity measurements was difficult to determine

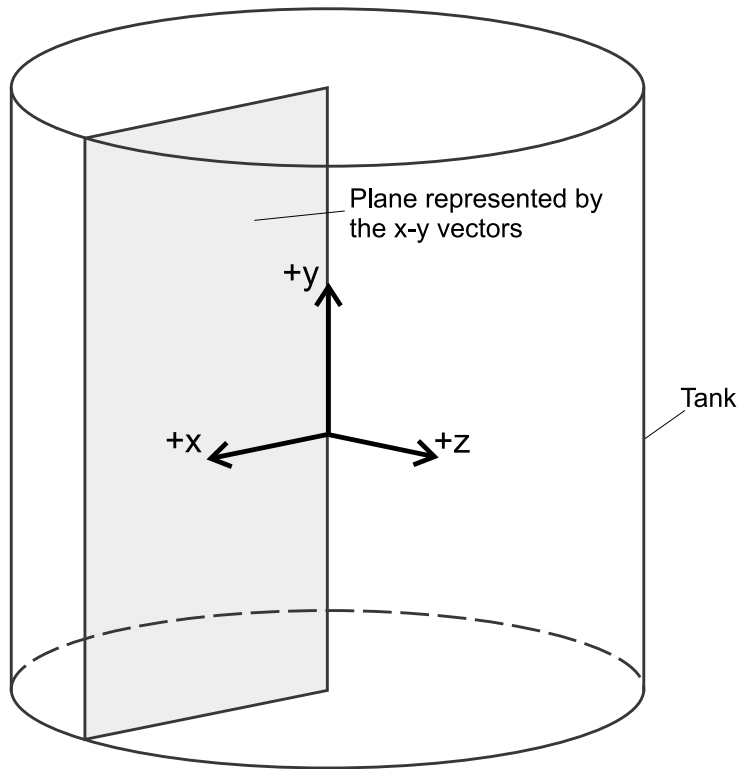


**Figure 15.** Three-dimensional view of the test tank at the U.S. Army Corps of Engineers, Waterways Experiment Station, Vicksburg, Mississippi, showing velocity-vector axes.

because of wind-induced circulation patterns that developed in the quarry after the initial velocity profile was collected.

#### Weakly Stratified Conditions

To demonstrate the mixing characteristics (velocity field, plunge point, and intrusion layer) and mixing patterns observed during weakly stratified conditions for a single aerator, the results from test eg964d in 1996 are presented in figure 26. Prior to test eg964d, the quarry was weakly stratified with a surface temperature of about 23°C, no defined thermocline except near the surface, a bottom temperature near 17°C, and the stratification in the quarry was relatively uniform horizontally.

The velocity data in figure 26 indicate a mixing pattern similar to the pattern observed during strong stratification; however, the axisymmetric intrusion layer was more difficult to define because fewer velocity measurements were available than the measurements shown in figure 22. The plunge point for this test was visually estimated to be about 9.1 m

from the center of the rising bubbles. The detrained water sank and intruded into a layer of neutral buoyancy at a depth of about 5.5–7.5 m from the surface. Fewer velocity measurements were collected in test eg964d than in eg962s (a.m.), so the thickness of the layer was difficult to obtain accurately. The intrusion layer could be observed only about 30 m laterally from the aerator (fig. 26).

The rate of entrainment into (or detrainment from) the plume in test eg964d was calculated using the velocities measured at 6 and 7 m below the surface (measurements were collected 1 m apart) at a distance of 33 m from the aerators. Similar to test eg962s (a.m.), only the eastern component of the velocity was used to define the depth of the intrusion layer and both the eastern and northern components (eq. 2) were used to compute a possible range in the velocities of the intrusion layer. The average horizontal velocity of the entire intruding layer was approximately 0.4–0.8 cm/s. The entrainment rate of the entire plume or the volume of the water being detrained from the plume was approximately 1.4–2.5 m<sup>3</sup>/s. The entrainment rate for test eg964d was difficult to determine because of the distance of the velocity measurements from the aerator and the few velocity measurements.

#### Multiple-Aerator Tests

The tests with two and four aerators, in addition to demonstrating large-scale circulation patterns, such as shown for a single aerator in figures 22 and 23, also demonstrated the extent of mixing or lack of mixing between the aerators. Mixing this area is especially important for preventing small areas of anoxia in a reservoir containing CSO's. To demonstrate an example of this type of mixing, the initial and final DO distributions between two aerators are shown for test eg964s (two aerators with strong stratification) in figure 27. After 4 hours of aerator operation, the water between the aerators became well mixed from the surface down to about 7 m. This upper area represents where the entrained water was released, which was moderately warm (20–22°C) with moderate DO concentrations (6.0–6.2 mg/L). These temperatures and DO concentrations represent the combination of the water entrained throughout the water column. In addition, the oxycline (depths with a rapid change in DO concentrations) and

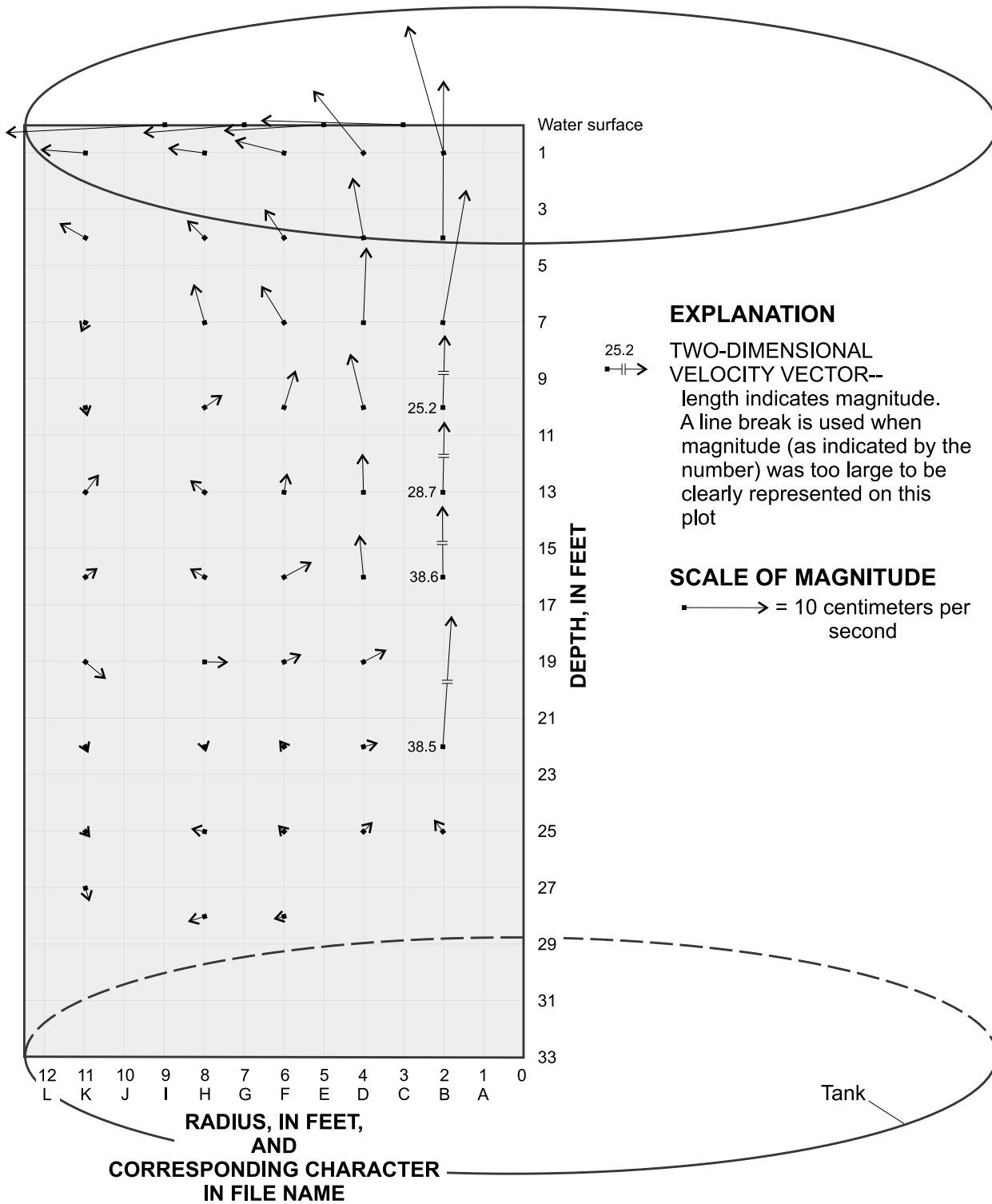


**Figure 16.** Two-dimensional plot of velocity vectors induced by aerators in a test tank (test ASA) at the U.S. Army Corps of Engineers Waterways Experiment Station, Vicksburg, Mississippi.

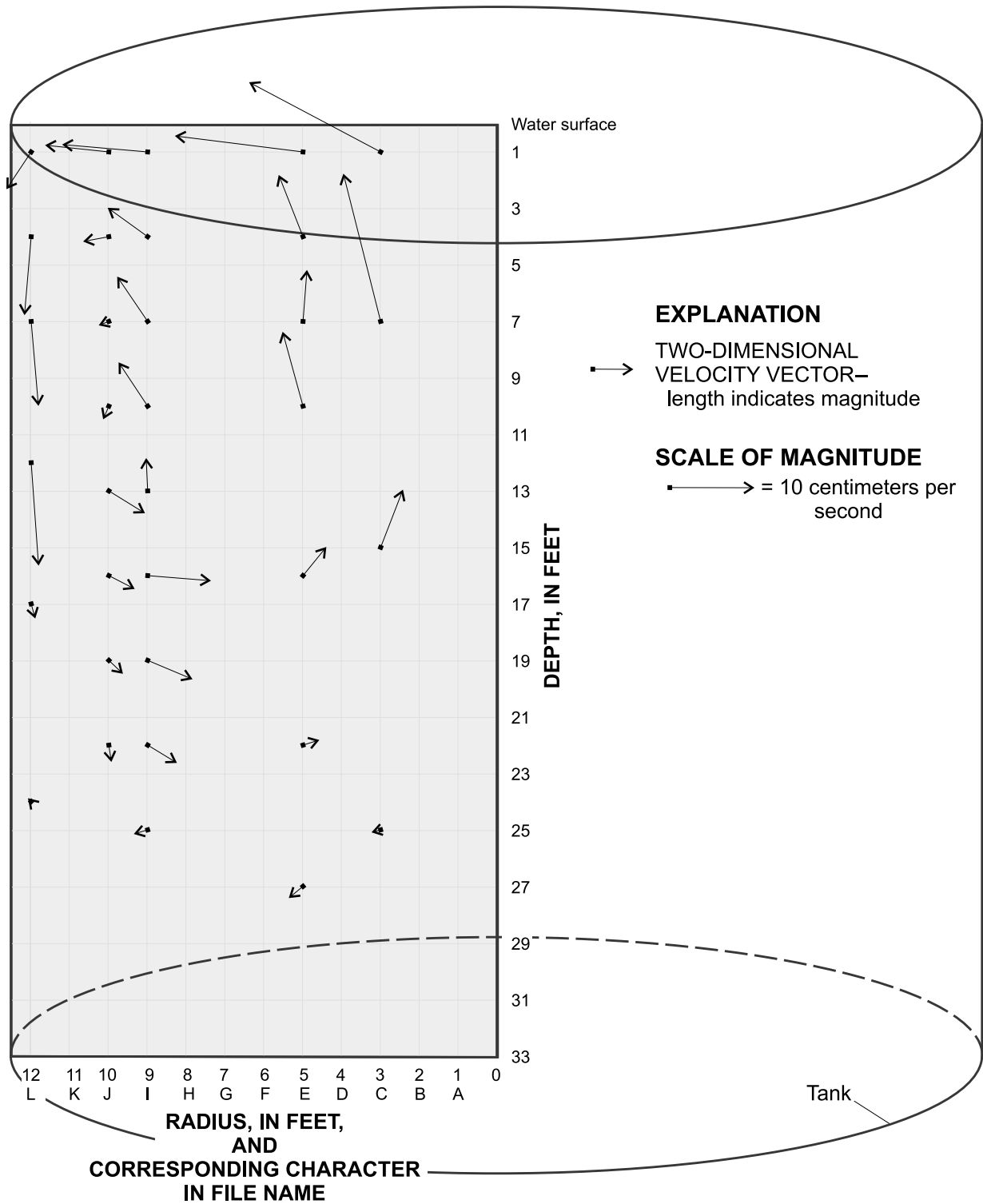


**Figure 17.** Two-dimensional plot of velocity vectors induced by aerators in a test tank (test ASB) at the U.S. Army Corps of Engineers Waterways Experiment Station, Vicksburg, Mississippi.

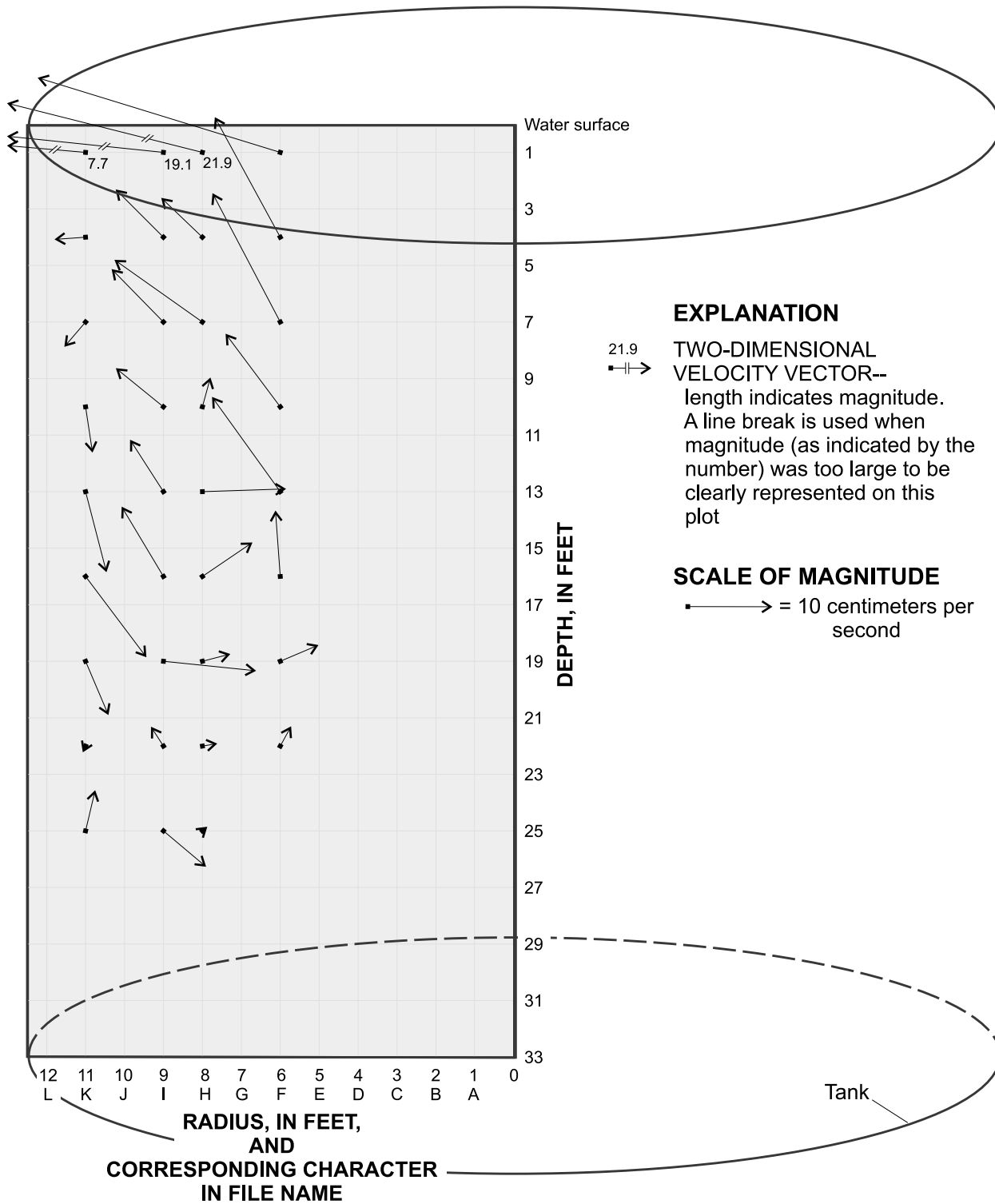


**Figure 18.** Two-dimensional plot of velocity vectors induced by aerators in a test tank (test ALC) at the U.S. Army Corps of Engineers Waterways Experiment Station, Vicksburg, Mississippi.

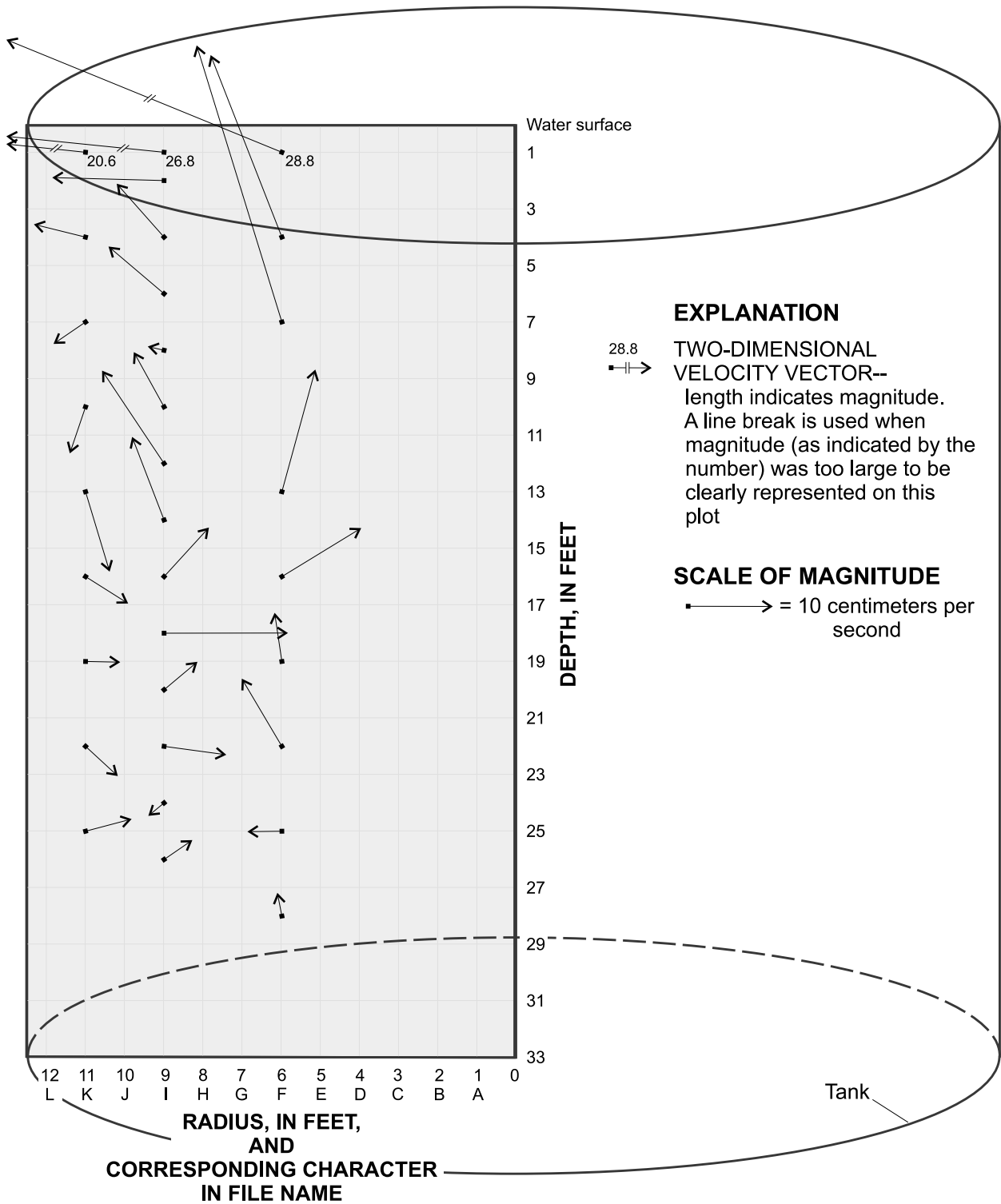


**Figure 19.** Two-dimensional plot of velocity vectors induced by aerators in a test tank (test ALD) at the U.S. Army Corps of Engineers Waterways Experiment Station, Vicksburg, Mississippi.

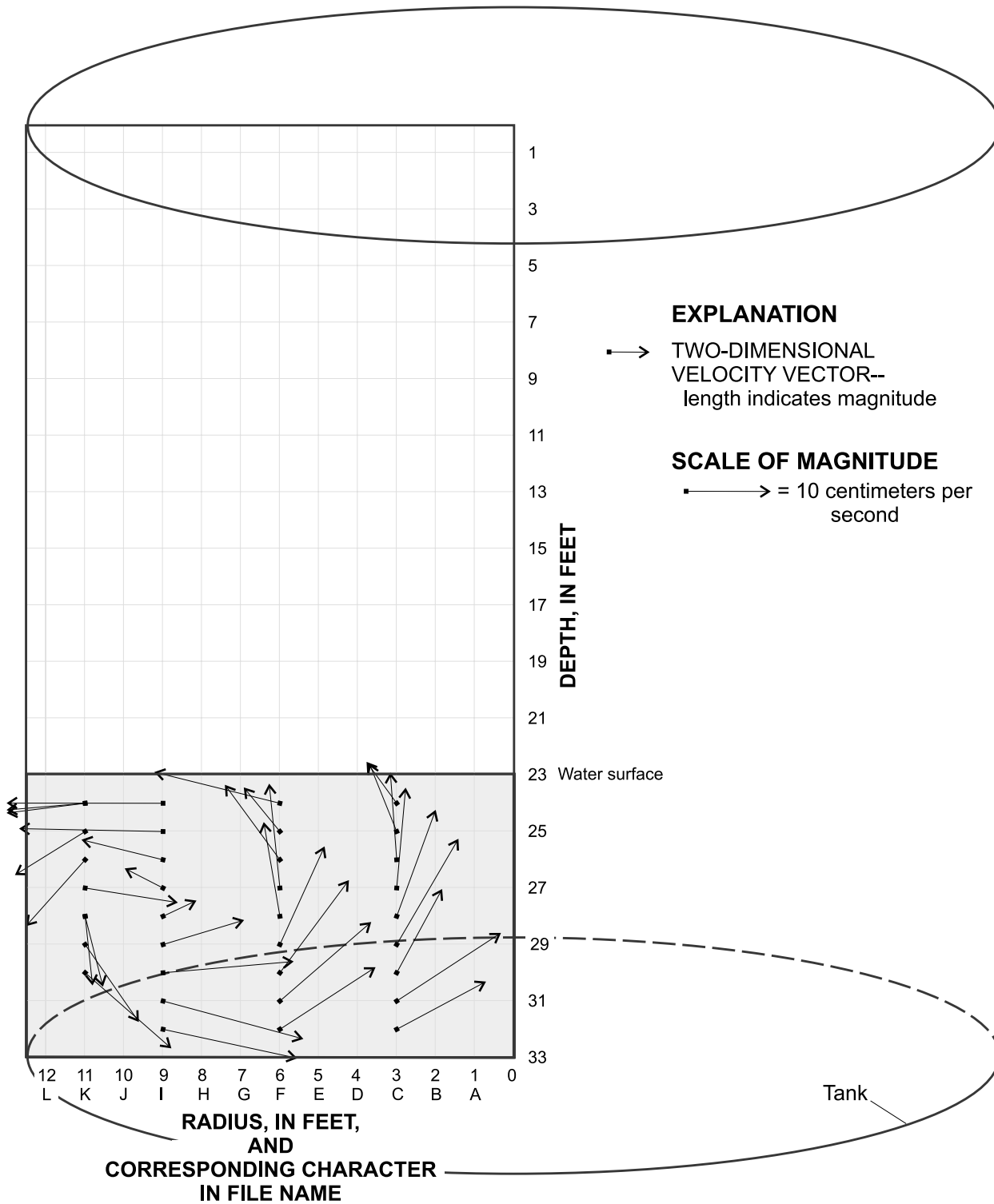


**Figure 20.** Two-dimensional plot of velocity vectors induced by aerators in a test tank (test BSE) at the U.S. Army Corps of Engineers Waterways Experiment Station, Vicksburg, Mississippi.

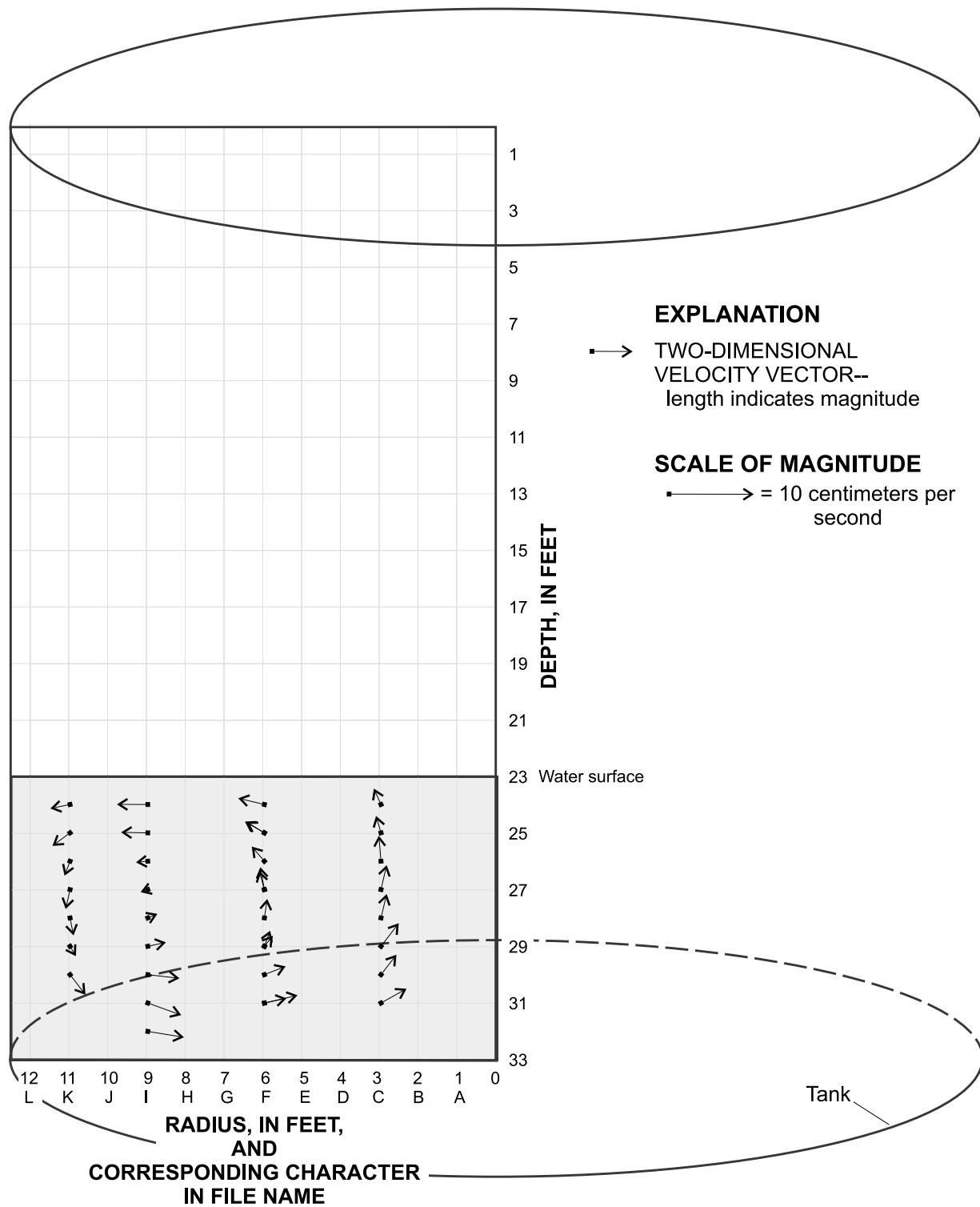


**Figure 21.** Two-dimensional plot of velocity vectors induced by aerators in a test tank (test BSF) at the U.S. Army Corps of Engineers Waterways Experiment Station, Vicksburg, Mississippi.

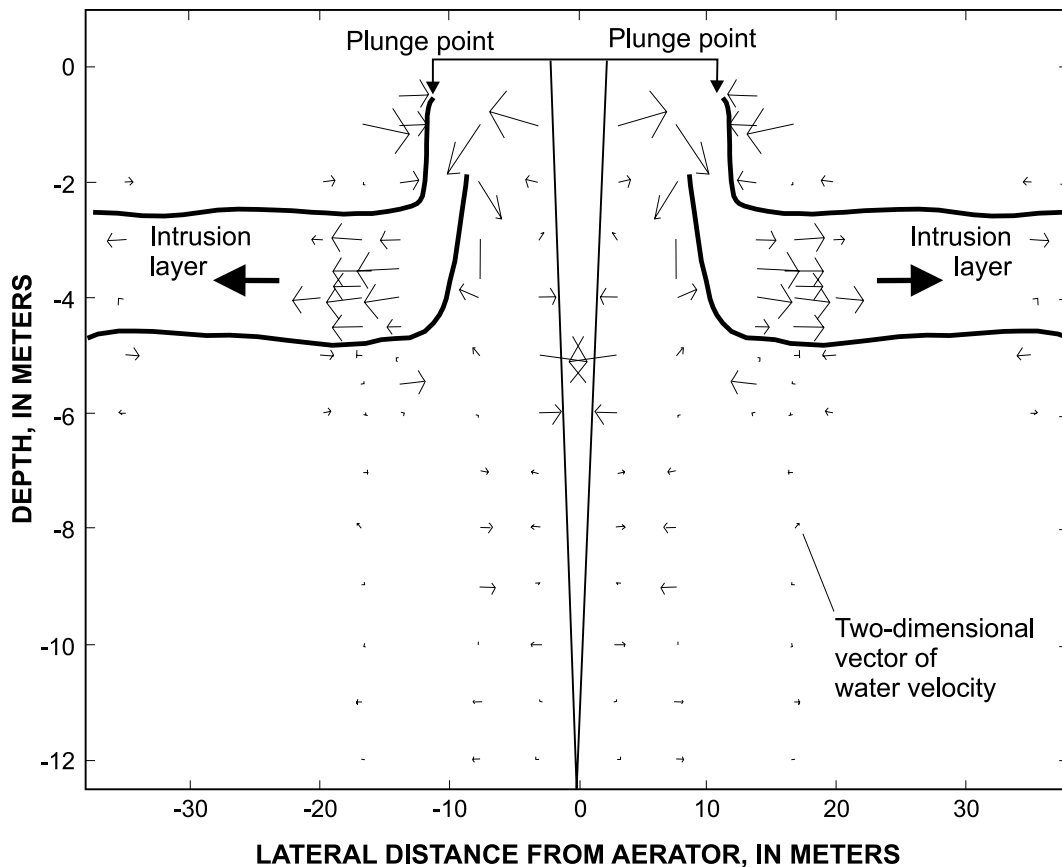


**Figure 22.** Velocity field induced from a single aerator during strongly stratified conditions [test eg962s (a.m.)], Egan Quarry, Schaumburg, Illinois, 1996.

thermocline became sharper and deeper. During the period of the test, the oxycline dropped from about 5 m to 7 m (fig. 27). Below the mixed layer, only small changes in DO and water temperature were observed. Water temperatures increased by 0.1°C at the bottom of the quarry and by 0.4°C at 2.5 m above the bottom. DO concentrations increased by 0.2 mg/L at the bottom of the quarry and by 0.3 mg/L at 2.5 m above the bottom. If aeration continued, this well-mixed area should continue to deepen and deep-water temperatures and DO concentrations should increase, although only very small water velocities were measured below 9 m even during weakly stratified conditions.

Although the analysis of the data is preliminary at the time of this publication, the data-collection methods used to characterize mixing patterns induced by bubble aerators appear successful in this application. An extensive data set has been collected and can continue to be analyzed.

### Measurements and Model Simulations of Plume Characteristics

Most dynamic models used to simulate the extent of mixing induced by bubble-plume aeration systems estimate various plume characteristics in the process of estimating mixing patterns. Therefore, one way to determine the accuracy of model simulations is to compare the simulated plume characteristics to field measurements, such as those conducted at Egan Quarry. Most models simulate the effects of a single aerator and then multiply these results by the total number of aerators to obtain the total effects. For example, in the DYnamic REservoir Simulation Model, DYRESM (Patterson and Imberger, 1989), the model simulates the total entrainment for one aerator as the plume rises through the water column, then that value is multiplied by the total number of aerators to obtain the total entrainment of the aeration system. The total volume of water then is inserted into a range of the depths centered around the depth with density similar to that estimated for the water being detrained from the plume.

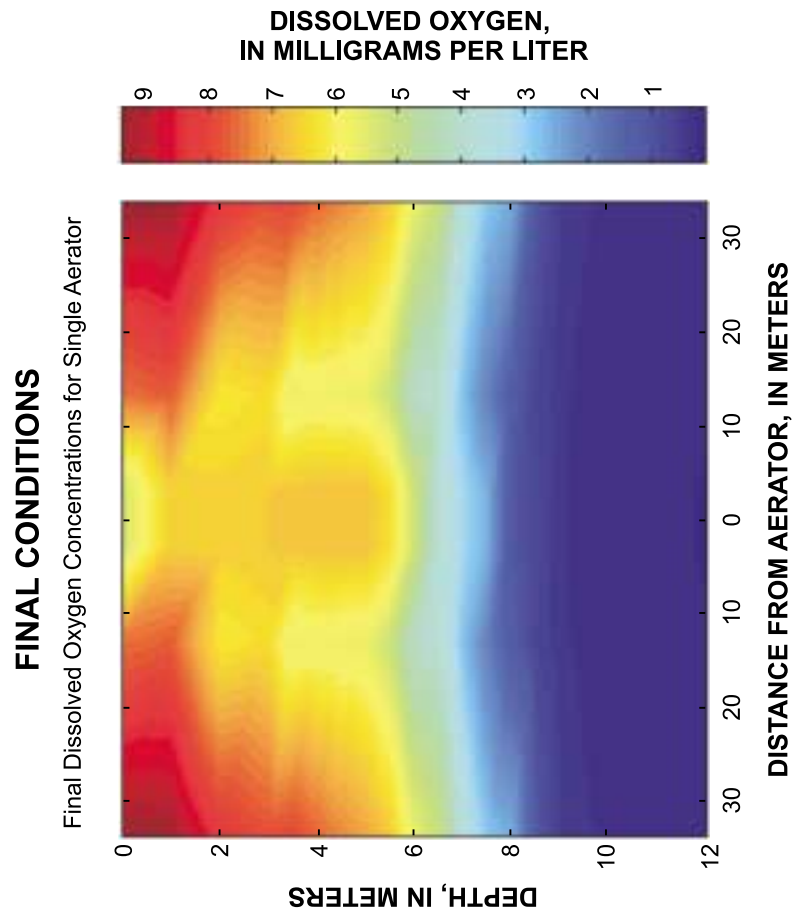
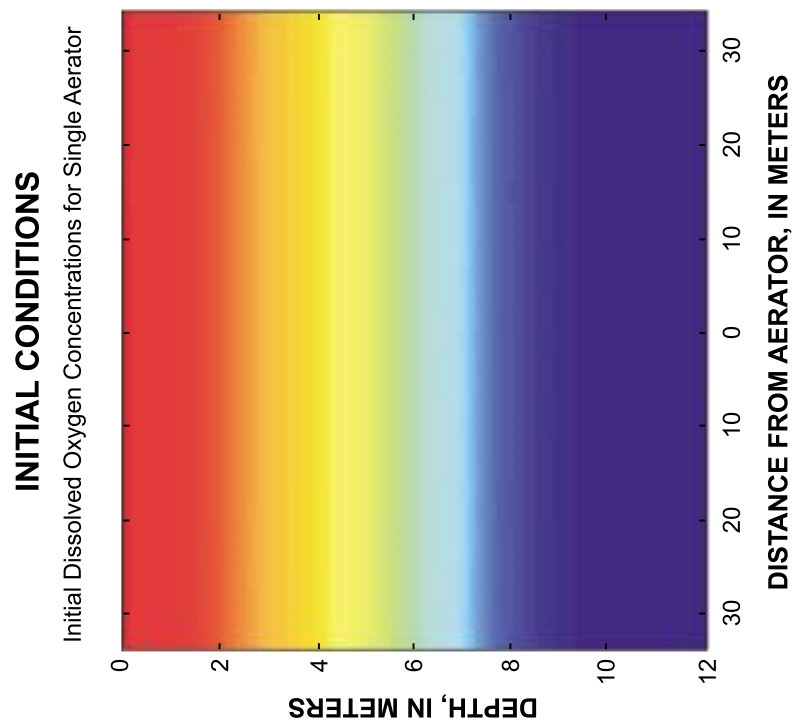


**Figure 23.** Dissolved oxygen concentrations prior to and during single-aerator test in strongly stratified conditions [test eg962s (a.m.)], Egan Quarry, Schaumburg, Illinois, 1996.

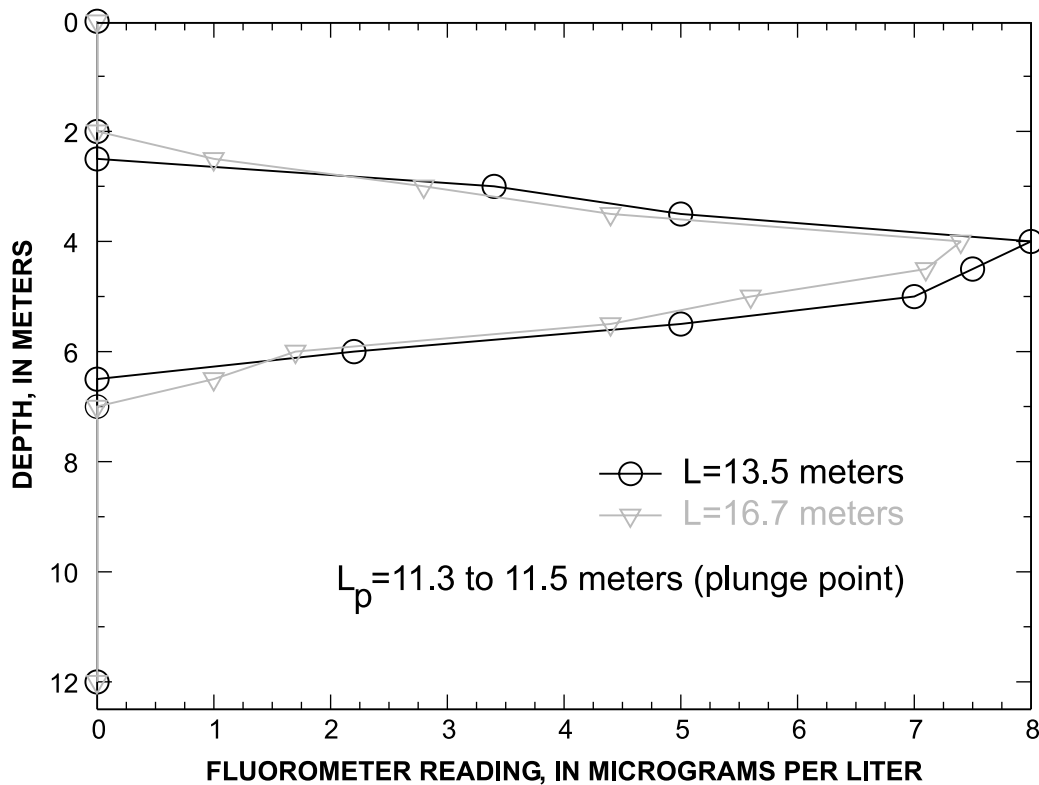


**Figure 24.** Fluorometric data recorded during single-aerator test eg962s (a.m.) after injection of dye at the aerator head, Egan Quarry, Schaumburg, Illinois, August 27, 1996. (L is the distance from the center of the rising-bubble plume.)

Therefore, carefully collected data describing a single-aerator bubble plume [tests eg962s (a.m.), eg962s (p.m.), eg963d, and eg964d] enable model users to test, calibrate, and verify aeration and stratification models and aid in further development of these models.

The plume characteristics estimated from measurements taken during the single-aerator tests with strongly stratified conditions and weakly stratified conditions (both with 0.022 SCMS [eg962s (a.m.) and eg964d]) are compared with those characteristics simulated with the dynamic bubble-plume model described by Schladow (1992) and those characteristics simulated with a set of empirical relations described by Lemckert and Imberger (1993) (table 10).

Schladow's model (1992) incorporates the physics described in McDougall (1978) for a bubble plume as it rises and entrains fluid in a density-stratified environment. In Schladow's model, the differential equations for the conservation of mass, momentum, and buoyancy are solved as the bubbles rise and entrain fluid in a one-dimensional, equispaced, Lagrangian grid. The water column is divided into 1 cm thick layers. For each time step in the model, the volume

of fluid entrained from each layer is computed and removed. The total volume of the detrained plume(s) then is inserted back into the water column at about the level(s) of neutral buoyancy. Two of the simulated plume characteristics in Schladow's model [volume of fluid entrained by the plume ( $Q_i$ ) and insertion depth] were estimated from measurements in Egan Quarry. The algorithm in Schladow's bubble-plume model (1992) is similar to the algorithm used in DYRESM (Patterson and Imberger, 1989); however, Schladow's model does not include the external meteorological forcing and a different layering scheme is applied.

Schladow's model was used to simulate 3 hours of aerator operation with the initial temperature conditions set to conditions measured just prior to tests eg962s (a.m.) and eg964d, an air-flow rate of 0.022 m<sup>3</sup>/s, and an aerator placed 0.6 m above the bottom of a 12.2-m water column. The input to and the output from the model are shown for test eg962s (a.m.) with strong stratification in figure 28. Changes in stratification as a result of the 3 hours of aeration also are shown in figure 28 (compare the initial temperature and density profiles with the final density profile). This

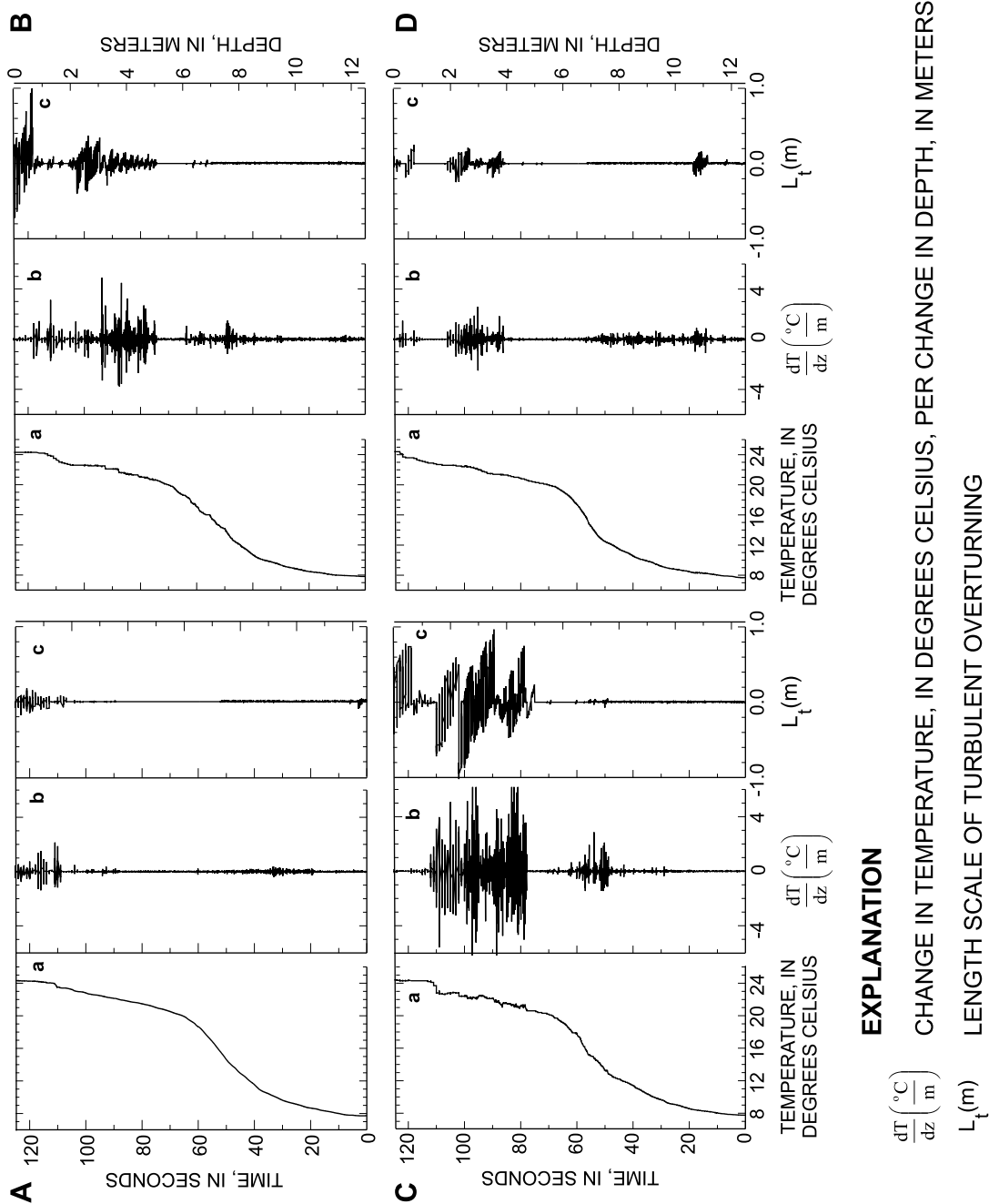


**Figure 25.** Microstructure data collected as the microprofiler ascended vertically to the water surface of Egan Quarry, Schaumburg, Illinois (A) prior to turning on the air compressor (initial conditions) on August 27, 1996, at 11:33 a.m., (B) at 12.3 meters from the center of the rising-bubble plume at 12:19 p.m., (C) at 10.7 meters from the center of the rising-bubble plume at 12:35 p.m. and (D) at 29.0 meters from the center of the rising-bubble plume at 1:03 p.m. The presented data are (a) water temperature, (b) corresponding temperature gradient, and (c) length scales of turbulent overturning as a visual aid to define the vertical extent of the events.

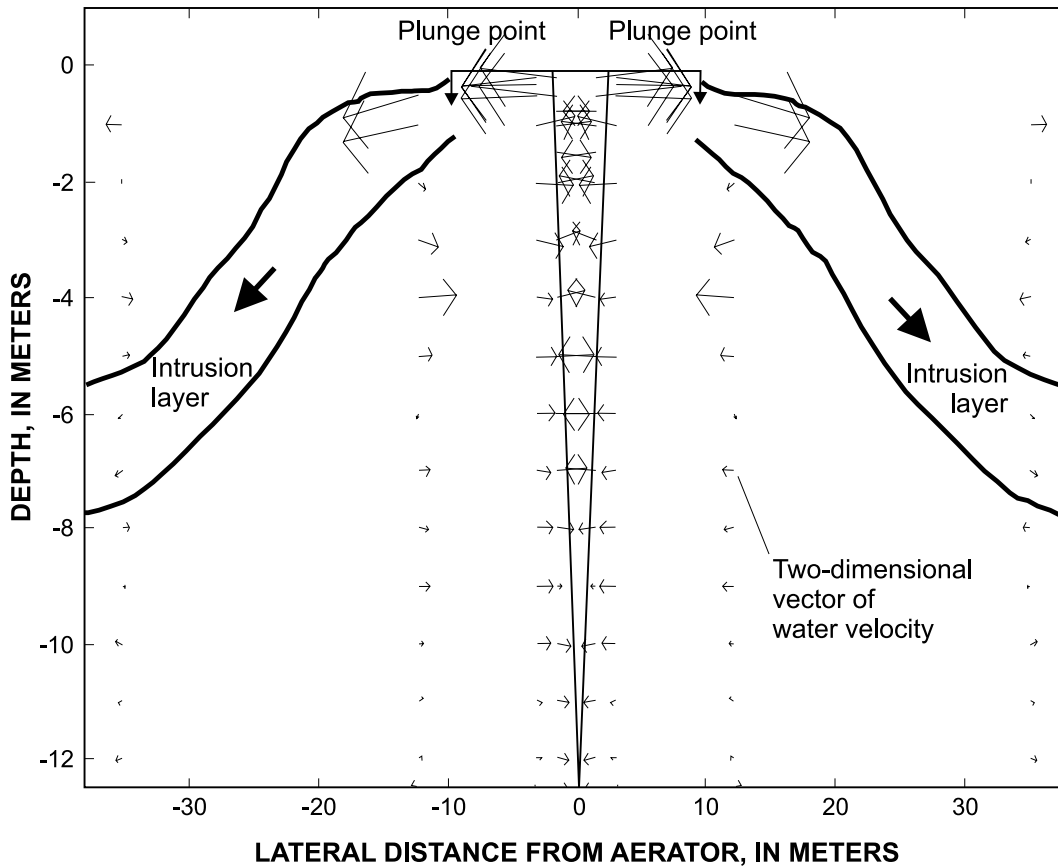


**Figure 26.** Velocity field induced from a single aerator during weakly stratified conditions (test eg964d), Egan Quarry, Schaumburg, Ill., 1996.

figure demonstrates the cooling and deepening of the epilimnion and an increase in the gradient of the thermocline. The radius of the bubble plume as it rises in the water column and the depth where the detrained water is inserted back into the water column also are shown in figure 28. The plume was inserted into a very narrow depth band—apparently narrower than measured in Egan Quarry (figs. 22–24). The vertical velocity of the rising-bubble plume also is shown in figure 28. The vertical velocity decreases as the plume rises through the water column but does not reach 0 m/s; therefore, the plume reaches to the surface before detraining. Also, the input to and the output from Schladow’s model are shown in figure 29 for test eg964d with weak stratification. During weaker stratification, the model simulated the detrained

plume to be inserted at about 8.5–9.2 m above the bottom.

Lemckert and Imberger (1993) used data from field and laboratory experiments to investigate the dynamics of bubble plumes in a water column with a specified stratification. Scaling arguments, in conjunction with experimental data from aerators in three different reservoirs and several laboratory experiments, were used to derive empirical equations to describe the radial extent of the plunge point,  $L_p$  (eq.3), and the total entrainment (or detrainment) rate,  $Q_i$  (eq. 4). These characteristics are a function of  $Q_o$  (volumetric air-flow rate at atmospheric pressure),  $Q_b$  (volumetric air-flow rate at the aerator),  $g$  (the acceleration due to gravity),  $N_e$  (equivalent linear stratification strength), and  $H$  (the depth of the aerator). Plume characteristics simulated

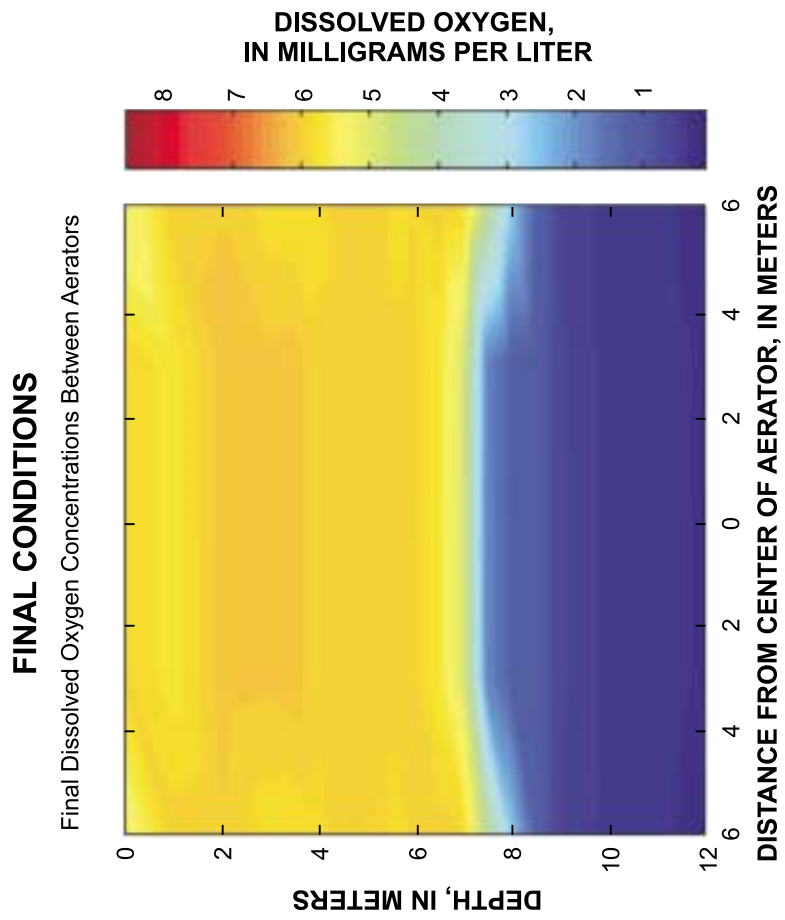
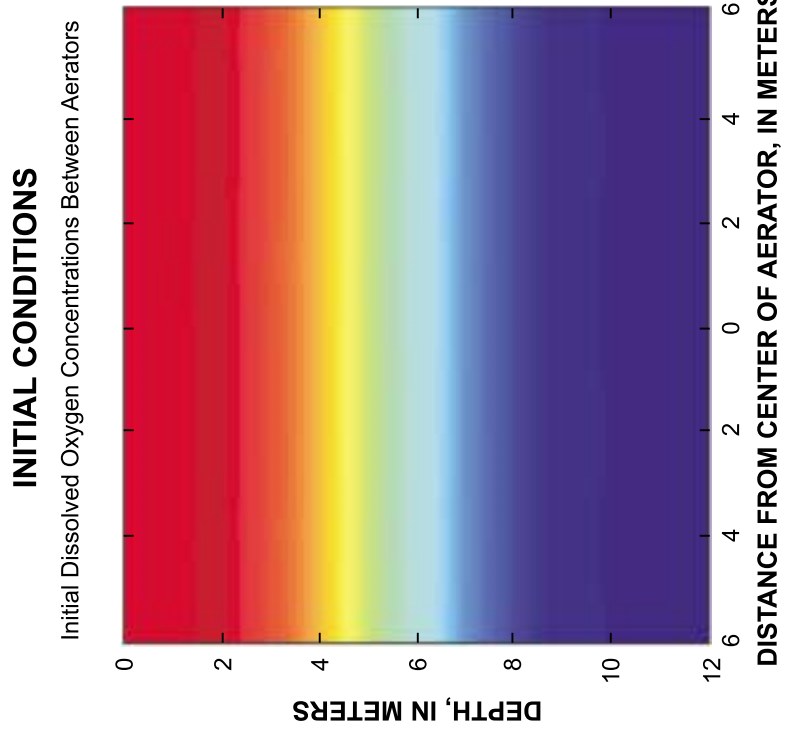


**Figure 27.** Dissolved oxygen concentrations prior to and during a two-aerator test in strongly stratified conditions (test eg964s), Egan Quarry, Schaumburg, Illinois, 1996.

**Table 10.** Comparison of measured and estimated plume characteristics for eg962s (a.m.) (strongly stratified) and eg964d (weakly stratified) at Egan Quarry, Schaumburg, Ill.

[NA, not available]

Method	Plunge-point radius (meters)	Insertion depth (meters from the surface)	Detrainment rate (cubic meters per second)
<b>Strong stratification [eg962s (a.m.)]</b>			
Measurements in Egan Quarry	11.4	2.5–5.5	5.4–6.6
Dynamic model (Schladow, 1992)	NA	5.8–6.3	3.2
Empirical (Lemckert and Imberger, 1993)	6.3	NA	6.5
<b>Weak stratification (eg964d)</b>			
Measurements in Egan Quarry	9.1	5.5–7.5	1.4–2.5
Dynamic model (Schladow, 1992)	NA	3.0–3.7	3.2
Empirical (Lemckert and Imberger, 1993)	10.4	NA	15.1

using equation 3 and 4 for the ambient conditions of test eg962s (a.m.) and eg964d are given in table 10.

$$L_p = 0.97 \times \left( \frac{Q_o \times g}{N_e^3} \right)^{0.25} \quad (3)$$

$$Q_i = 0.74 \times \left( \frac{(Q_b \times g)^3}{N_e^5} \right)^{0.25} \times \left( \frac{(Q_b \times g)}{0.0023 \times H} \right)^{0.11} \quad (4)$$

The observed radius of the plunge point in Egan Quarry was 11.4 m [test eg962s (a.m.), strong stratification] and 9.1 m (test eg964d, weak stratification). Lemckert and Imberger's relations simulated the plunge-point radius to increase with a decrease in stratification: 6.3 m during test eg962s (a.m.) (strong stratification) and 10.4 m during test eg964d (weak stratification). Equation 3 worked very well during weak stratification but underestimated the radius of the plume during strong stratification. Schladow's one-dimensional model does not simulate a plunge-point radius.

The depth of insertion of the extruding plume was from 2.5 to 5.3 m during strong stratification and 5.5 to 7.5 m during weak stratification. During strong stratification, Schladow's model indicated the extruding plume should have been deeper and narrower (5.8–6.3 m) than the plume observed during strongly stratified conditions, and shallower and narrower (3.0–3.7 m) than the plume observed during weakly stratified conditions. Part of this difference in the thickness of the extruding layer may be the result of where

the insertion depth was observed. The plume was observed from 23 to 33 m away from the aerator where the width was still narrowing, whereas the model is one dimensional and simulates an average depth and width over the entire water body. The depth of the insertion is strongly dependent on the background stratification; therefore, Lemckert and Imberger did not attempt to develop relations to simulate insertion depth.

The total entrainment rate into the plume or the volumetric intrusion rate of the axisymmetric intrusion layer was estimated to be about 5.4–6.6 m<sup>3</sup>/s during strong stratification [test eg962s (a.m.)] and 1.4–2.5 m<sup>3</sup>/s during weak stratification (test eg964d). The estimate is given as a range because two mean velocities were determined in the following manner: one on the basis of using just the eastern components of the velocities and one on the basis of the combined eastern and northern components of the velocities. The difference in these estimated entrainment rates may be partially due to the difference in the resolution of the two tests. The results for test eg962s (a.m.) probably were more accurate than the results for test eg964d because the plume was much better defined in test eg962s (a.m.). On the basis of the conditions prior to test eg962s (a.m.) and test eg964d, Schladow's model estimated an entrainment rate of 3.2 m<sup>3</sup>/s for both tests, and Lemckert and Imberger's empirical relations simulated a rate of 6.5 m<sup>3</sup>/s during test eg962s (a.m.) and 15.1 m<sup>3</sup>/s during test eg964d. Only the entrainment rates were compared for test eg962s (a.m.) because of the uncertainties in the estimated entrainment rate for test eg964d. Lemckert and Imberger's model simulates an entrainment rate similar to the rate measured during test eg962s (a.m.) (presumably the most accurate test),

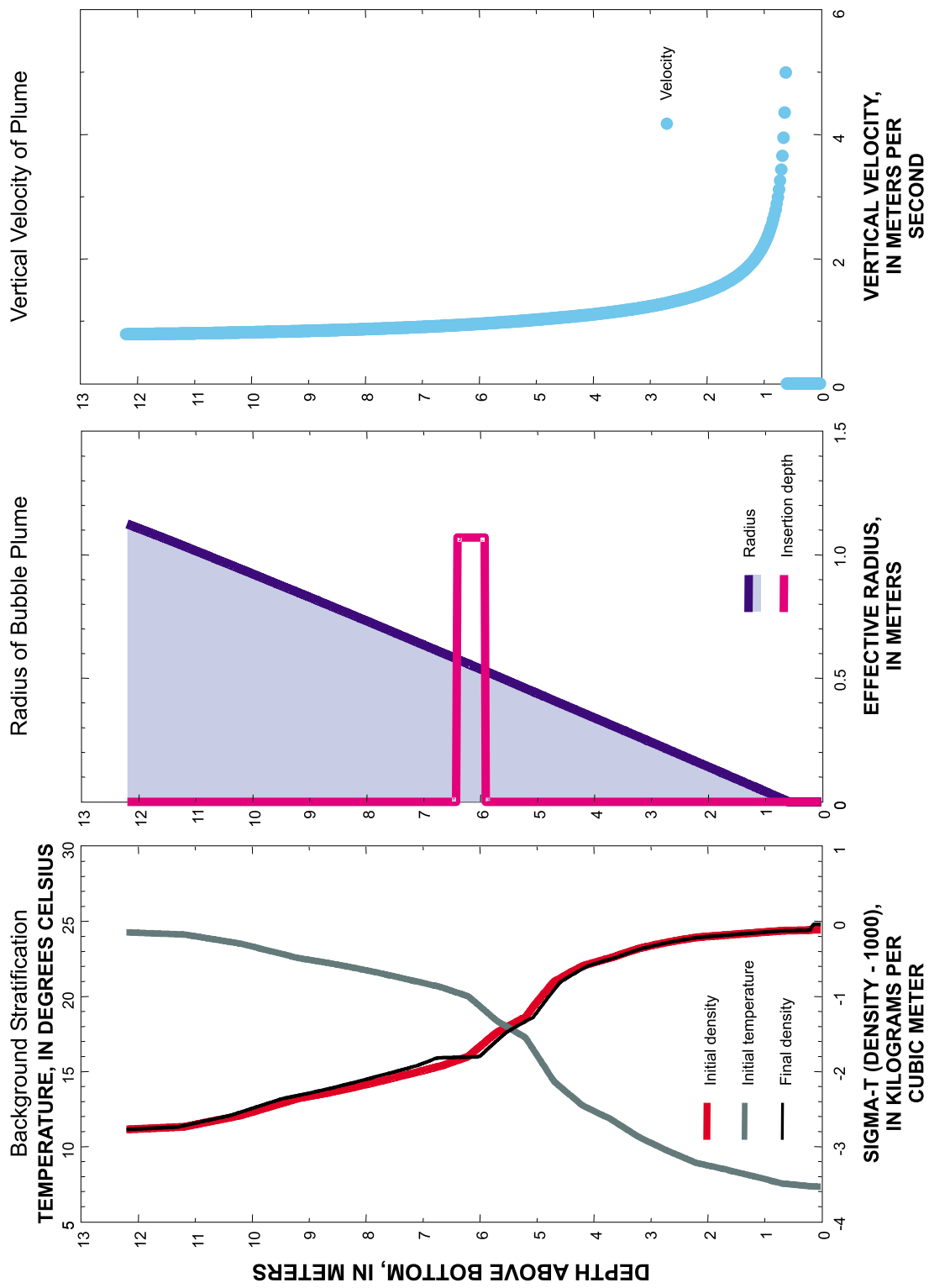


**Figure 28.** Physical characteristics of a rising bubble-plume from Schladow's (1992) model for a bubble plume rising through a 12.2-meters strongly stratified water column with an aerator at 11.6 meters and an air-flow rate of 0.022 cubic meter per second, Egan Quarry, Schaumburg, Ill.

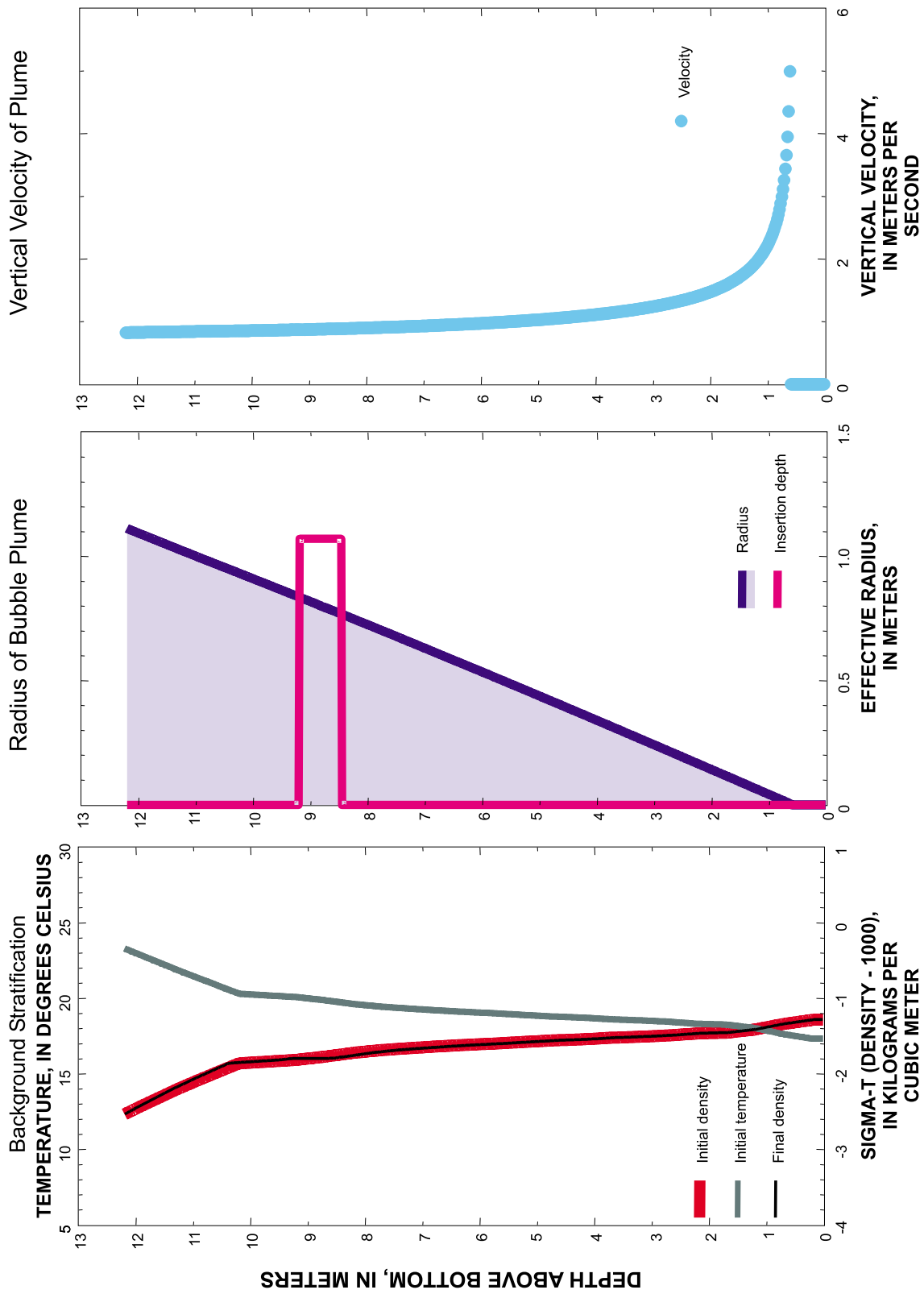


**Figure 29.** Physical characteristics of a rising bubble-plume from Schladow's (1992) model for a bubble plume rising through a 12.2-meters weakly stratified water column with an aerator at 11.6 meters and an air-flow rate of 0.022 cubic meter per second, Egan Quarry, Schaumburg, Ill.

whereas Schladow's model appears to underestimate the total entrainment rate by about 40 to 50 percent.

The apparent underprediction in the plume entrainment rate (detrainment rate) by Schladow's dynamic model along with insertion at a depth deeper than observed in test eg962s (a.m.) may indicate too little water was entrained into the bubble plume near the surface. This result was caused by the model only calculating entrainment for a rising plume, whereas, in reality, much of the entrainment occurs as the detrained water descends away from the plume. When the water descends away from the rising plume, the radius is actually much larger than the radius shown in figure 28. Therefore, this model may underestimate the total effect of the aeration system and the underestimation would result in conservative aerator designs. In deep reservoirs where the plunge depth is much less than the total depth of the reservoir, the additional entrainment near the surface may not be as significant as demonstrated for Egan Quarry. To improve the dynamic model, the entrainment rate near the surface should be increased to account for the much larger radius of the detrained water. This modification would increase the entrainment rate, decrease the density of the detrained water, and result in the insertion of detrained water at a shallower depth.

### **Breakdown of Stratification in Egan Quarry**

After the field tests during strongly stratified conditions were completed in 1996 (table 2), all four aerators were operated during the daytime for 5 days beginning on August 29, 1996, to destratify the quarry. The operation schedule for these 5 days is summarized in table 2. The total air-flow rate used during this time was about 0.090 SCMS (approximately 0.022 SCMS through each aerator). The destratification in the quarry was done in preparation for tests during weakly stratified conditions. To document the breakdown of stratification, the thermistor string on the floating dock platform in the far field (yellow dock) collected hourly water temperature data (illustrated in fig. 30). Water temperatures in the quarry were significantly affected by the operation of the bubble-plume system. The profiles presented in figure 30 are from 12:00 a.m. on August 28 (Julian day 241) to 12:00 a.m. on September 3 (Julian day 248).

Prior to activating the four aerators (12:00 a.m. on August 28), temperature stratification was very strong, with temperatures ranging from over 24°C near

the surface to just over 7°C at the bottom. Additional temperature profiles demonstrated the stratification was nearly horizontal throughout the quarry, as would be expected in an undisturbed lake. The thermocline was approximately 5 m from the bottom with a temperature gradient of nearly 4°C per meter. Prior to activating the four aerators, the epilimnion was larger and better mixed than the hypolimnion.

After running the aerators for 5.5 hours on August 28 (Julian day 241), the thermocline lowered over 1 m to a depth of approximately 3.5 m above the bottom. With the lowering thermocline, the epilimnion thickened and became more thermally homogeneous. The surface temperature decreased by about 1°C, which may be due to entrainment of cool, deep water and cooling at the surface at night. Temperatures at the bottom of the epilimnion fell from 21°C to 18°C (fig. 30). The thermocline not only was lowered from operation of the aerators but also was compacted. The volume of the hypolimnion decreased because hypolimnetic water was entrained into the rising plume and released at a shallower depth. After the aerators were discontinued on August 28, the changes in the quarry stopped and the thermocline remained at a constant depth.

During the next 4 days, the destratification progressed in a very similar manner to that of the first day. Destratification resulted in a step-wise descent of the thermocline, whereas the epilimnion volume increased and the hypolimnion volume decreased. These changes in the quarry are contradictory to the results of Schladow and Fischer (1995), who found destratification to cause the hypolimnion volume to grow at the expense of the epilimnion. The discrepancy was probably caused by (1) the relatively higher air-flow rate used in Egan Quarry and (2) the relatively shallower depth of Egan Quarry when compared to the air-flow rates and depths in the reservoirs studied by Schladow and Fischer. The relatively higher air-flow rate used in Egan Quarry resulted in much more entrainment near the surface, resulting in the depth of the plume insertion above the thermocline, whereas detrainment in the reservoirs occurred in and below the thermocline. The bottom of the thermocline in Egan Quarry eventually reached the bottom of the quarry on about August 31 (Julian day 244). From this point forward, the bottom of the thermocline continually eroded with little change in the rest of the quarry.

During the 5 days of destratification, the temperature of the top 0.5 m of the quarry changed in response to daily heating and cooling from the

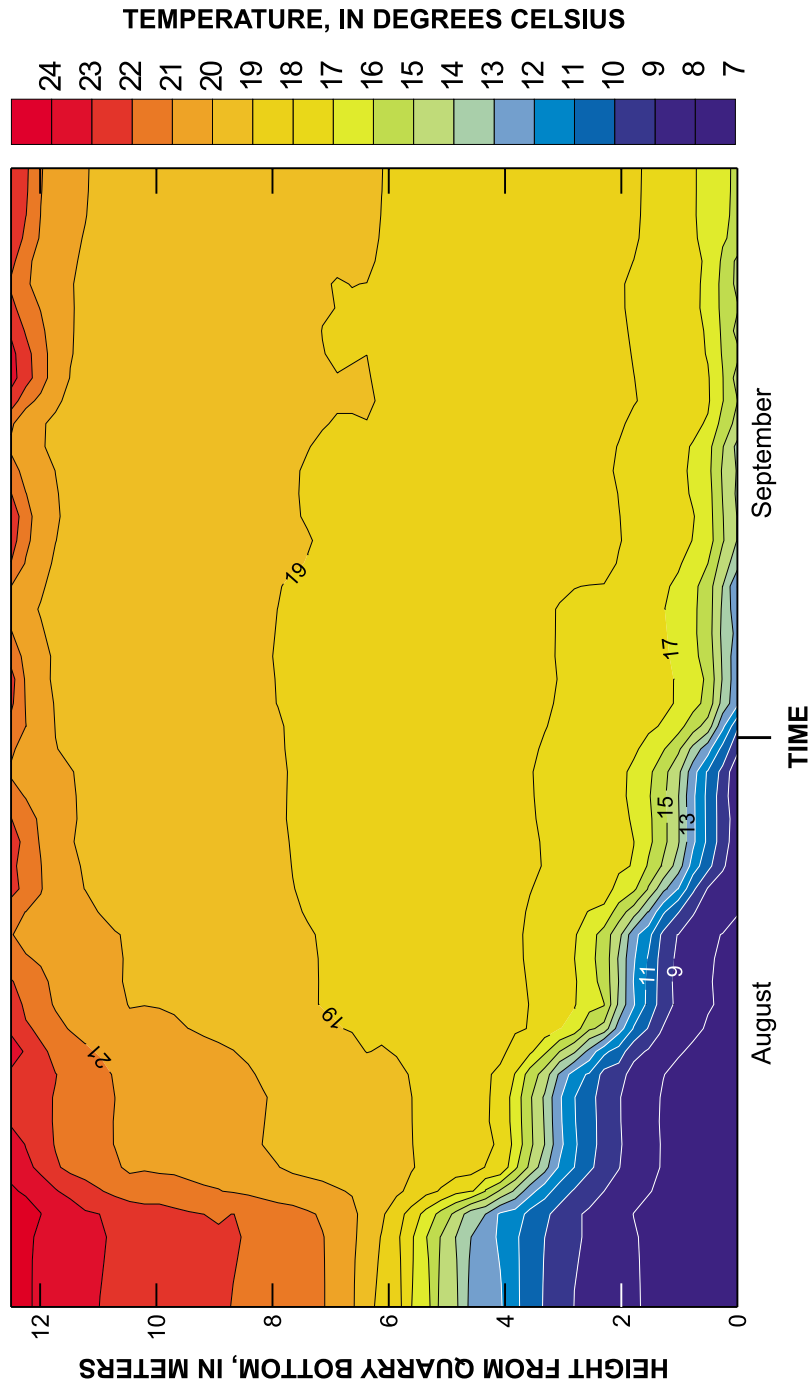


Figure 30. Observed water temperature from August 28 to September 3, 1996, in Egan Quarry, Schaumburg, Ill.

atmosphere, whereas the rest of the epilimnion became relatively well mixed. Daily heating and cooling resulted in a fairly sharp temperature gradient at the top of the epilimnion during the middle of the day, with the middle and bottom relatively isothermal at about 18–19°C. If aeration continued through the night, the stratification near the surface may have been eliminated.

To determine whether the changes in the thermal structure of Egan Quarry could be simulated with a numerical simulation model, the Dynamic Lake Model (DLM) was applied to the quarry (McCord and others, 2000). DLM is a one-dimensional lake and reservoir model, modified from the DYRESM (Imberger and Patterson, 1981). These models are process-based and have been successfully used to simulate changes

in the vertical temperature structure of many lakes and reservoirs. The model is based on parameterizations of each individual mixing process, so site-specific model calibration is not necessary. DLM is based on a Lagrangian layer scheme in which the lake is represented by a series of horizontal layers, each with uniform properties but variable thickness. Mixed-layer deepening is modeled as convective overturn, resulting from surface cooling, wind stirring at the surface, seiche induced shear at the pycnocline, and billowing at the pycnocline resulting from shear instability. Turbulent transport in the hypolimnion is modeled as a diffusionlike process, with an eddy diffusivity depending on the local density gradient and rate of dissipation of kinetic energy. Inflows and outflows are confined to narrow regions adjacent to the insertion level and outflow area of the water body (Patterson and Imberger, 1989).

A bubble-plume model was added to these models in an attempt to simulate mixing by bubble-plume destratification systems (Schladow, 1992). Each aerator is treated as a point source, and the bubble plume is modeled by integrating the equations for mass, momentum, and buoyancy from the bottom of the water body to the surface. As the plume rises through each computational layer, entrained water is added and plume density changed. If the plume width exceeds the source spacing at any height, the combined plumes can be treated as a line source, as outlined by Robertson and others, 1991. If the vertical velocity of the plumes decreases to zero, the water is detrained at that height and a new plume is started as a new source at the depth of detrainment. The water detrained from the rising plume then is inserted into the water column as a line source similar to tributary input. Therefore, the detrained water only effects the computational layers adjacent to the intrusion but will spread out vertically as a result of other mixing processes (Schladow, 1992).

Inputs to DLM include lake morphometry, meteorological data, inflow and outflow data, and initial water-temperature profiles. Daily averages of air temperature, vapor pressure, wind speed, and river temperature are used as inputs to DLM. Daily total values for river inflows, river outflows, long wave and short wave radiation, and rainfalls are used as inputs to DLM. To simulate the operation of an aeration system, the total air-flow rate, number of aerators, depth of aerators, and aerator spacing are required. To simulate the temporal changes in the operation of the aerators (table 2), DLM was modified to incorporate hourly

operation schedules of the bubble-plume system rather than the operation over an entire day as required in the original DLM and produce hourly output, if requested. This version of the model is called DLM-hr. Additional data required for DLM-hr are the hours of operation of the aeration system for each day.

To simulate destratification in Egan Quarry, the morphometry from figure 3 was used with meteorological data from St. Charles (approximately 30 km northwest of the quarry; for a full description of the meteorological data see Olson, 1998) and the operational schedule of the aeration system (table 2).

The changes in water temperature in the quarry were well simulated with DLM-hr (fig. 31). The model was able to accurately simulate the step-wise descent of the thermocline and the increase in the epilimnetic volume at the expense of the hypolimnetic volume. The water temperature of most of the epilimnion was simulated to be approximately 19–21°C compared with the observed 18–20°C. The model was unable to describe most daily increases in temperature near the surface. Another apparent discrepancy was in the temperatures at the very bottom of the quarry. Results of DLM-hr simulation indicated strong stratification should have remained within 1 m of the quarry bottom, whereas only very weak stratification was observed. The strong stratification simulated in the bottom meter of the quarry may have been present in the quarry; however, temperatures immediately above the sediment-water interface (0.5 m) were not measured.

Overall, the changes in the stratification in the quarry were well simulated in the model, including the short-term daily changes. Therefore, this model is appropriate for simulating one-dimensional changes as a result of aeration. The model was further applied to see how stratification would have changed in the quarry if the aeration system was not applied and only daily variability in meteorological conditions occurred (fig. 32). Without the operation of the aeration system, stratification in the quarry would have changed very little during the 5-day period. The only change that would have occurred was small diurnal heating and cooling.

## **Egan Quarry Tests (1997)**

### **Aerators and Submersible Mixer**

During summer 1997, several tests were conducted at Egan Quarry to investigate mixing

### Dynamic Lake Model-hr Simulation of Egan Quarry With Aeration

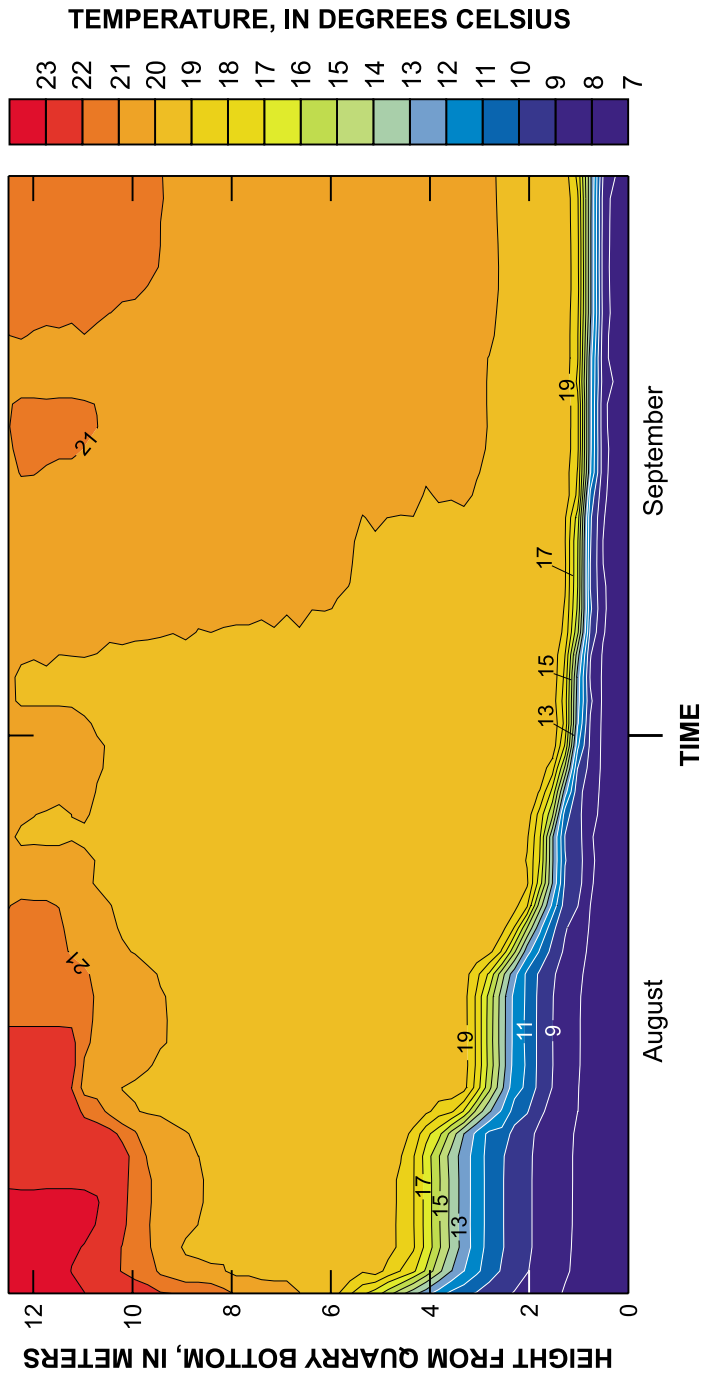


**Figure 31.** Simulation by the Dynamic Lake Model-Hourly (DLM-hr) of water temperature in Egan Quarry, Schaumburg, Ill., with aeration, in 1996.

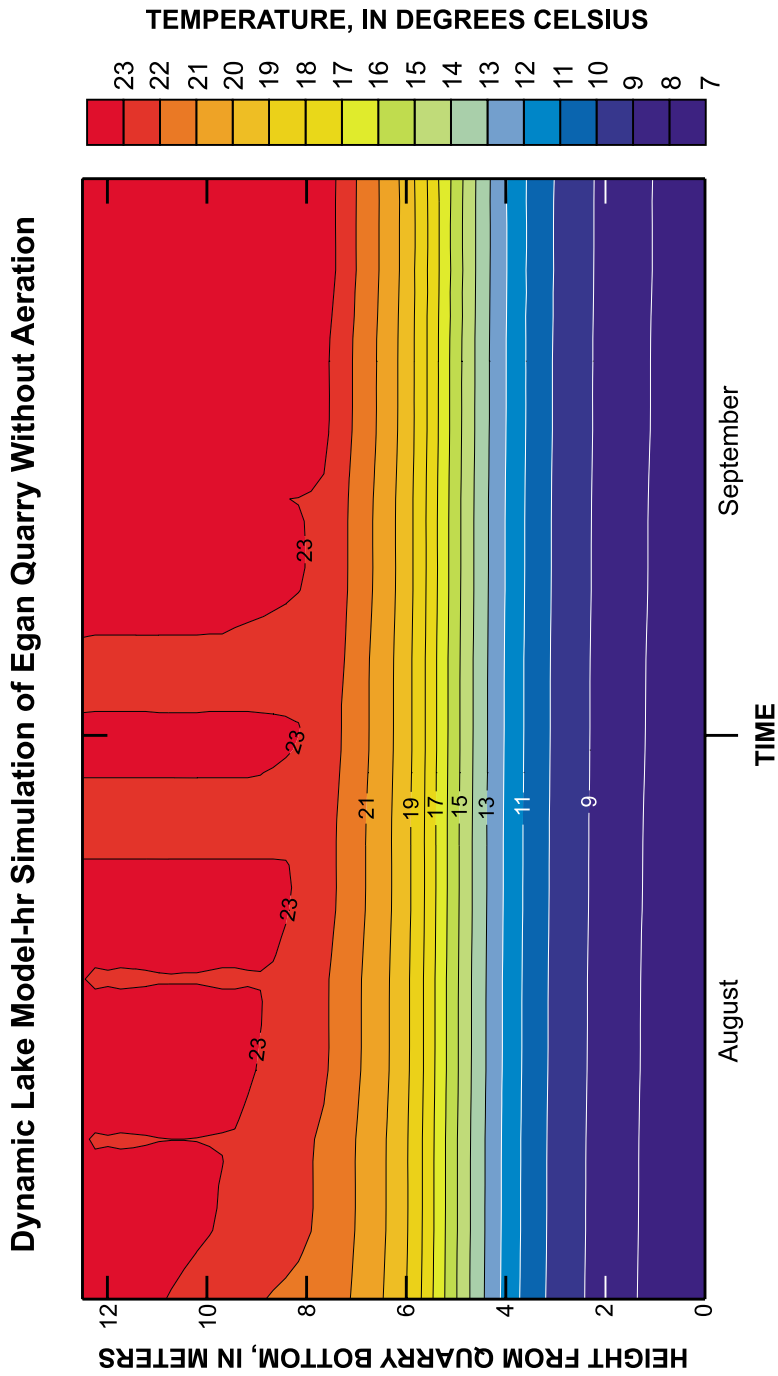


**Figure 32.** Simulation by the Dynamic Lake Model-Hourly (DLM-hr) of water temperature in Egan Quarry, Schaumburg, Ill., without aeration, in 1996.

patterns induced by combinations of aerators and/or a submersible mixer. Four aerators were placed 0.6 m above the quarry bottom in a 19.8 m by 27.2 m rectangle (see maps in appendix 1 for locations of aerators, mixers, and data-collection points). The submersible mixer was placed in two different locations and pointed in several different directions (see table 3 for a description of the aerator/mixer configurations for all tests in 1997). Tests were done during strongly stratified and weakly stratified conditions. A few observations made during these tests are described below.

During test eg973s, the submersible mixer was pointed due west and parallel to the quarry bottom (aerators were not in operation). The water velocities induced by the operation of the submersible mixer were evident at location O, 6.1 m due west of the mixer (fig. 33). Velocities were essentially 0 cm/s from the water surface down to about 11 m deep. Around a depth of 11.0 m, velocities increased dramatically and were as high as 55 cm/s due west. These high velocities along the quarry bottom continue radially outward and were still measurable (as high as 22 cm/s due west) at a distance of 32 m west of the mixer.

During test eg975s, all four aerators operated at 0.022 SCMS, and the submersible mixer was oriented directly up in the middle of the four aerators. Data were collected at several locations throughout the quarry. At location D, which was on the line between the northwest aerator and the submersible mixer about 4.6 m southeast of the northwest aerator, the interaction of the aerators and the mixer could be observed. At this location, the surface-water velocities induced by the northwest aerator encountered the surface water velocities induced by the submersible mixer. The result was consistent downward velocities of over 10 cm/s down to a depth of at least 8 m.

During test eg974d, all four aerators were operated at 0.022 SCMS, and the submersible mixer was in the middle of the two north aerators, oriented due south, and parallel to the quarry bottom. The same downward mixing pattern as in the eg975s test was observed; the surface-water velocities induced by the aerators encountered each other and plunged downward. These consistent downward velocities were as high as 11 cm/s, until they reached the bottom of the quarry where the submersible mixer began to affect the water.

The north/south velocities remained within plus or minus 2 cm/s down to a depth of 11 m. Suddenly, at 11 m, the velocities increased to 11 cm/s toward the

south, then the velocities increase to 48 cm/s toward the south at 12 m. The strong velocities directly away from the submersible mixer were still as high as 16 cm/s near the quarry bottom at location AA, 19.8 m directly south of the submersible mixer.

### Surface Mixer

Three tests were conducted to investigate mixing patterns induced from the operation of the surface mixer. During all three tests, the floating mixer was moored using cables in the middle of the quarry, oriented due east, and angled down at a 45° angle toward the quarry bottom. Measurement locations are shown on the maps in appendix 1. A few observations of the data collected during these tests are described below.

During test SM2, at location 55 (16.7 m due east of the mixer), water velocities were as high as 78 cm/s due east at the surface but below a depth of about 3 m were not significantly affected by the mixer (fig. 34a). At location 14 (49 m due east of the mixer), water velocities near the surface were still in the east direction (as high as 19.3 cm/s) but were reversed nearer to the bottom and headed back towards the mixer (fig. 34b). This probably resulted because of the interference from a quasi-boundary effect from the quarry wall that was about 80 m due east of the mixer.

Dissolved oxygen data were collected along 10 radial taglines (fig. 35) from the mixer to the shore prior to, during, and after test SM3 and used to quantify the net change in dissolved oxygen as a result of operating the surface mixer. Dissolved oxygen concentrations along the west-east transect are shown for the initial and final conditions (just prior to shutting off the mixer) along with the change in concentrations as shown in figure 36. The black areas in the figure represent the bottom of the quarry. In figure 36c, the dark blue areas represent areas with a net decrease in DO and the yellow and red areas represent areas with a net increase in DO. In general, DO concentrations decreased throughout the epilimnion and increased in areas where the thermocline deepened.

The total mass of DO, prior to and after operating the surface mixer, was calculated by segmenting the quarry into separate volumes, computing the mass of DO in each volume, and then summing those quantities. The total mass of DO in the quarry decreased by about 35.3 kg during the 7 hours of mixer operation, indicating a net loss of oxygen from the quarry. Decreases in the mass of dissolved oxygen may have been caused

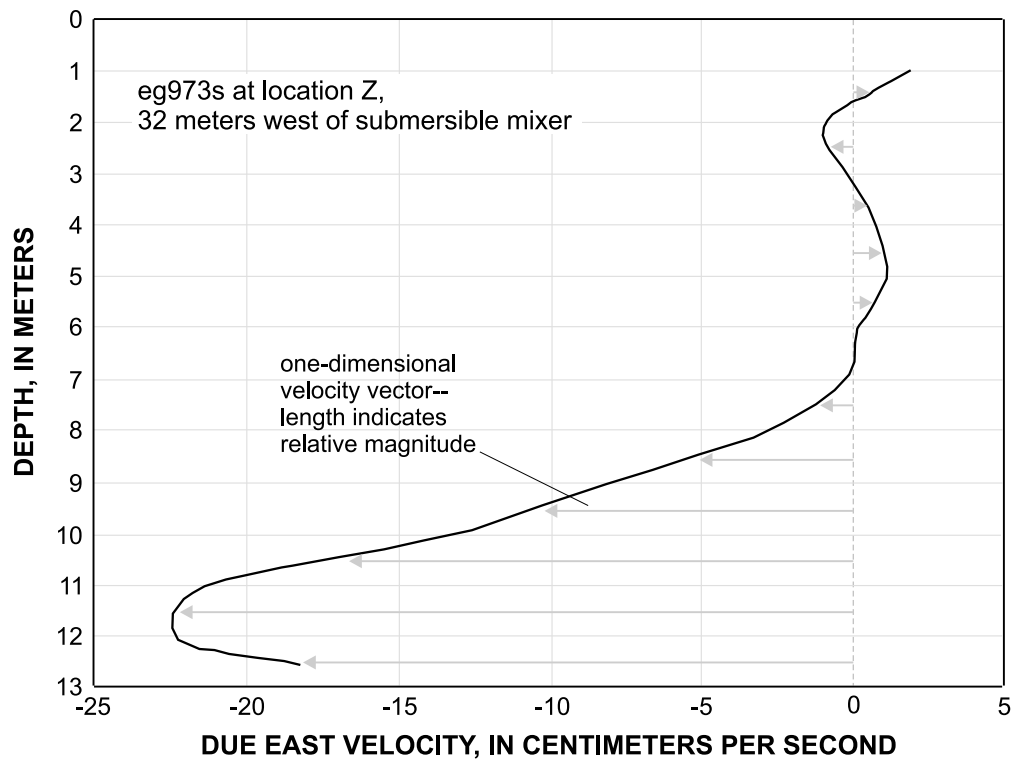
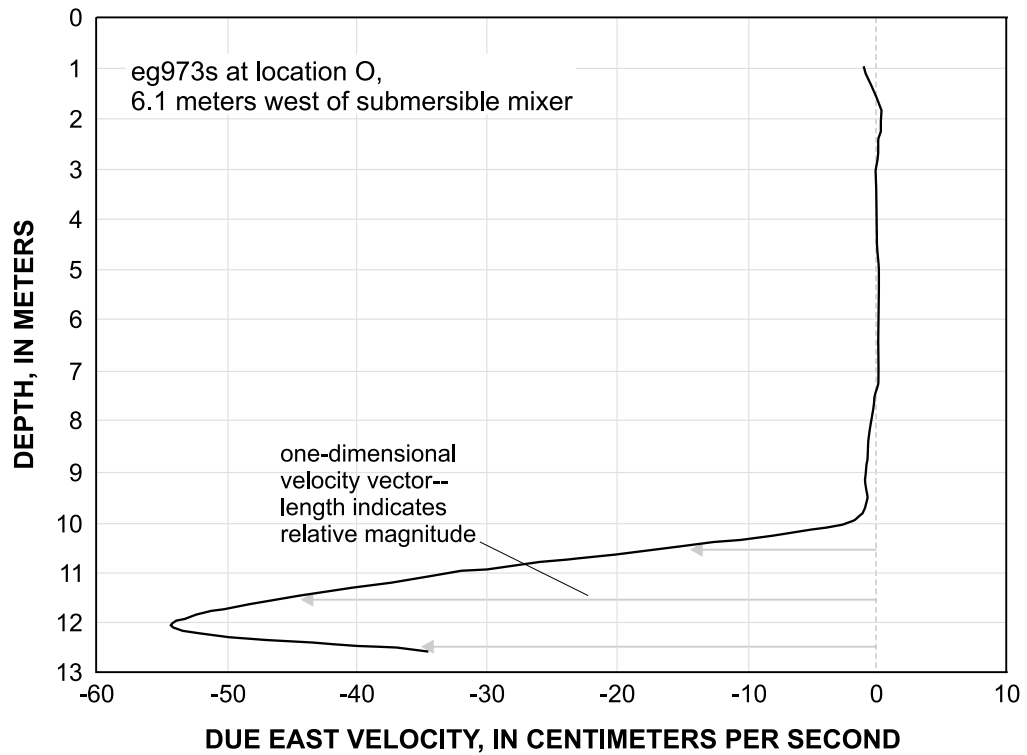


**Figure 33.** Water-velocity profiles during test eg973s, 6.1 meters west and 32 meters west of the submersible mixer, Egan Quarry, Schaumburg, Illinois, 1997.

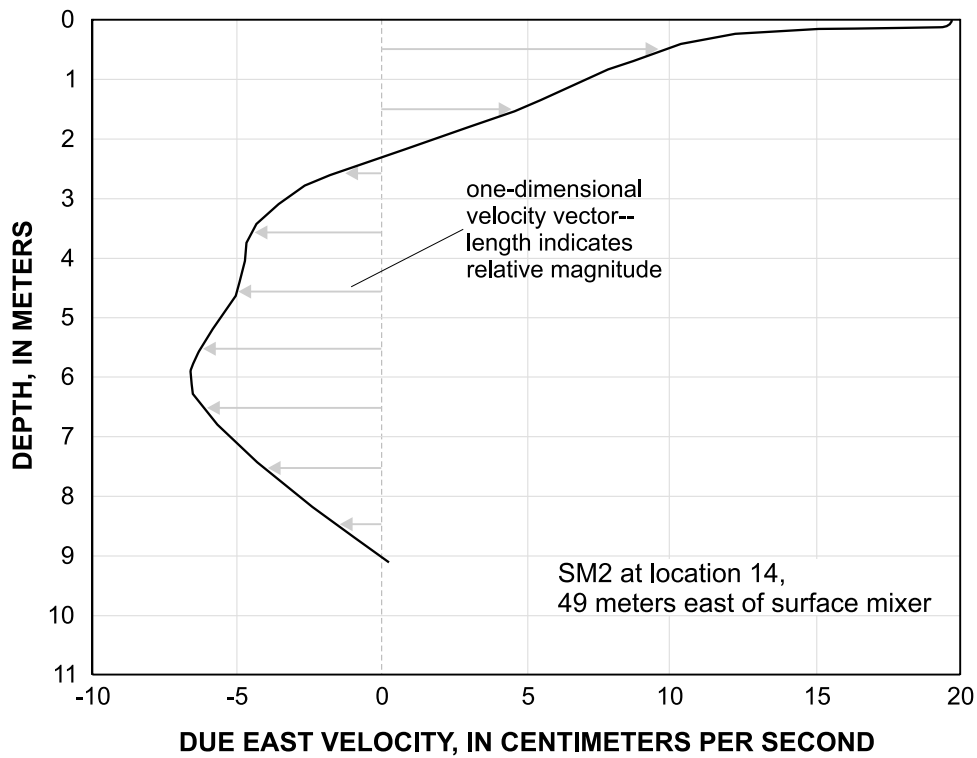
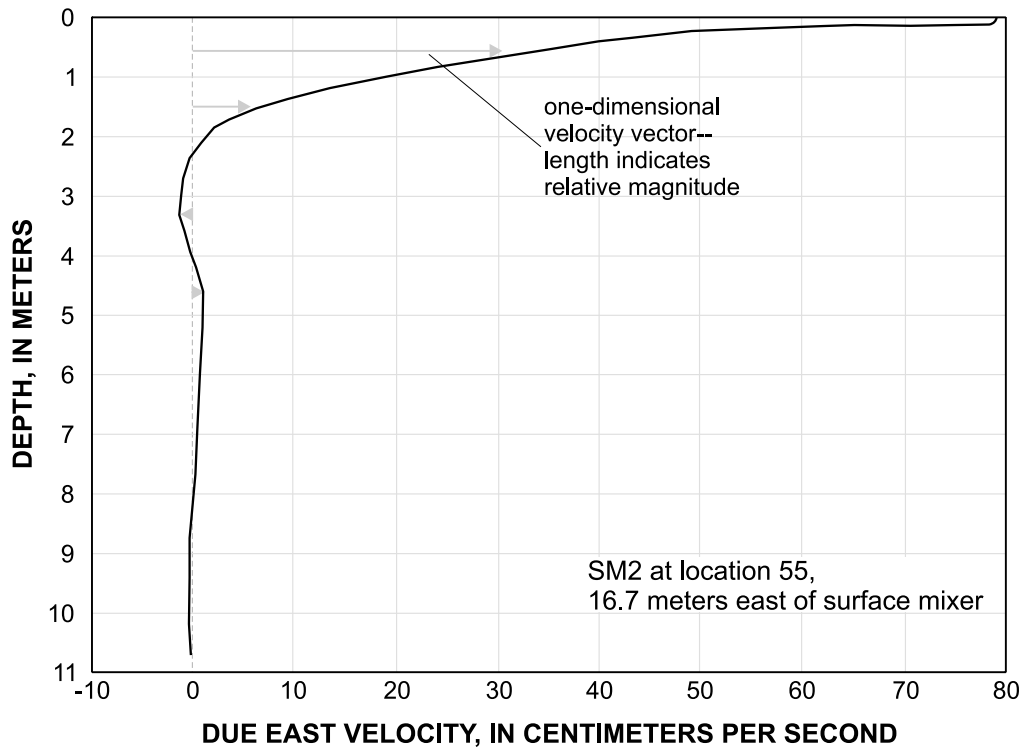


**Figure 34.** Water-velocity profiles during test SM2, 16.7 meters east and 49 meters east of the surface mixer, Egan Quarry, Schaumburg, Illinois, 1997.



**Figure 35.** Data collection set-up during the SM3 test, Egan Quarry, Schaumburg, Ill., July 24, 1997.

by an increase in water temperature throughout the epilimnion and associated reduction in saturation concentrations as the day progressed. Increases in the DO concentrations near the thermocline appear to be caused by the epilimnion (with higher DO concentrations) being depressed down field of the mixer.

## SUMMARY

The U.S. Geological Survey, in cooperation with the U.S. Army Corps of Engineers, collected data to describe mixing patterns induced by aerators and mixers, which will aid in the calibration and verification of the three-dimensional hydrodynamic model, MAC-3D. The model will be used to design an aeration system for a combined sewer overflow storage reservoir. This report describes the test designs, configurations, instrumentation, methods, and data analysis used in the pilot-scale tests and the data collection

in September 1995 in a test tank at the Waterways Experiment Station in Vicksburg, Mississippi, and the field-scale tests, data collection, and analysis at Egan Quarry, Schaumburg, Illinois, during the summers of 1996 and 1997.

Three-dimensional water-velocity profiles were collected during operation of fine-bubble and coarse-bubble aerators in a test tank during September 1995. During summer 1996 and summer 1997, three-dimensional water-velocity and water-temperature, dissolved-oxygen-concentration, and specific-conductivity profiles were collected during operation of a coarse-bubble aerator in a reservoir during strongly stratified and weakly stratified conditions. During summer 1997, the effects of a submersible mixer and a surface mixer also were investigated. The water-mixing patterns induced by the operation of aerators, submersible mixers, and surface mixers were described.

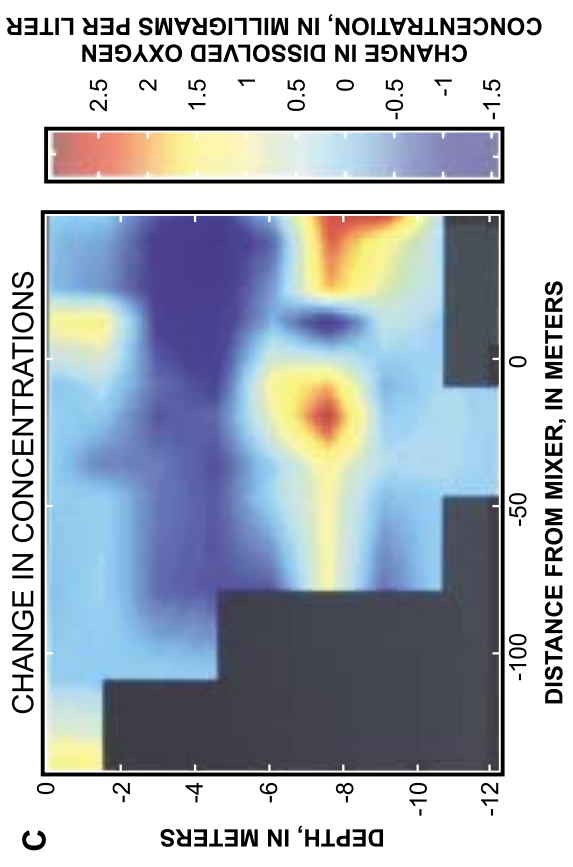
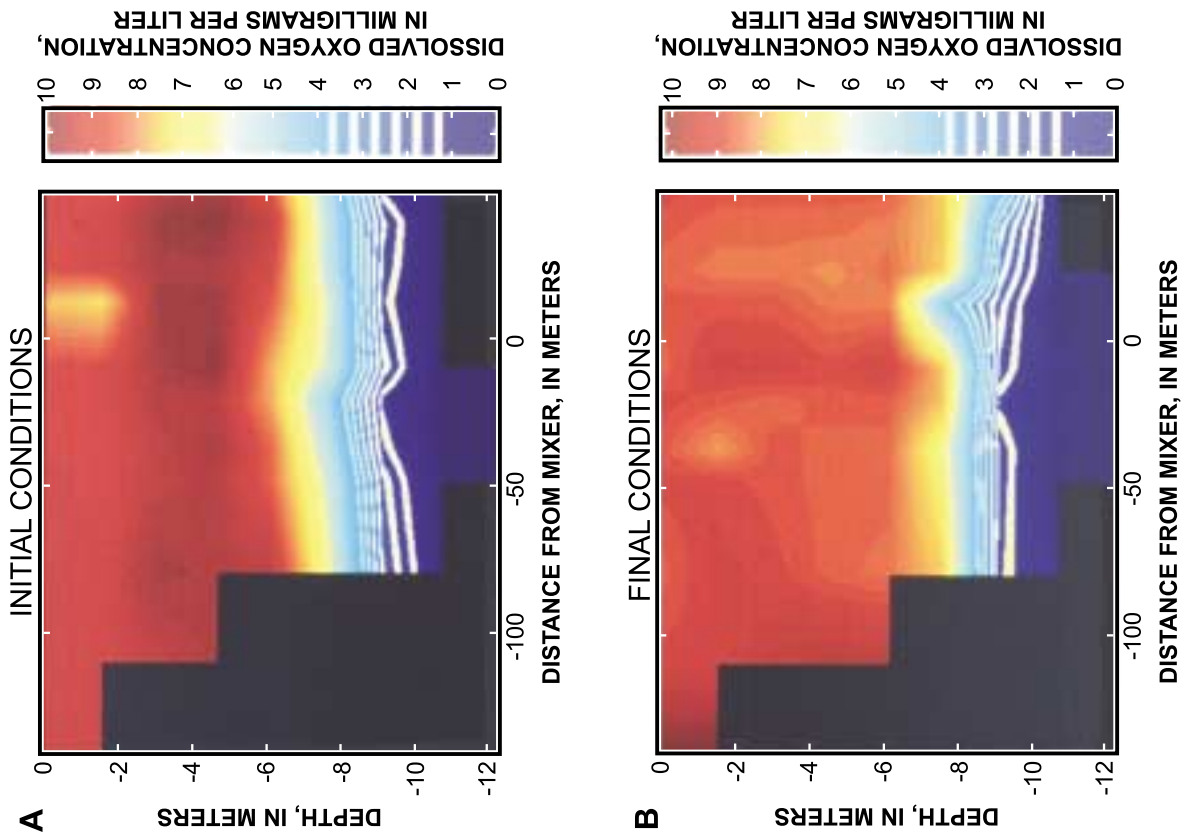


**Figure 36.** Dissolved oxygen data of a west to east cross-section in Egan Quarry during test SM3, Schaumburg, Illinois, July 24, 1997.

Characteristics of the mixing patterns induced by the aerators and mixers during tests in strongly stratified and weakly stratified water were compared to results from simulations with different numerical models. Changes in the stratification of Egan Quarry during a 5-day period of continuous aerator operation during daylight hours also were compared to simulations from the one-dimensional Dynamic Lake Model (DLM). This model accurately simulated changes in the water temperature of Egan Quarry during the period.

Finally, on the basis of temporal and spatial measurements of dissolved oxygen concentrations, the volumetric quantity of oxygen in the reservoir was quantified before and after operation of a submersible mixer. A net loss of oxygen was calculated, which may have been the result of increases in water temperature in the epilimnion and an associated reduction in dissolved oxygen concentrations.

## REFERENCES CITED

- Bernard, R.S., 1996, Preliminary validation of the MAC-3D numerical flow model, *in* Proceedings of the North American water and environment Congress '96: Anaheim, Calif., A.S.C.E. Conference, session C-160, June 22–28, 1996.
- 1997, Extension and validation of the MAC-3D numerical model for applications involving bubble diffusers, *in* Proceedings of the 27th Congress of the International Association for hydraulic research, theme B: San Francisco, Calif., August 10–15, 1997.
- Cooke, G.D., Welch, E.B., Peterson, S.A., and Newroth, P.R., 1986, *Lake and reservoir restoration*, Butterworths: Stoneham, Mass.
- Hornewer, N.J., Johnson, G.P., Robertson, D.M., and Hondzo, M., 1997, Field-scale tests for determining mixing patterns associated with coarse-bubble air diffuser configurations, Egan Quarry, Illinois *in* Proceedings of the 27th Congress of the International Association for hydraulic research, theme B: San Francisco, Calif., August 10–15, 1997, p. 57–63.
- Hydrolab, 1991, Surveyor 3 brochure, Bulletin no. SVR3-BRO2 Apr1991: Austin Texas, Hydrolab Corporation.
- Imberger, J., and Patterson, J.C., 1981, A dynamic reservoir simulation model- DYRESM: 5, Transport models for inland and coastal waters, *in* Fischer, H.B., ed., Academic: New York, p. 310–361.
- Lemckert, J.C., and Imberger, J., 1993, Energetic bubble plumes in arbitrary stratification: *Journal of Hydraulic Engineering*, vol. 119(6), p. 680–703.
- McCord, S.A., Schladow, S.G., and Miller, T.G., 2000, Modeling artificial aeration kinetics in ice-covered lakes: *Journal of Environmental Engineering*, vol. 124, no. 1, p. 21–31.
- McDougall, T.J., 1978, Bubble plumes in stratified environments: *Journal of Fluid Mechanics*, vol. 85, p. 655–672.
- Olson, D.T., 1998, The thermal response of a small water body to bubble-plum destratification: M.S. thesis, Department of Civil Engineering, University of Illinois at Urbana-Champaign, 162 p.
- Patterson, J.C., and Imberger, J., 1989, Simulation of bubble plume destratification systems in reservoirs: *Aquatic Science*, vol. 51(1), p. 3–18.
- RD Instruments, 1995, Direct reading and self-contained Broadband Acoustic Doppler Current Profiler technical manual, P/N 951-6046-00 (Aug 95 C1): San Diego, Calif., RD Instruments.
- Robertson, D.M., Schladow, S.G., and Patterson, J.C., 1991, Interacting bubble plumes: the effect on aerator design, *in* Lee, J.H.W. and Cheung, Y.K. eds., *Environmental Hydraulics: Hong Kong, Balkema, Rotterdam*, Proceedings of the International Symposium on Environmental Hydraulics, p. 167–172.
- Schladow, S.G., 1992, Bubble plume dynamics in a stratified medium and the implications for water quality amelioration in lakes: *Water Resources Research*, vol. 28(2), p. 313–321.
- Schladow, S.G., and Fischer, I.H., 1995, The physical response of temperate lakes to artificial destratification: *Journal of Limnology and Oceanography*, vol. 40 (2), p. 359–373.
- Sontek, 1994, ADV information and specifications brochure: San Diego, Calif., Sontek Company.
- Zic, K., Stefan, H.G., and Ellis, C., 1992, Laboratory study of water destratification by a bubble plume: *Journal of Hydraulic Research*, vol. 30:1, p. 7–26.

---

---

## APPENDIX

---

---



APPENDIX 1. MAPS OF DATA-COLLECTION LOCATIONS

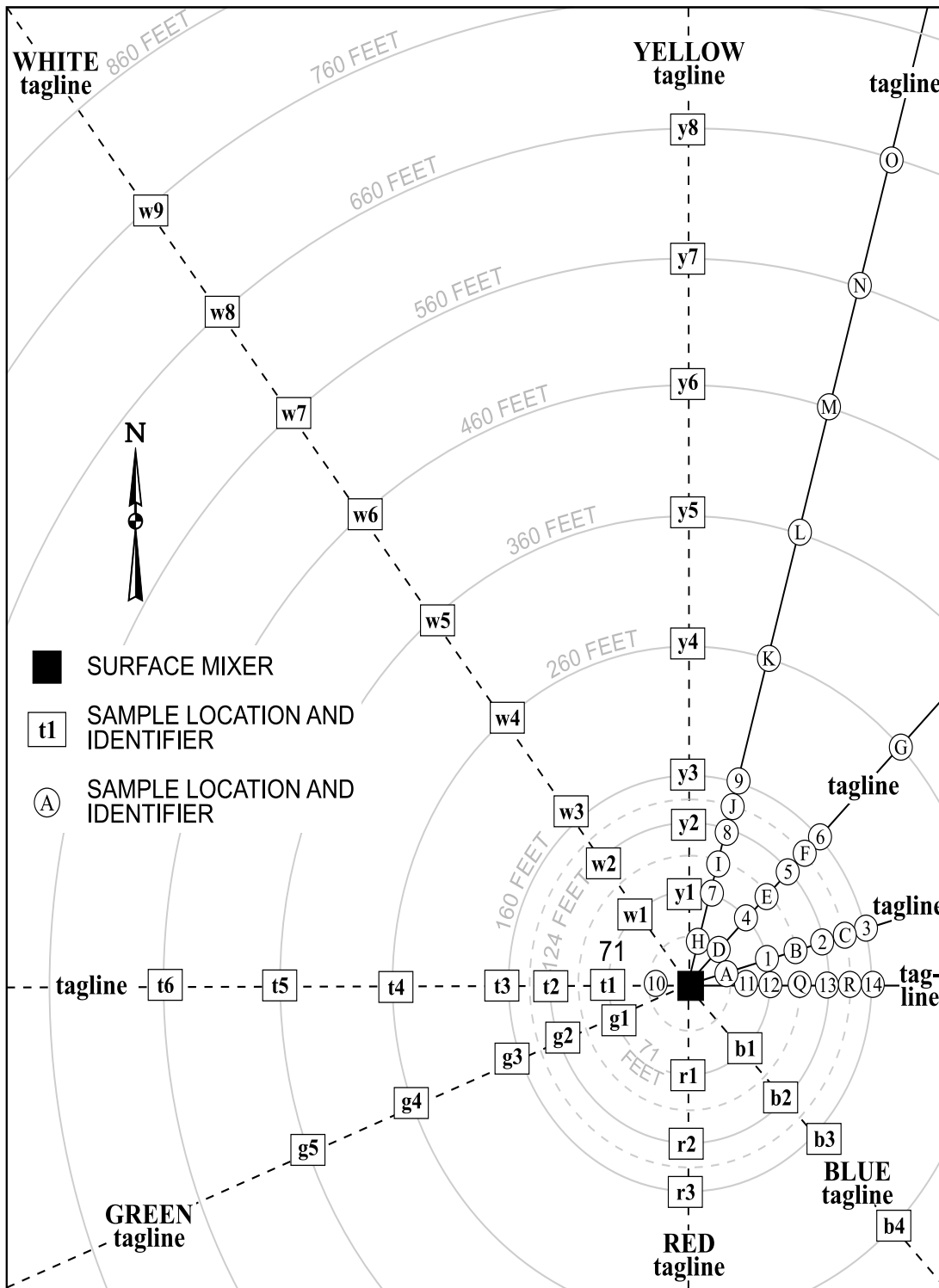


Figure 1-1. Layout for three surface-mixer tests, SM1, SM2, and SM3.

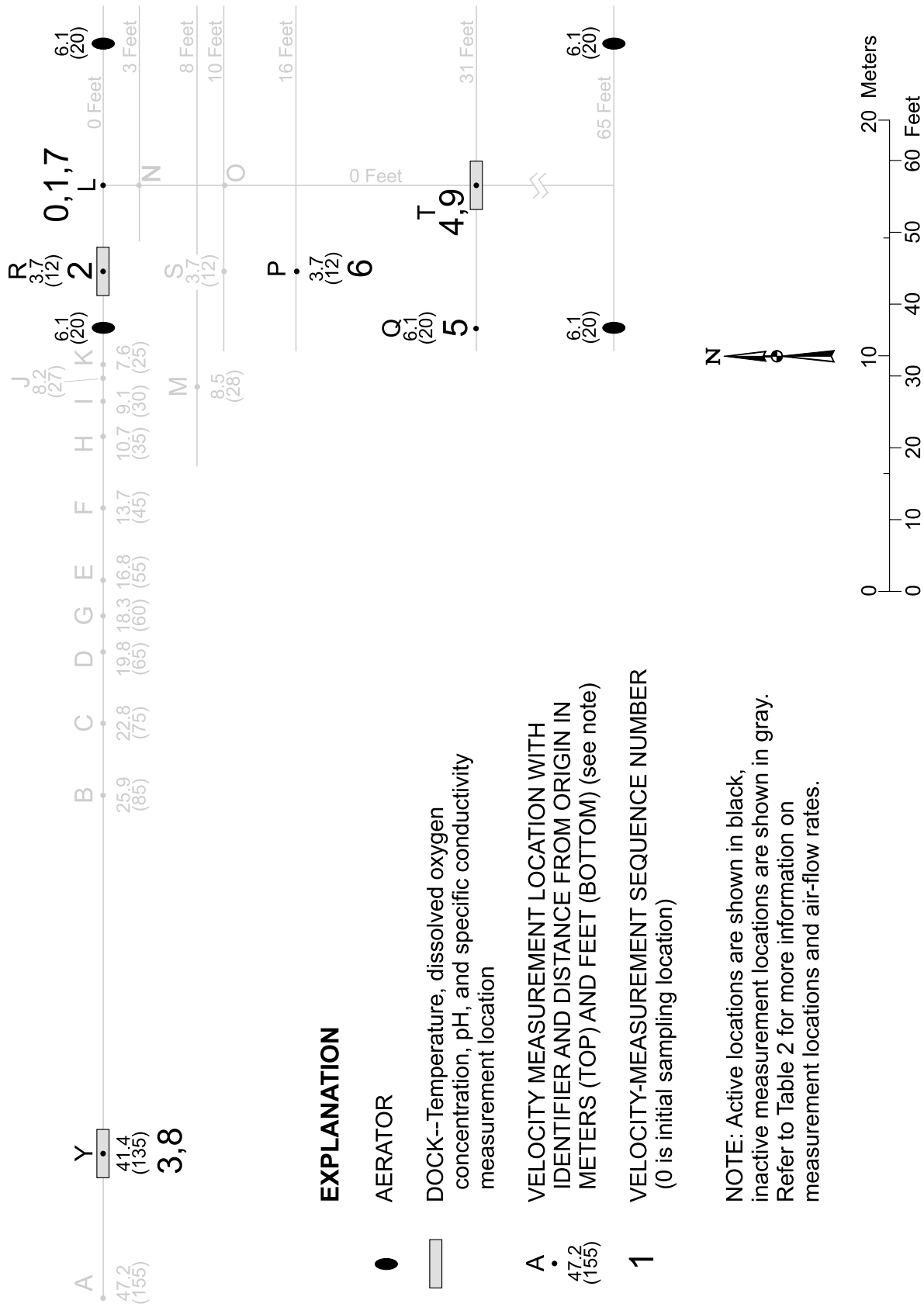
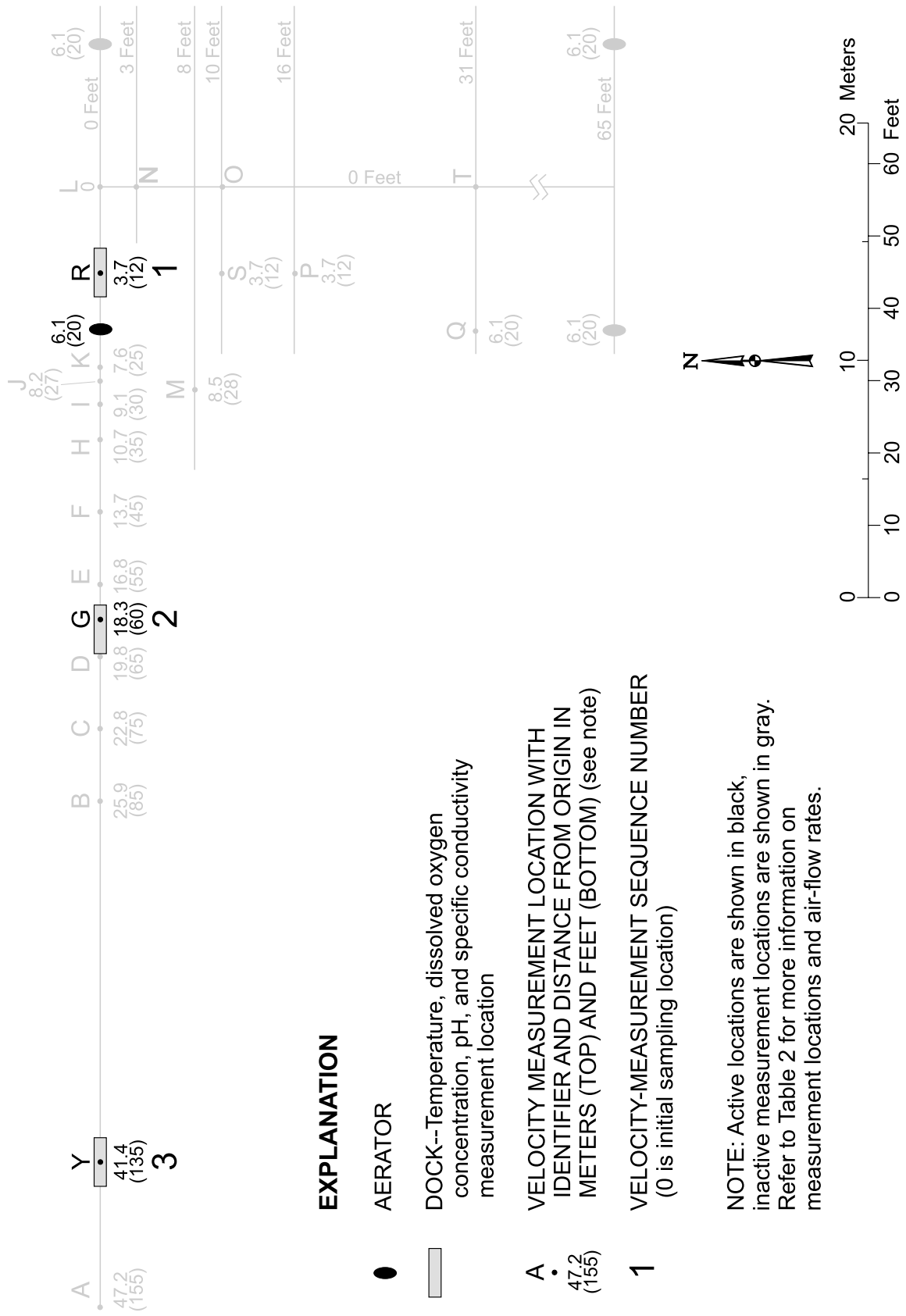


Figure 1-2. Layout for test "eg961d" on September 3, 1996.



**EXPLANATION**

● AERATOR

▭ DOCK-- Temperature, dissolved oxygen concentration, pH, and specific conductivity measurement location

● VELOCITY MEASUREMENT LOCATION WITH IDENTIFIER AND DISTANCE FROM ORIGIN IN METERS (TOP) AND FEET (BOTTOM) (see note)

1 VELOCITY-MEASUREMENT SEQUENCE NUMBER (0 is initial sampling location)

NOTE: Active locations are shown in black, inactive measurement locations are shown in gray. Refer to Table 2 for more information on measurement locations and air-flow rates.

Figure 1-3. Layout for test "eg961s" on August 22, 1996.

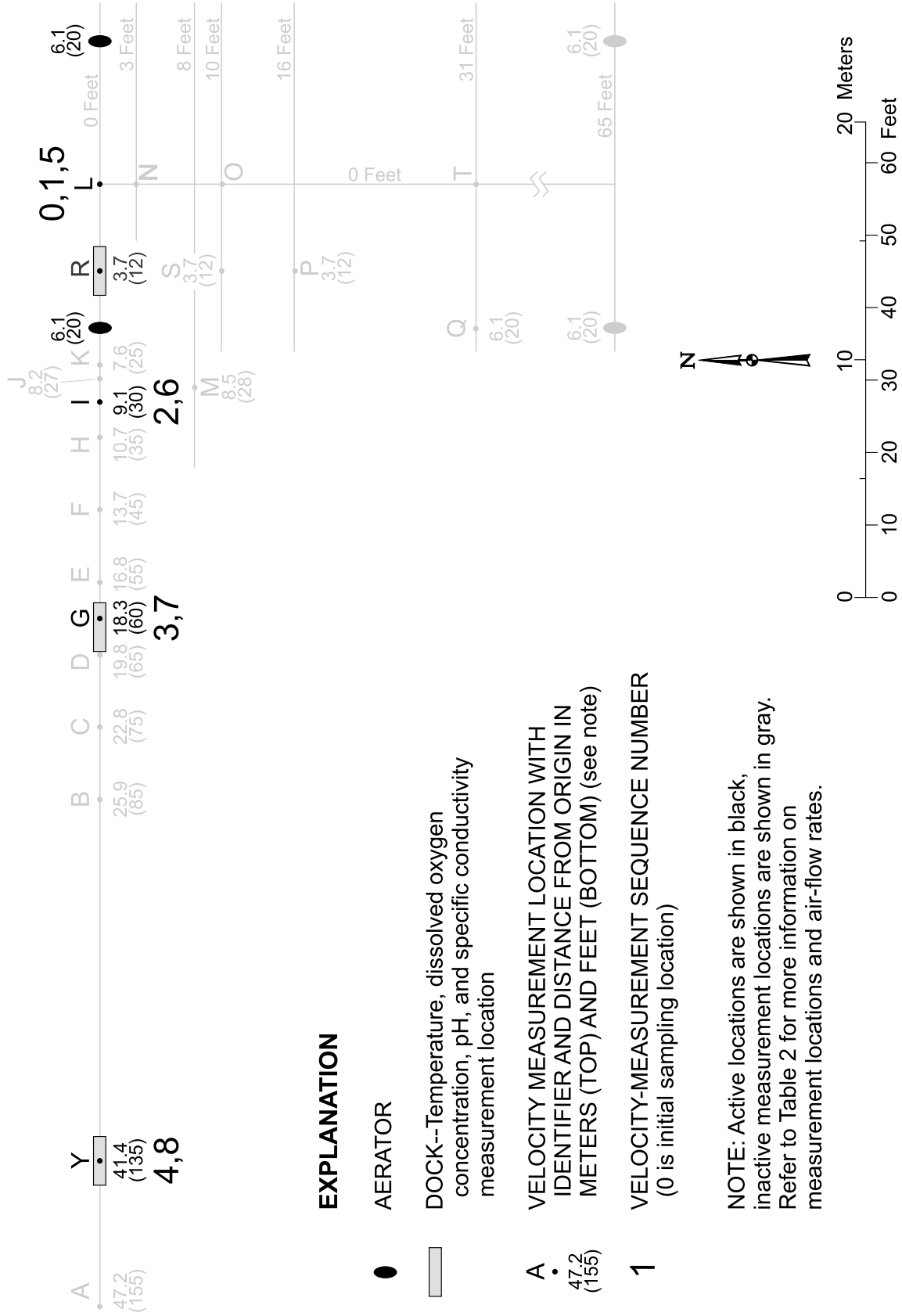


Figure 1-4. Layout for test "eg962d" on September 4, 1996.

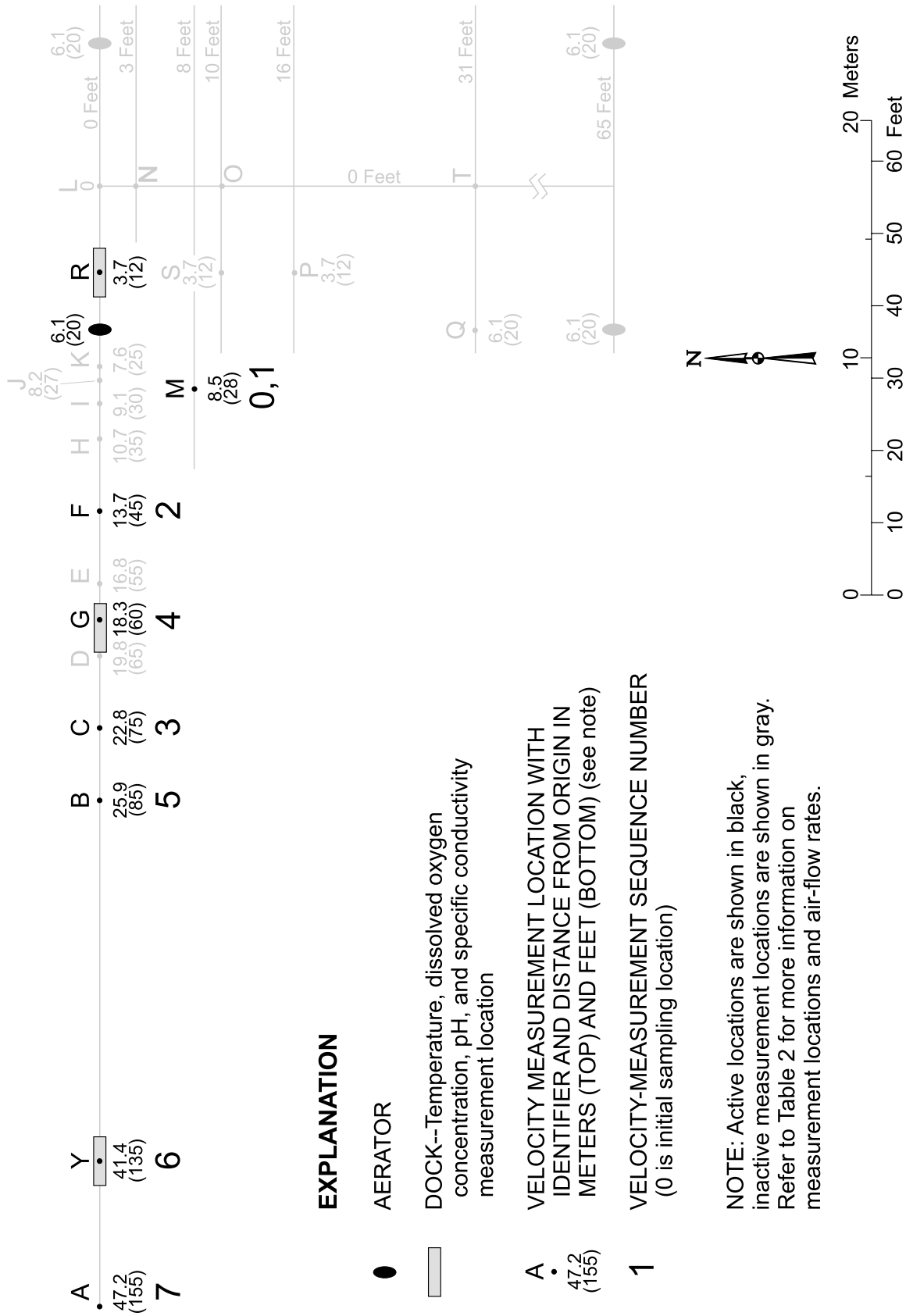


Figure 1-5. Layout for test "eg962s" on August 27, 1996.

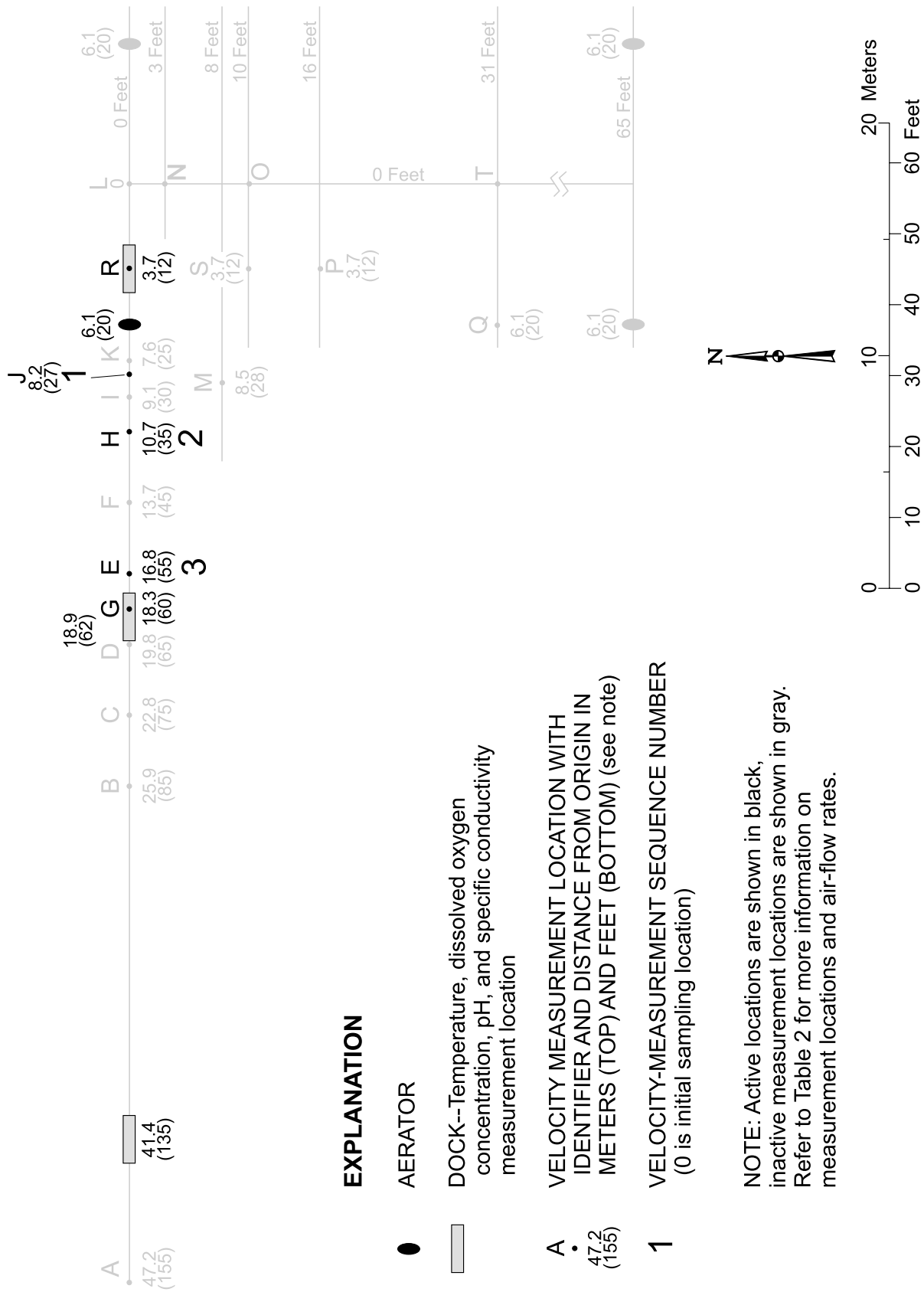
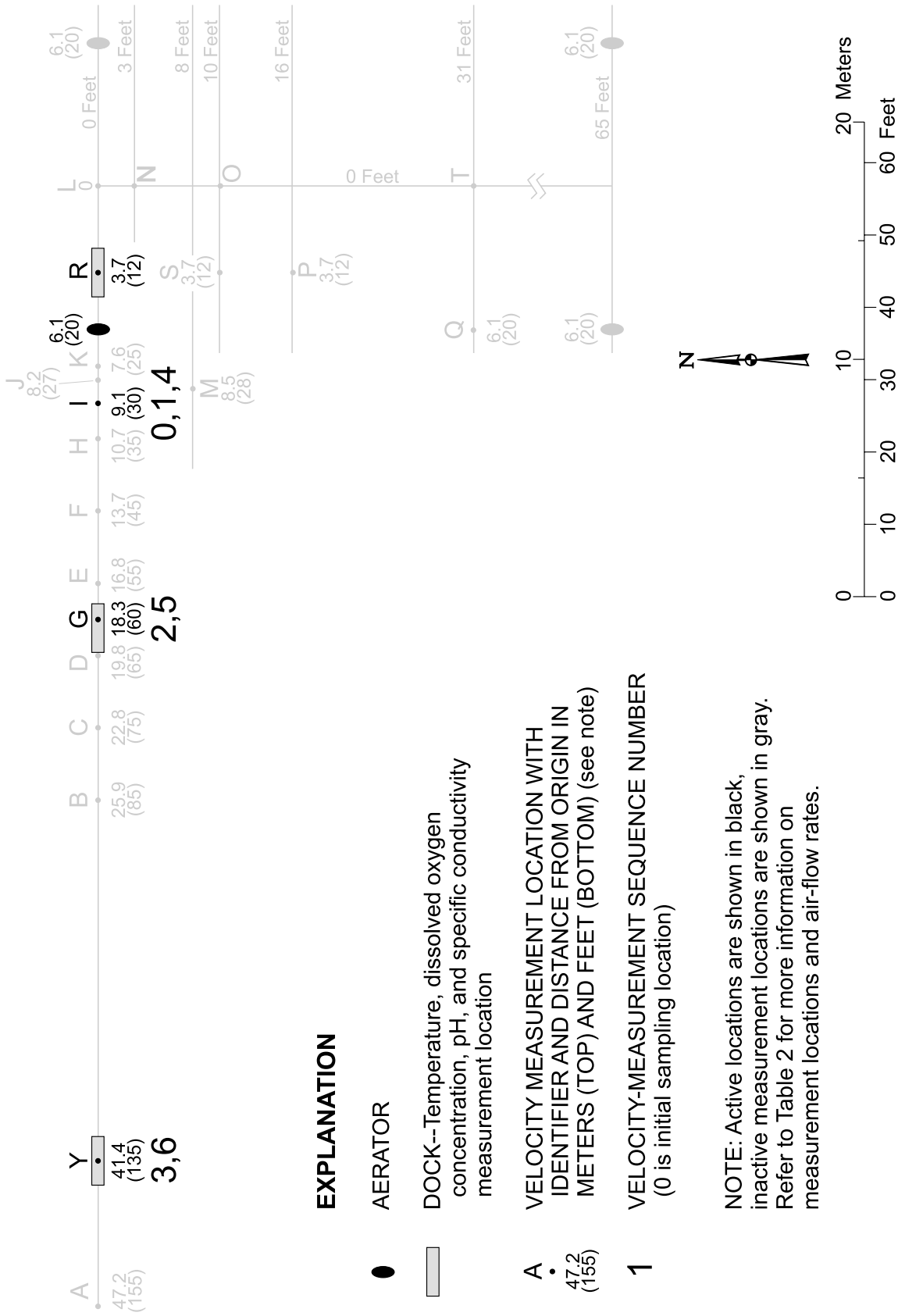


Figure 1-6. Layout for test "eg962s" on August 27, 1996.



**EXPLANATION**

● AERATOR

▬ DOCK-- Temperature, dissolved oxygen concentration, pH, and specific conductivity measurement location

A ● VELOCITY MEASUREMENT LOCATION WITH IDENTIFIER AND DISTANCE FROM ORIGIN IN METERS (TOP) AND FEET (BOTTOM) (see note)

1 VELOCITY-MEASUREMENT SEQUENCE NUMBER (0 is initial sampling location)

NOTE: Active locations are shown in black, inactive measurement locations are shown in gray. Refer to Table 2 for more information on measurement locations and air-flow rates.

Figure 1-7. Layout for test "eg963d" on September 5, 1996.

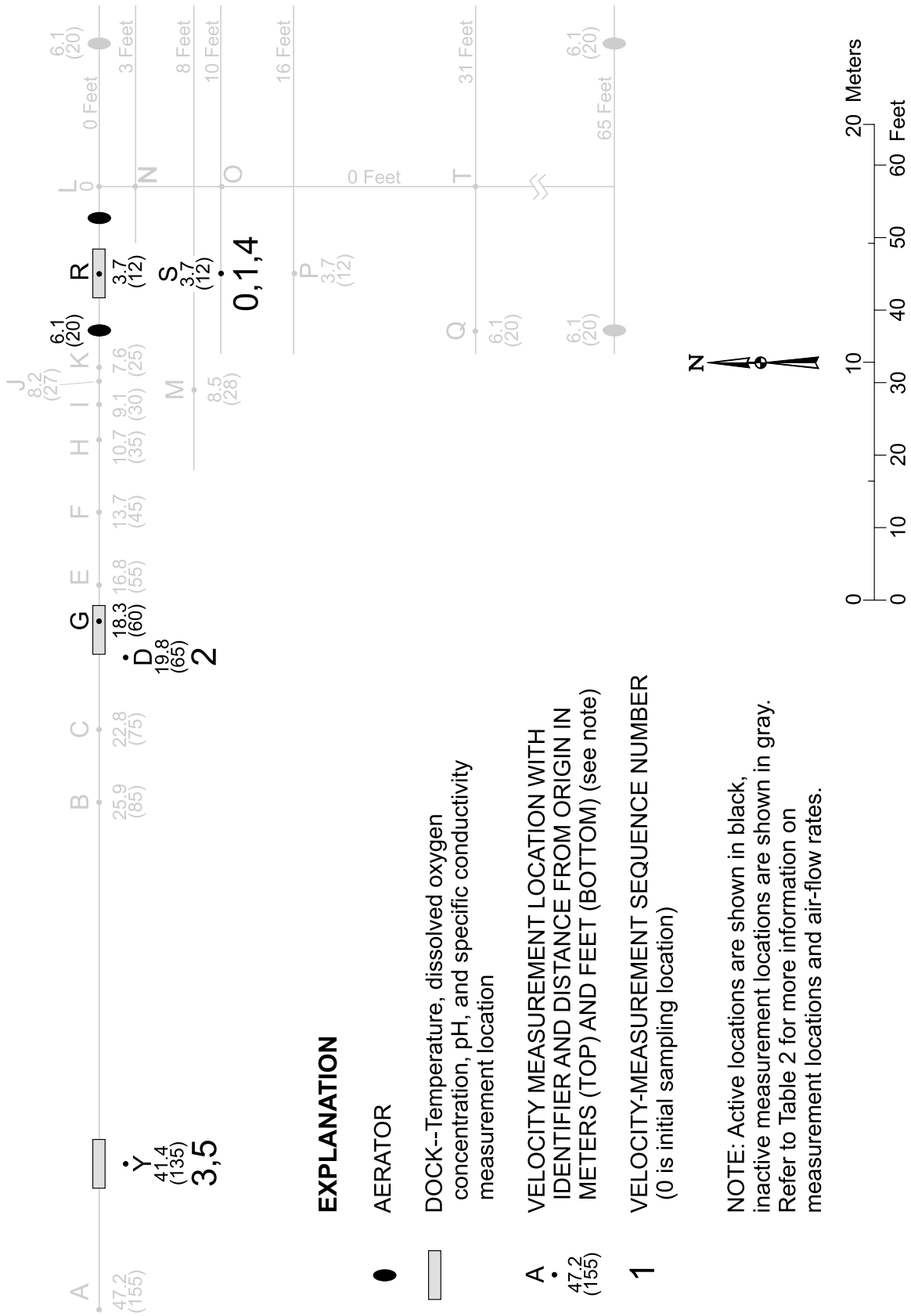


Figure 1-8. Layout for test "eg963s" on August 23, 1996.

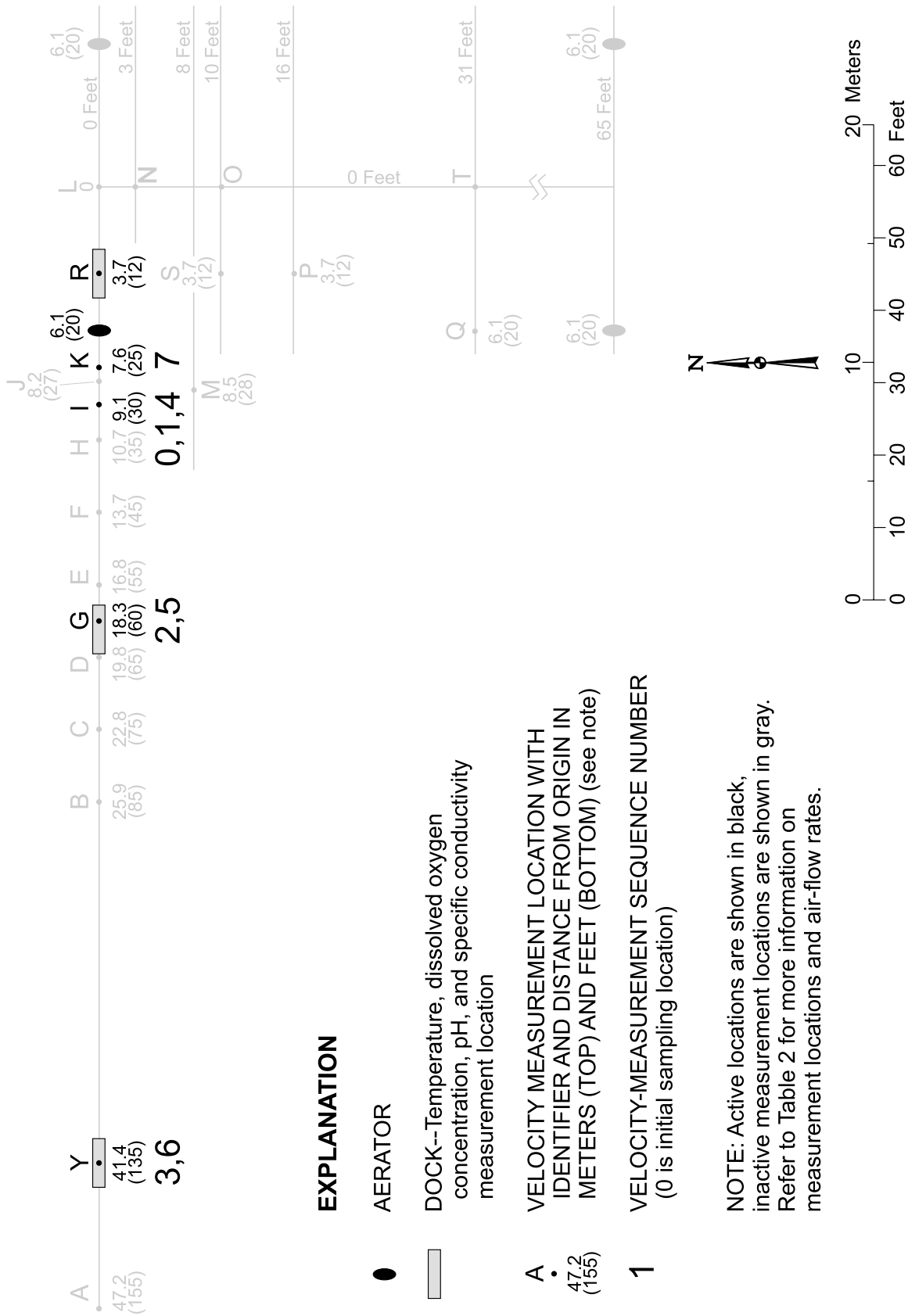


Figure 1-9. Layout for test "eg964d" on September 5, 1996.

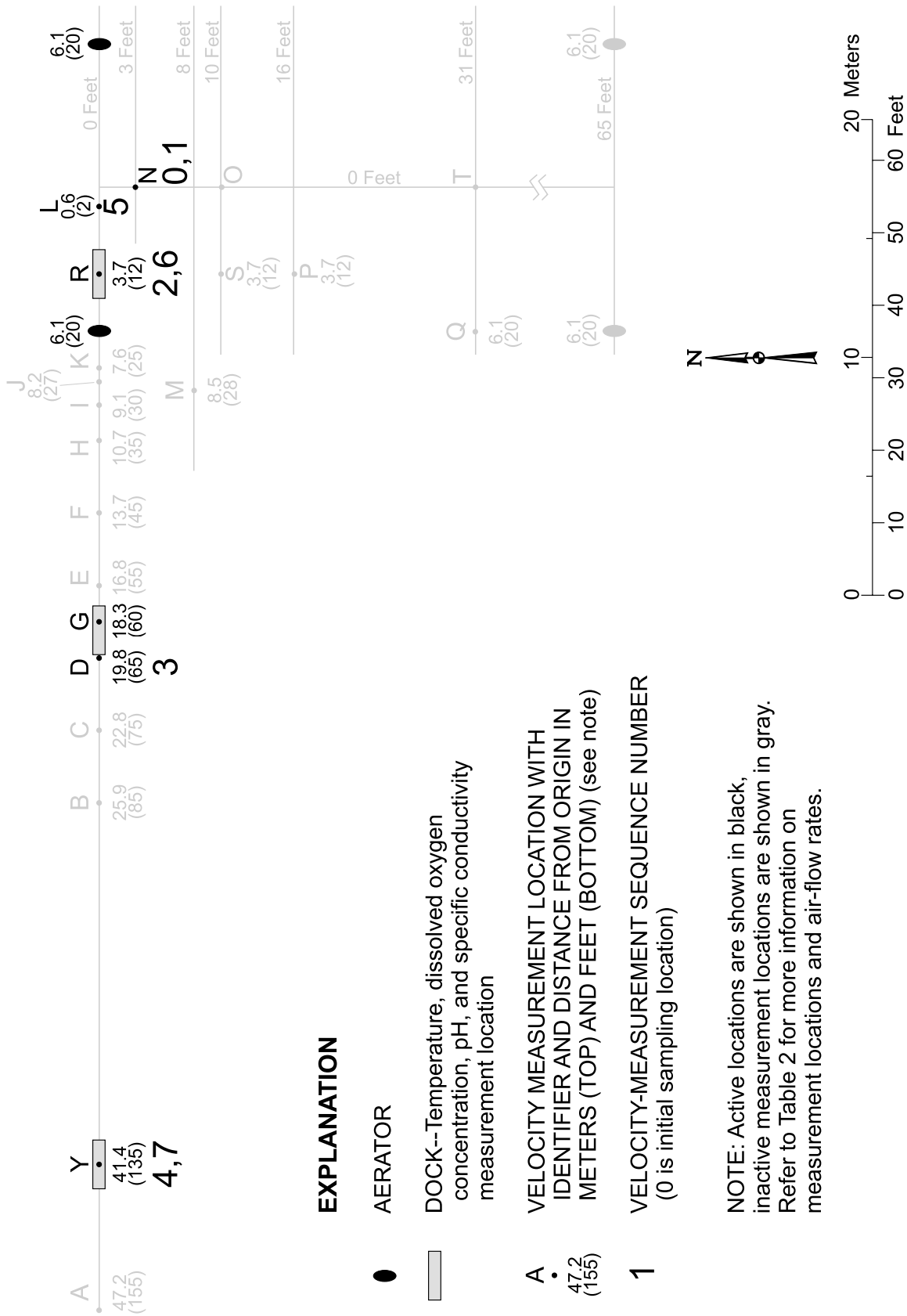


Figure 1–10. Layout for test "eg964s" on August 26, 1996.

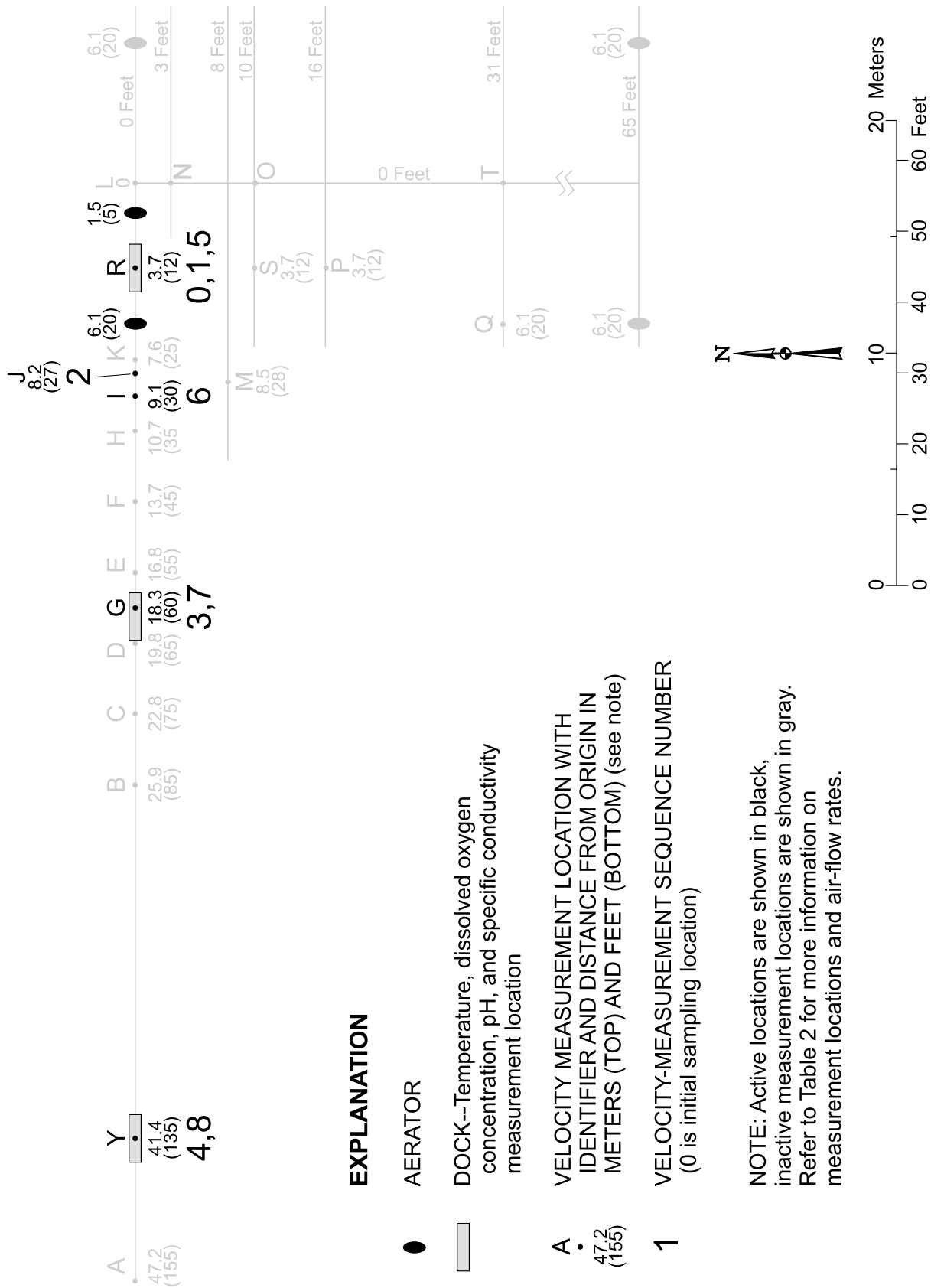


Figure 1-11. Layout for test "eg965d" on September 6, 1996.

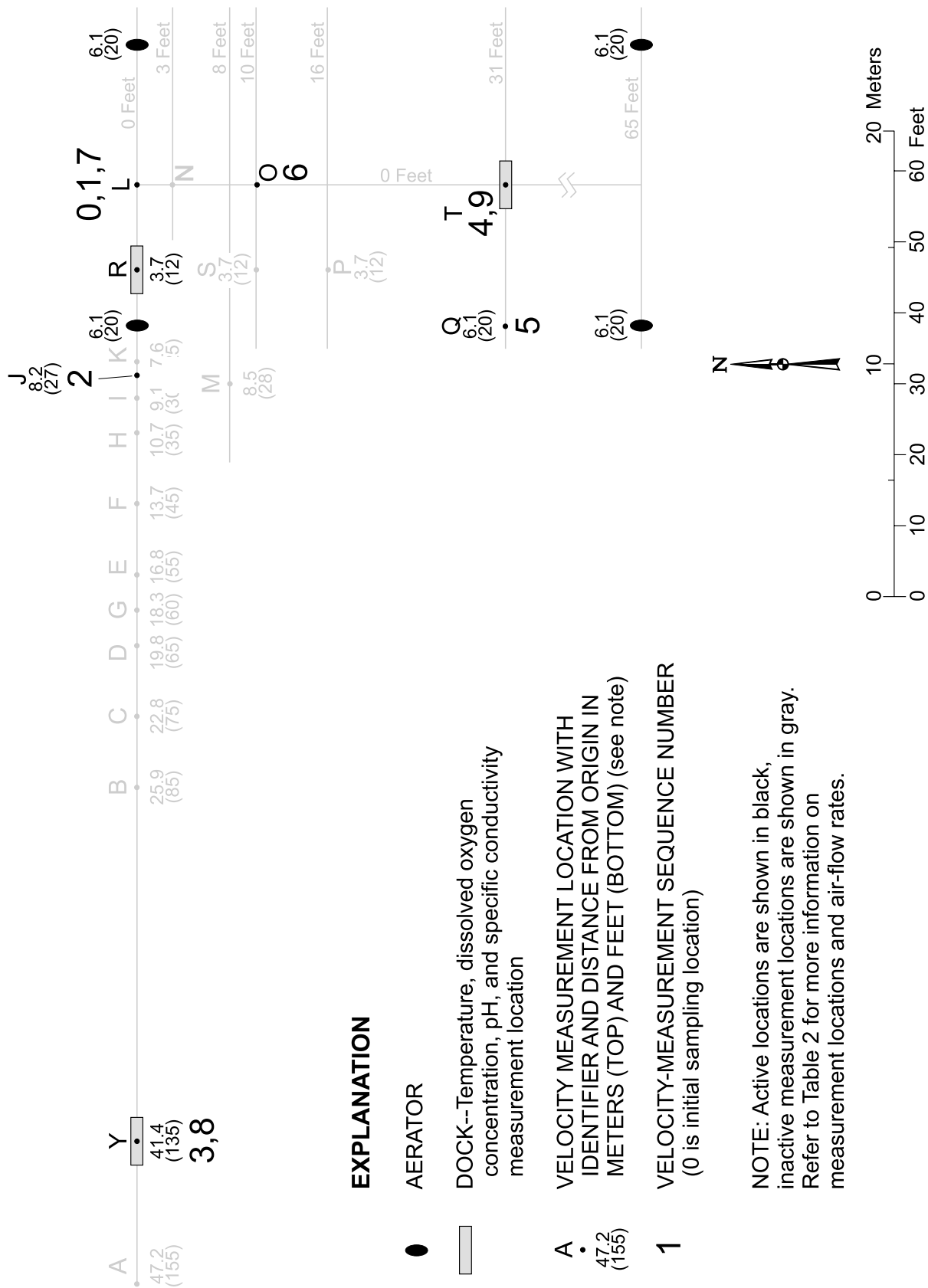


Figure 1-12: Layout for test "eg965s" on August 28, 1996.

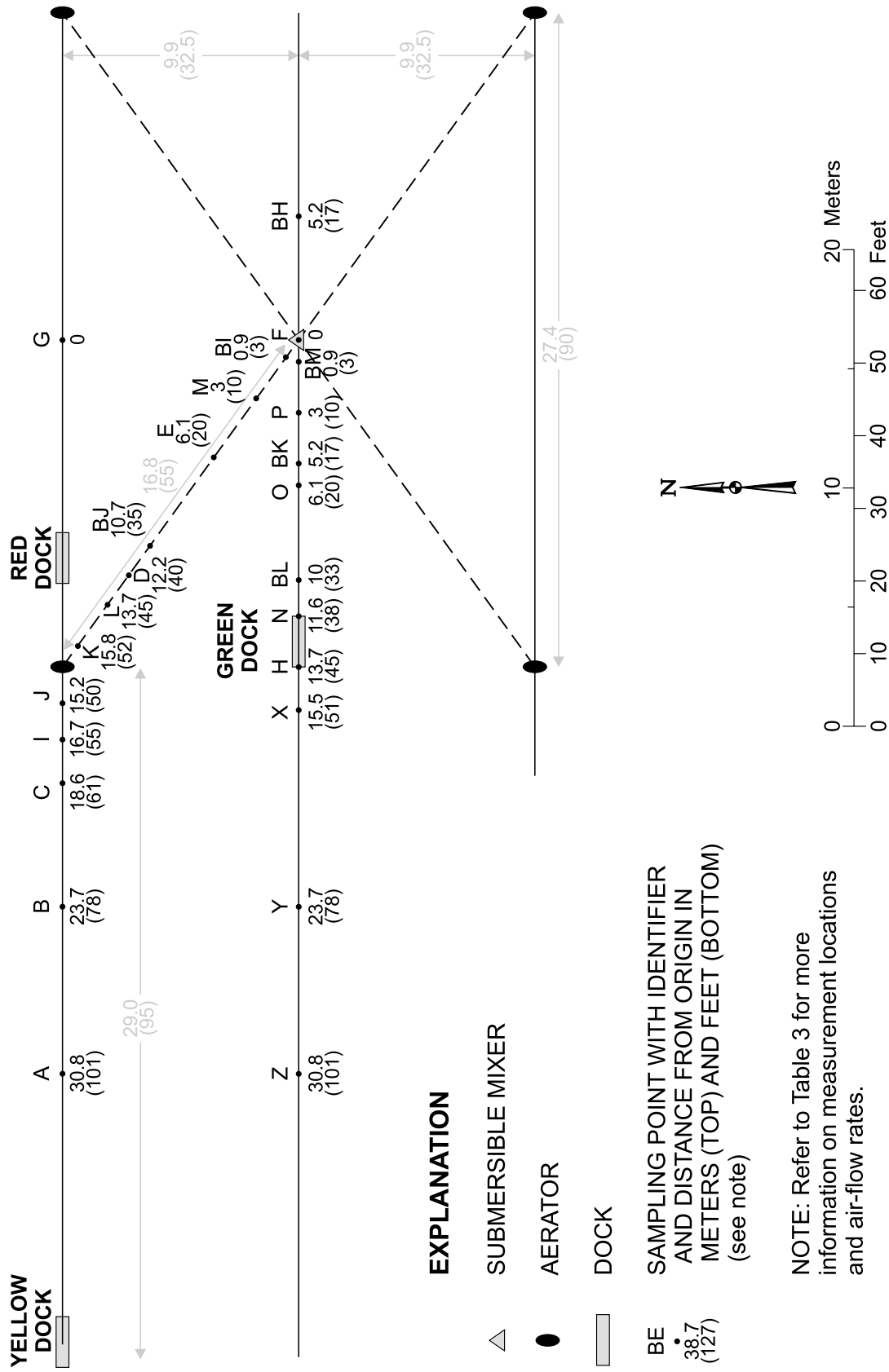


Figure 1-13. Layout for test "eg971d" on June 16, 1997.

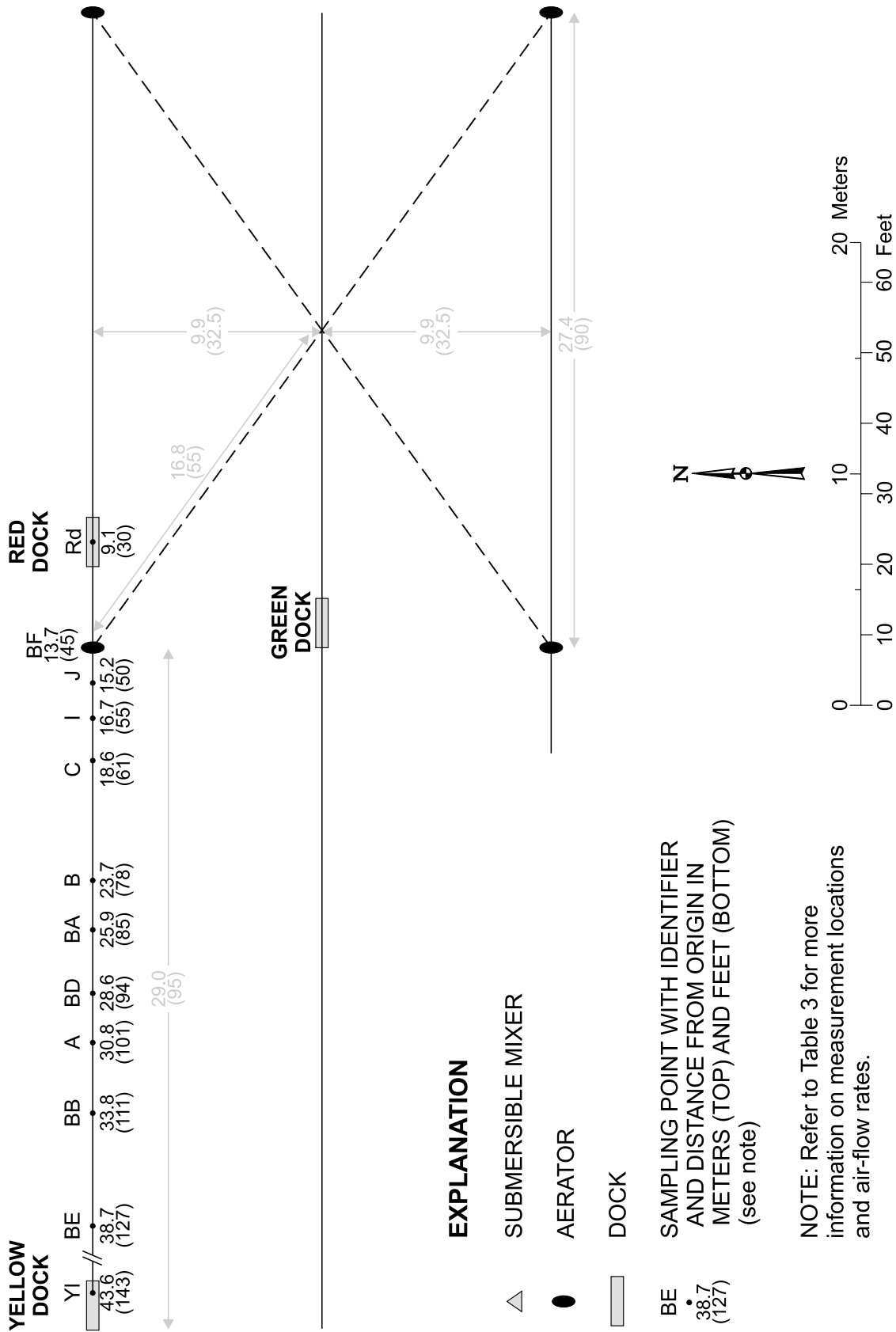


Figure 1-14. Layout for test "eg971s" on June 3, 1997.

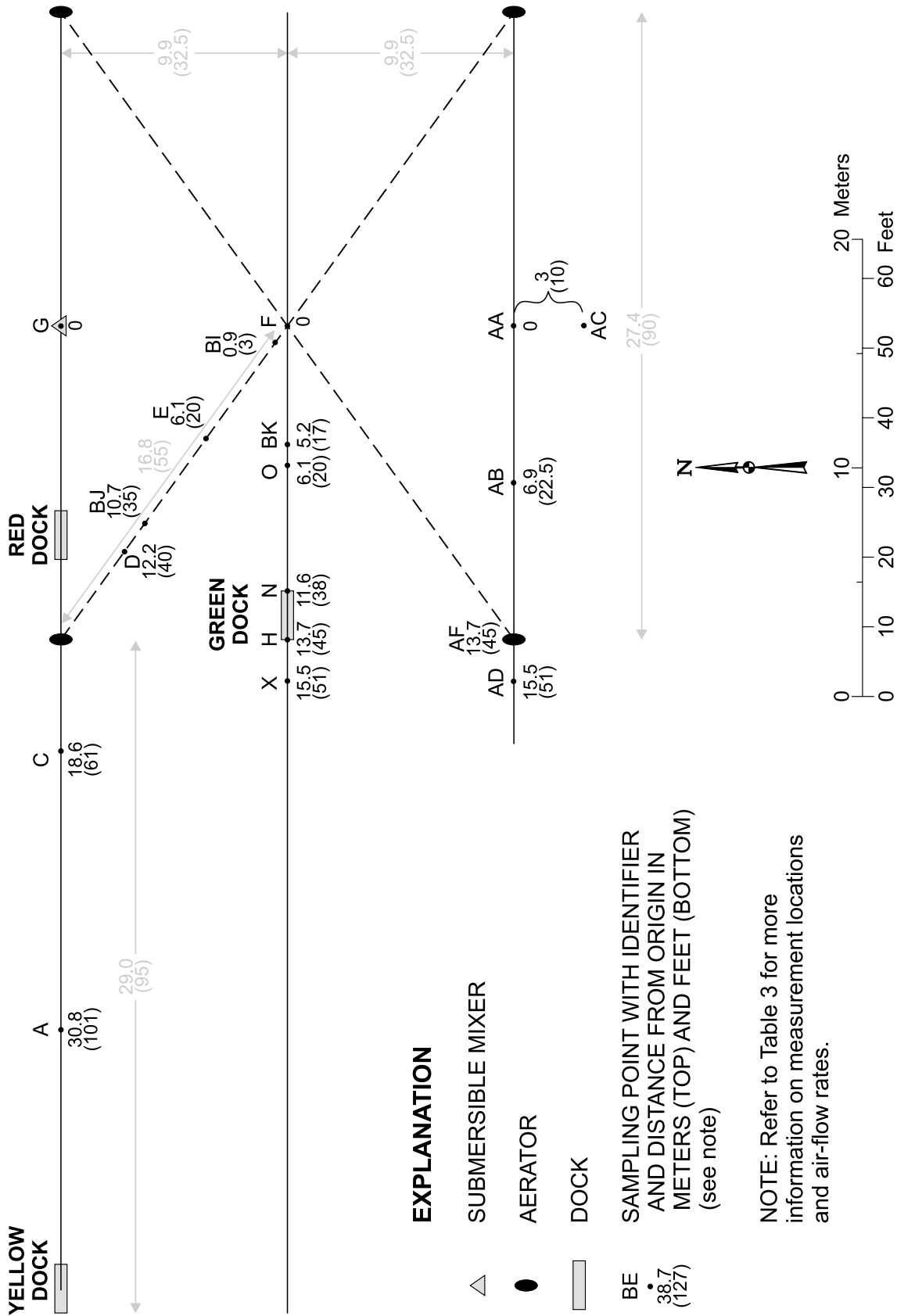


Figure 1-15. Layout for test "eg972d" on June 17, 1997.

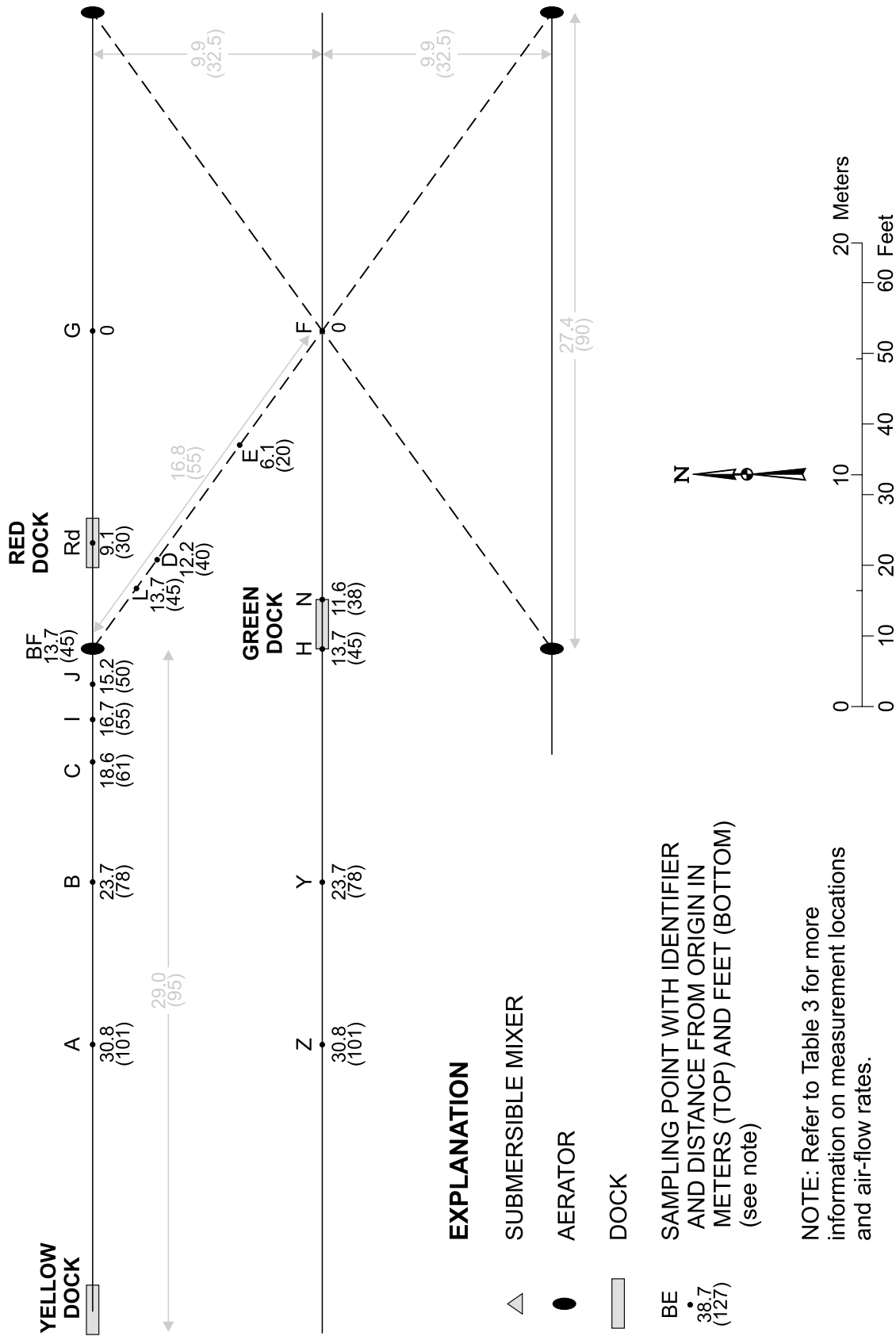


Figure 1-16. Layout for test "eg972s" on June 4, 1997.

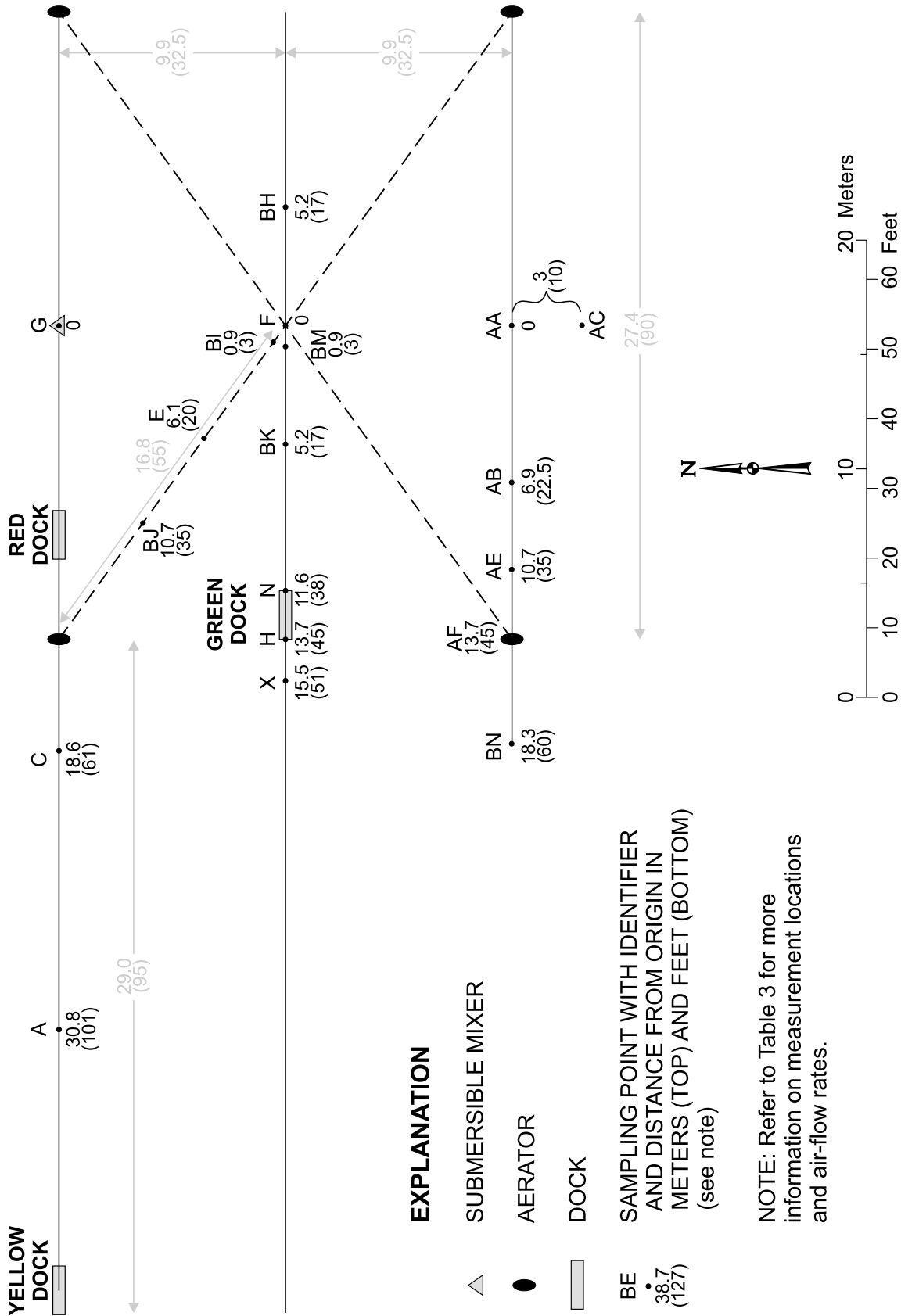


Figure 1-17. Layout for test "eg973d" on June 18, 1997.

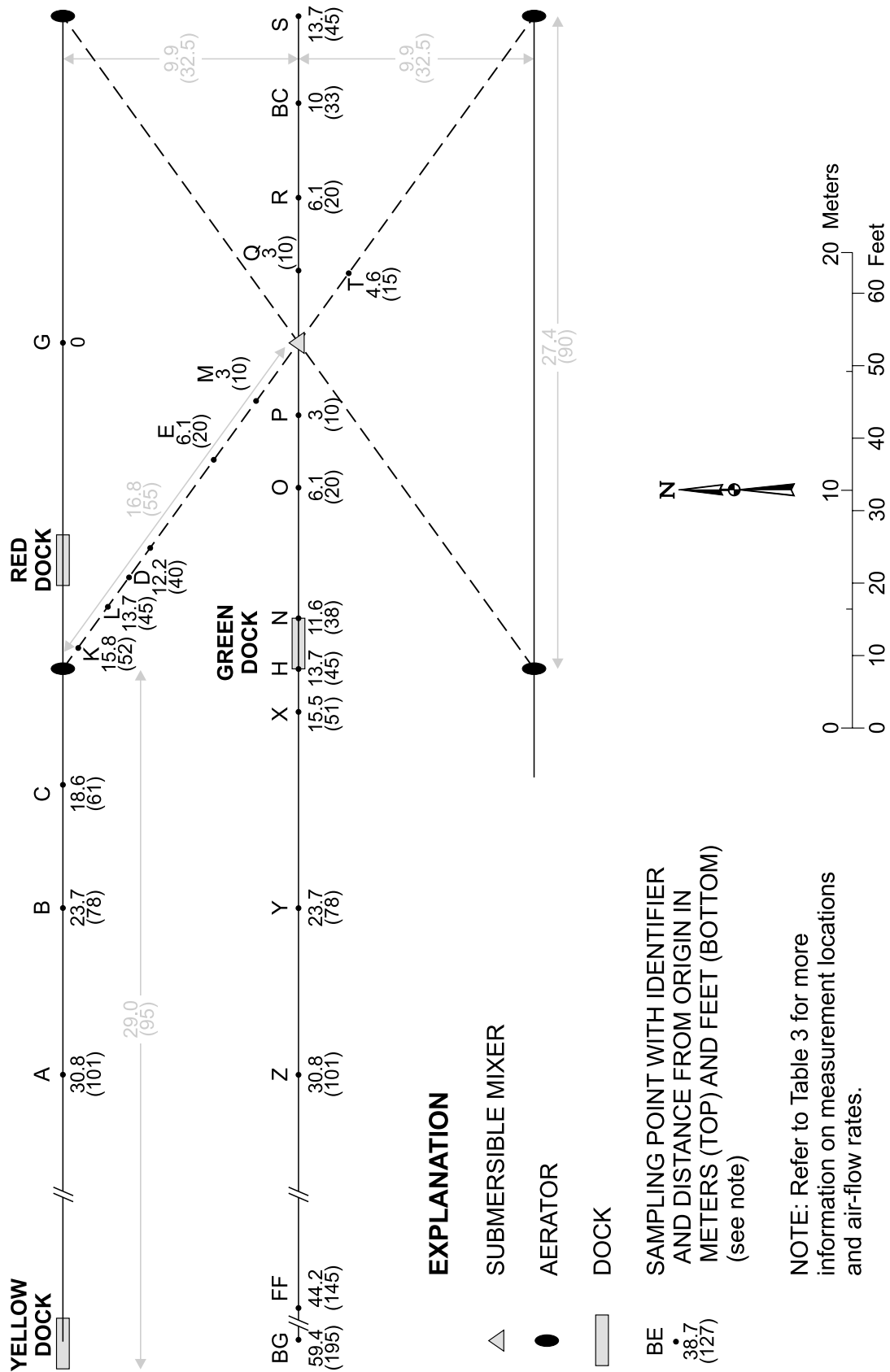


Figure 1-18. Layout for test "eg973s" on June 10, 1997.

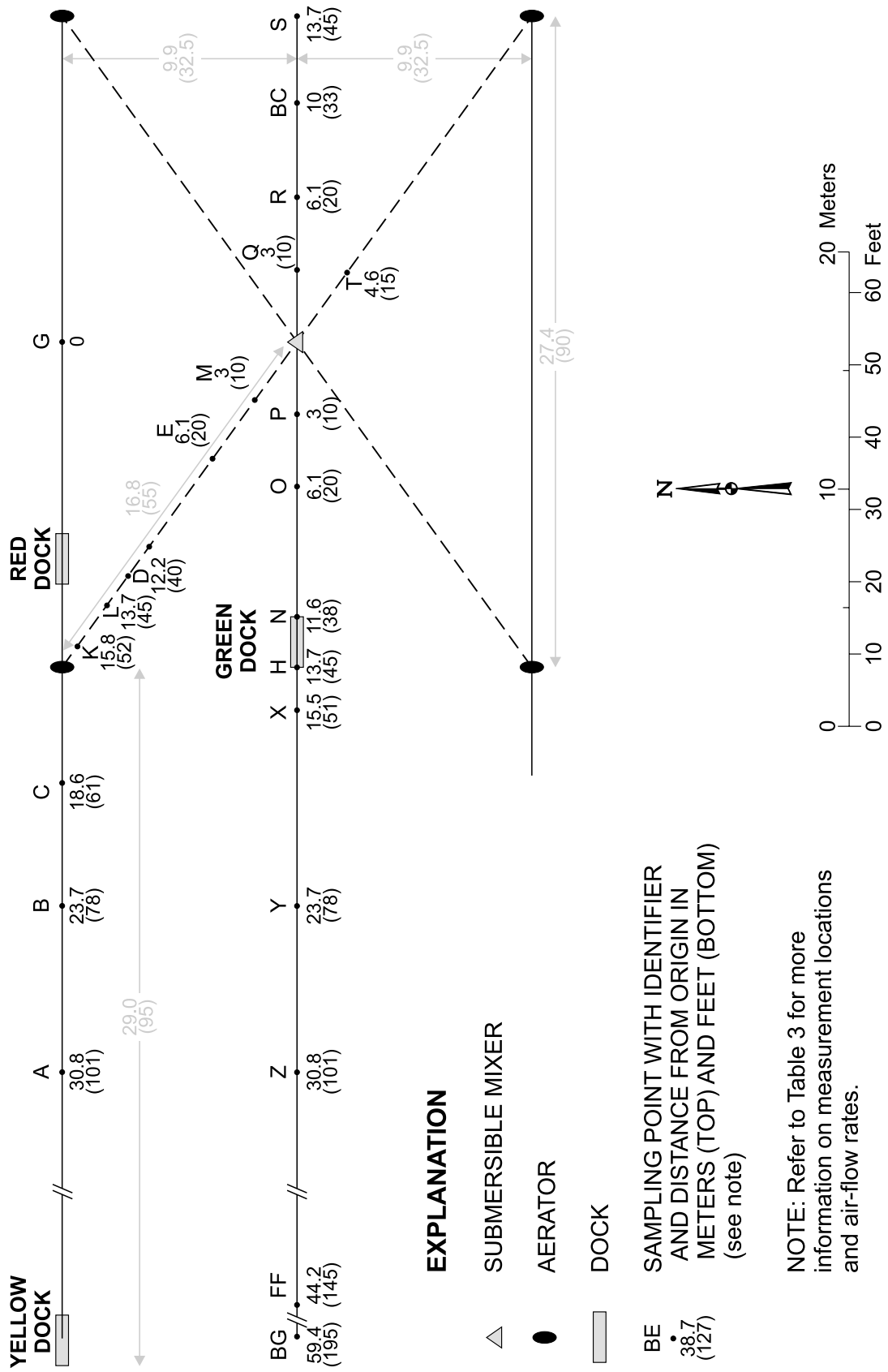


Figure 1-19. 69

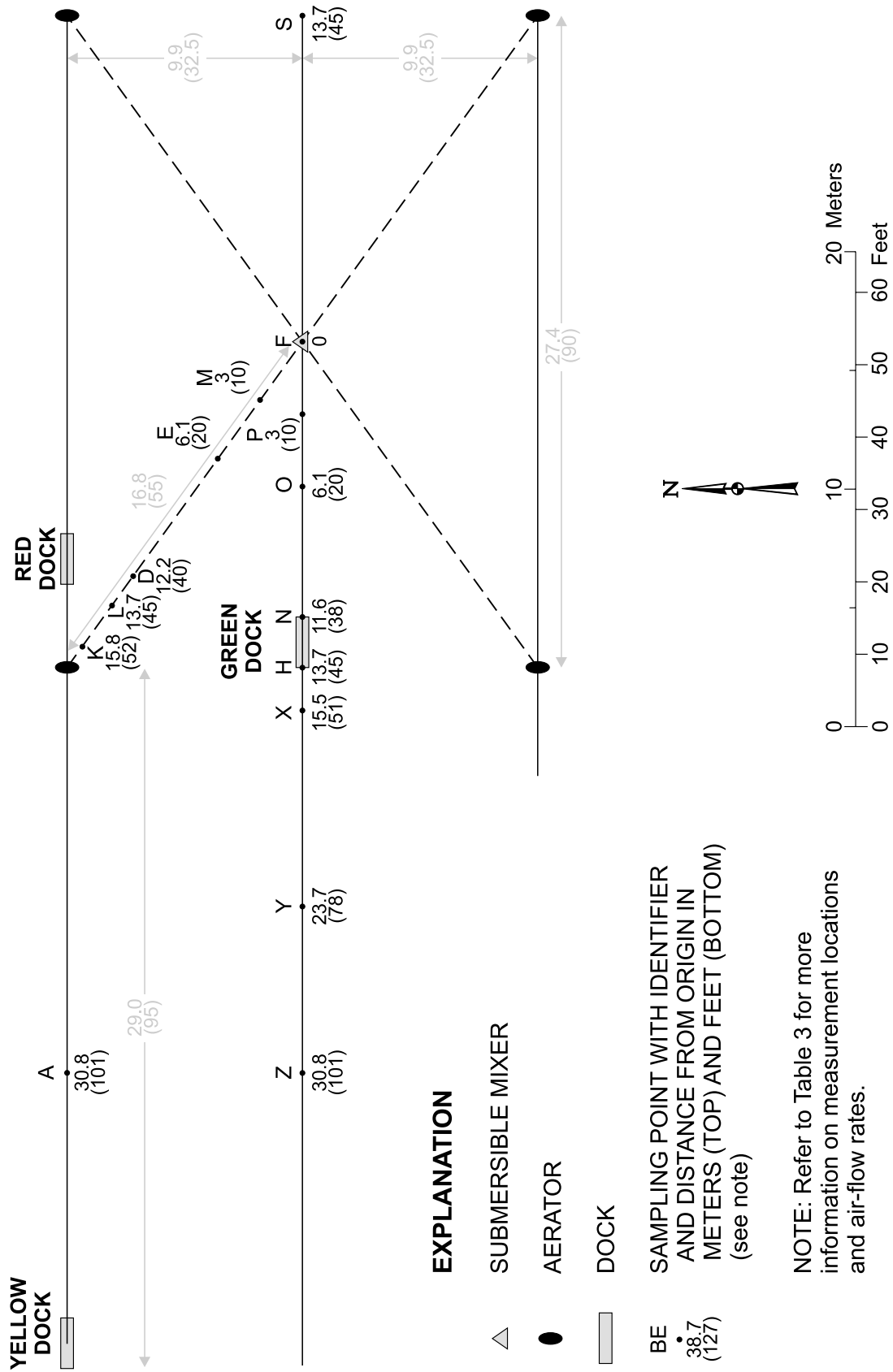


Figure 1-20. Layout for test "eg974s" on June 11, 1997.

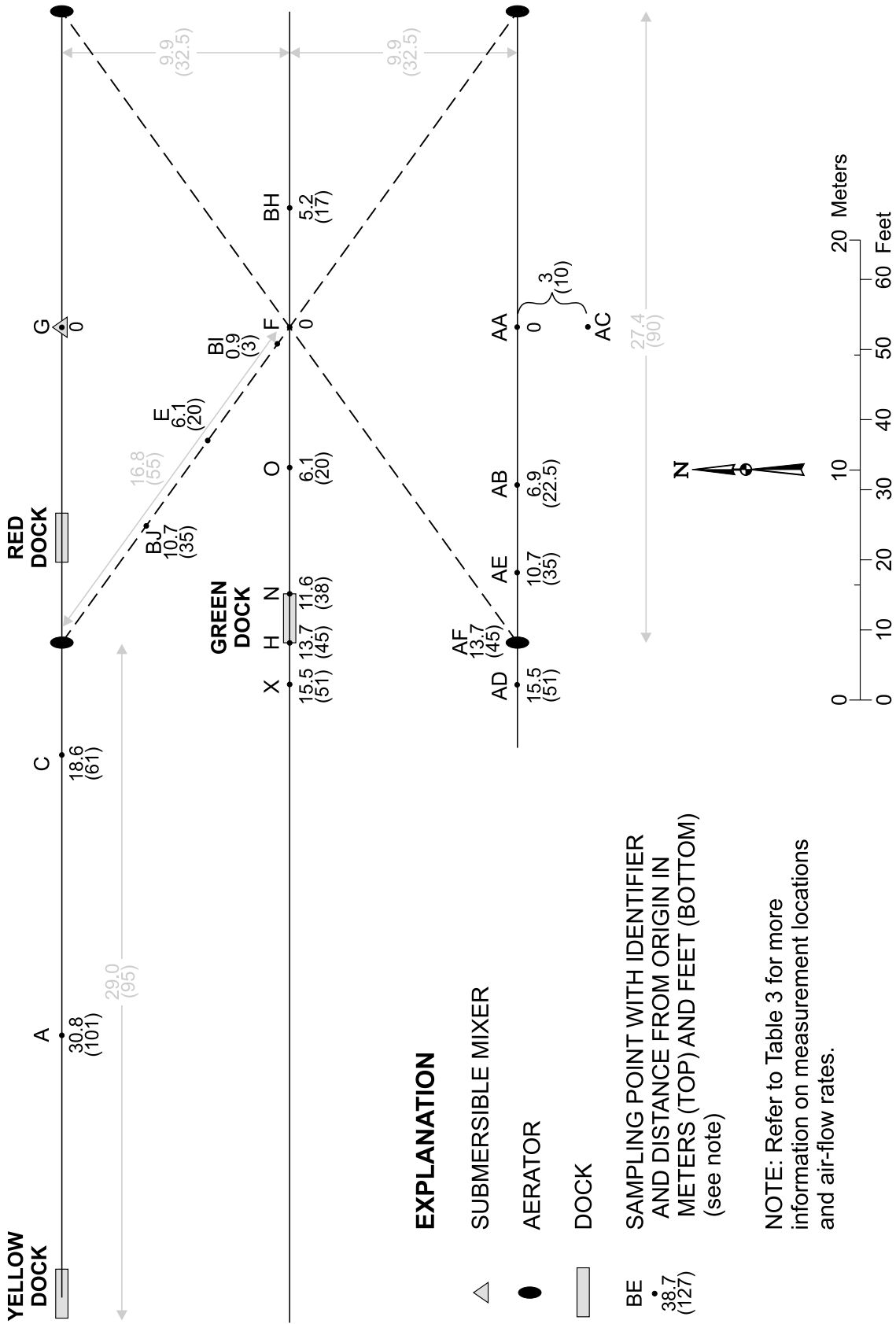


Figure 1-21. Layout for test "eg975d" on June 19, 1997.

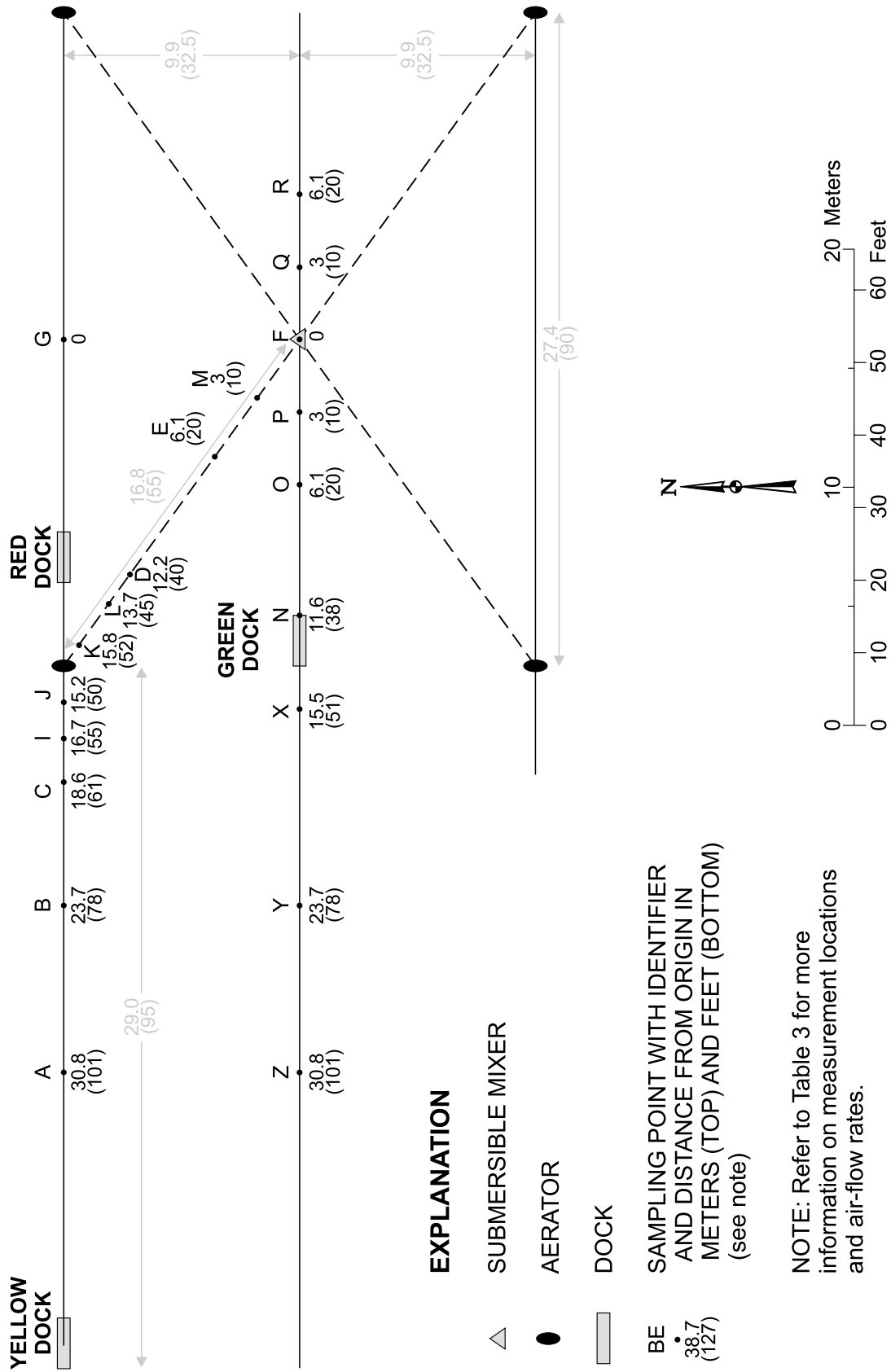


Figure 1-22. Layout for test "eg975s" on June 11, 1997.

U.S. GEOLOGICAL SURVEY  
221 NORTH BROADWAY AVE.  
URBANA, ILLINOIS 61801



Johnson and others—METHODODOLOGY, DATA COLLECTION, AND DATA ANALYSIS FOR DETERMINATION OF WATER-MIXING PATTERNS INDUCED  
BY AERATORS AND MIXERS—U.S. Geological Survey Water-Resources Investigations Report 00-4101